Open Research Online

The Open University's repository of research publications
and other research outputs

Analysis of target-derived factors regulating axon guidance in the visual system of Drosophila.

Thesis

How to cite:

Bazigou, Eleni (2006). Analysis of target-derived factors regulating axon guidance in the visual system of Drosophila. PhD thesis The Open University.

For guidance on citations see FAQs.

© 2006 Eleni Bazigou

https://creativecommons.org/licenses/by-nc-nd/4.0/

Version: Version of Record

Link(s) to article on publisher's website:
http://dx.doi.org/doi:10.21954/ou.ro.0000fe21

Copyright and Moral Rights for the articles on this site are retained by the individual authors and/or other copyright owners. For more information on Open Research Online's data policy on reuse of materials please consult the policies page.

oro.open.ac.uk

UNRESTRICTED

ANALYSIS OF TARGET-DERIVED FACTORS REGULATING AXON GUIDANCE IN THE VISUAL SYSTEM OF *DROSOPHILA*

Eleni Bazigou, B.Sc.

Thesis submitted to the Open University for the degree of

Doctor of Philosophy in Neurobiology

27th of March, 2006

Division of Molecular Neurobiology

National Institute for Medical Research

Mill Hill, London

AUTHOR NO: W3266751
DATE OF SUBMISSION: 27 MARCH 2006
DATE OF AWARD: 24 JULY 2006

ProQuest Number: 13917216

All rights reserved

INFORMATION TO ALL USERS
The quality of this reproduction is dependent upon the quality of the copy submitted.

In the unlikely event that the author did not send a complete manuscript
and there are missing pages, these will be noted. Also, if material had to be removed,
a note will indicate the deletion.

ProQuest 13917216

Published by ProQuest LLC (2019). Copyright of the Dissertation is held by the Author.

All rights reserved.
This work is protected against unauthorized copying under Title 17, United States Code
Microform Edition © ProQuest LLC.

ProQuest LLC.
789 East Eisenhower Parkway
P.O. Box 1346
Ann Arbor, MI 48106 – 1346

ACKNOWLEDGMENTS

Most good things in life you cannot really plan, opportunities arise and you have to take them, even if you are not sure of their benefit. I put my trust on two people to undertake this project, Iris Salecker and Vassilis Pachnis, and here I am, finishing my PhD after almost three years of effort and reward. As the first student in the lab and a working project to start with, Iris provided me with a safe environment and a lot of support and guidance during my first steps and throughout my studentship. She introduced me to the world of fly genetics and showed me that in order to reach excellence you need to work hard, be imaginative and have a critical mind, yet be respectful of other people's work. Importantly, while in the early days of the lab, Iris let me deviate from my original project and gave me the opportunity to work with something I was very much interested in, "aspects of metamorphosis".

A great part responsible for enjoying my work in the lab I ought to my past and present lab fellows, Wendy Leung, Carole Chotard, Justine Oyallon, Holger Apitz and Zoe Ludlow. Interaction between us, especially during our initial collaboration with Wendy, Carole and Iris in the screen but also later on when we each undertook our own projects, was great and constructive criticism and suggestions have proved invaluable. The working environment in NIMR has been great even in its extended version. For this reason, I would like to say a special thanks to the two other labs working with flies at the Institute (Alex Gould's lab and Jean Paul Vincent's lab), as well as to everyone working in the division of Molecular Neurobiology, for their suggestions and for creating a wonderful environment to work in.

Being a student in NIMR not only gave me the opportunity to participate in high quality science, but to also practise teamwork in the volleyball and football pitch. Many special thanks to all the friends I have made during the last three years through both scientific and social interactions. I am very grateful to my friends in London for helping

me adapt to the new environment and sharing laughter and many hours of good fun by teaching me of new ways, like French, Spanish, Italian, German, Mexican, and of course English. Thankfully, the Greek society in NIMR helped me not to forget the Greek ways! I am also grateful to my old friends in Athens for showing me that distance in time and space cannot overcome friendship. Also, a big thank you to Maria Ilia, with whom I worked during my studentship at the Institute of Psychiatry, for encouraging me and helping me to pursue a scientific career.

I would especially like to say a special thanks to all the people that took the time to read and suggest corrections for my thesis, including all the members of my lab, as well as Irene Miguel-Aliaga, Despina Stamataki, Babis Rallis and Steen Ooi. They have all been very supportive and inspirational throughout my PhD and during the writing of my thesis.

This thesis is dedicated to my father and mother, and my sister. Without their constant support throughout my studies, I would have not managed to be where I am today. Mum and dad, I could never describe how much your love, affection and faith in me have helped me get over many obstacles along my way over these past few years, even some scientific ones. My beloved sister, Faidra, thank you for staying younger than me to remind me of little silly things that can make me smile when I feel stressed, and proving to be more mature than me when I think the end of the world is just around the corner. One end has finally come with the submission of this thesis...

PREFACE

This PhD project has been conducted and completed in the laboratory of Dr Iris Salecker in the Division of Molecular Neurobiology at the National Institute for Medical Research.

This thesis describes my original work and has not been previously submitted as part of any other degree course or to another university. References are cited where appropriate. I have acknowledged all materials that have been used as well as findings obtained by my colleagues. Chapter 3 includes findings from the genetic screen, which has been conducted in a collaborative effort by C. Chotard, W. Leung, I. Salecker and myself. Section 3.1 refers to work performed by Iris Salecker and Wendy Leung prior to my involvement in the project. My contribution to the genetic screen is described in section 3.2. This included the setting up of genetic crosses, immunostainings of mutant mosaic animals, and assessing of phenotypes. I further sequenced the first mutant candidate of interest.

CONTENTS

LIST OF FIGURES AND TABLES

Chapter 1

Chapter 2

Chapter 3

Chapter 4

ABSTRACT

The developing visual system of *Drosophila* is characterized by complex and stereotyped patterns of neuronal connections. The *Drosophila* compound eye consists of approximately 800 ommatidia, each containing 8 photoreceptor cells (R-cells, R1-R8). Each of these R-cell groups have distinct spectral sensitivity and target specificity. R1-R6 axons terminate in the first optic ganglion called the lamina, inbetween two rows of glial cells, the epithelial and marginal glia, whereas R7 and R8 axons project through the lamina and terminate in the second optic ganglion, the medulla.

Previous studies have demonstrated that epithelial and marginal glia regulate target layer selection of R1-R6 in the lamina. To systematically address the molecular mechanisms through which glial cells as well as target neurons guide R-cell axons to establish initial projection pattern, the lab devised an FLP/FRT system-based genetic approach (ELF system) to generate somatic clones specifically in target cells. Using ELF in a large-scale mutagenesis screen for the left arm of the second chromosome, we isolated mutant candidates with R-cell projection defects caused by genes required in the target.

In a candidate approach, the role of the *Drosophila* homolog of the receptor tyrosine kinase Anaplastic lymphoma kinase (Alk) and its activating ligand Jelly belly (Jeb), known for their role in the development of the *Drosophila* visceral mesoderm, was addressed in our system. Alk and Jeb show a highly dynamic and initially complementary expression pattern in the target and in R-cells, respectively. Loss of *Alk* from the target and *jeb* from the eye has revealed common target specificity defects of R1-R6 axons in the lamina and R8 axons in the medulla during the refinement of axonal projections in the optic lobe. This novel anterograde signaling system in the *Drosophila* visual system may be regulating R1-R6 and R8 target specificity by controling the modulation of one or more axon guidance cues present in the target.

1.1 Overview of Mechanisms Underlying Axon Guidance

During the formation of the nervous system, newly born neurons migrate to their characteristic positions, differentiate and extend dendrites and axons, which connect with their appropriate synaptic partners. Dendrites and axons are required for synaptic input and output, respectively and thus are morphologically distinct. Dendrites do not extend very far away from the cell body and usually form elaborate branches that are characteristic of each neuron type (reviewed in Scott and Luo, 2001). Axons often have to travel long distances to reach their target. Along their trajectory they encounter guidepost cells, which help them to select or avoid a particular route towards their target area. Axons of early differentiating neurons pioneer scaffolds along which later extending axons project and then defasciculate to choose their synaptic partners (reviewed in Chotard and Salecker, 2004; Hutter, 2003). In the early sixties, Sperry proposed that synaptic specificity is determined by molecular labels distributed in complementary gradients on both projecting axons and their targets (chemoaffinity hypothesis; Sperry, 1963). These molecular labels exist in the form of attractive or repulsive cues, which growing axons receive and interpret through a specialized sensorimotor device present at their leading edge, called the growth cone (Tessier-Lavigne and Goodman, 1996; Figure 1). The formation of initial projection patterns and synaptic connections is genetically hardwired and in most cases activity-independent. However, during the lifetime of an organism these initial patterns of connections are refined as a result of activity-dependent mechanisms, including learning and experience (Sur and Rubenstein, 2005).

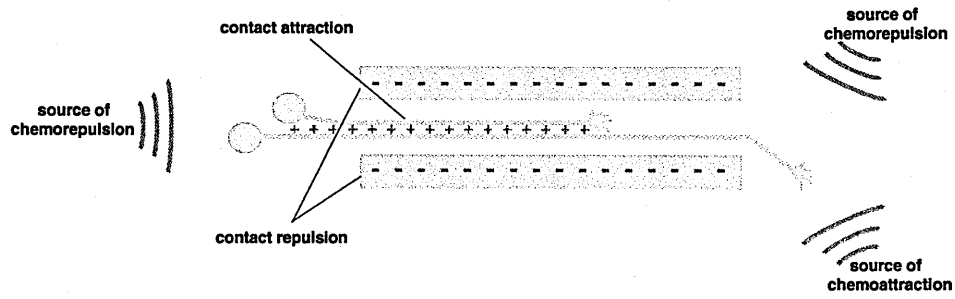

Figure 1. Guidance Forces.
Four types of mechanisms contribute to the guidance of axons: chemorepulsion (green waves), chemoattraction (red waves), as well as contact repulsion (-) and contact attraction (+). Adapted from Tessier-Lavigne and Goodman, 1996.

1.1.1 The Growth Cone

Growth cones are characterized by a central (C) domain rich in organelles and microtubules and a peripheral (P) domain containing actin filaments within veil-like protrusions, called lamellipodia, and spike-like protrusions, called filopodia. Polymerized F-actin from monomeric G-actin forms bundles within filopodia and a crossed-linked meshwork in lamellipodia. Growth cone motility depends on the balance between polymerization of actin bundles at the leading edge and retrograde flow of F-actin (Pantaloni et al., 2001; Suter and Forscher, 2000). Microtubules consist of tubulin polymers that extend into the growth cone from the axon shaft and provide structural support and regulate the axonal transport of organelles. In addition, microtubules found in the transition zone between the C and P domain are highly dynamic (Schaefer et al., 2002; Zhou et al., 2002), and can also play a role in steering the growth cone towards attractive cues or away from repulsive ones (Buck and Zheng, 2002; Suter et al., 2004). Finally, cross talk between the two polymer networks in the transition zone is important for the regulation of growth cone motility (Dent and Kalil, 2001; Lee et al., 2004; Zhou et al., 2002).

1.1.2 Rho GTPases

Depending on the concentration and combination of signals from extracellular cues, growth cones change their shape and perform tasks as extension, retraction or turning (Dent and Gertler, 2003). Small GTPases of the Rho family, such as Rac, Cdc42 and Rho, are key proteins in transducing these signals to the actin cytoskeleton and have been shown to play important roles in several aspects of neuronal morphogenesis and axon guidance (reviewed in Dickson, 2001; Ng et al., 2002).

The potential of the Rho GTPases to function as signaling switches resides in their ability to cycle between an active (GTP-bound) and inactive (GDP-bound) state. This cycling is regulated by guanine nucleotide exchange factors (GEFs) promoting the exchange of GDP for GTP, thereby activating GTPases, while GTPase activating proteins (GAPs) are negative regulators of Rho GTPases (Luo, 2000). GEFs and GAPs contain multiple motifs, such as Src homology (SH) domains 2 and 3 and PDZ (postsynaptic density 95/Discs large/zona occludens 1) domains, involved in intracellular signal transduction (reviewed in Luo, 2000). The best-studied GEF is Trio, containing two GEFs and one serine/threonine domain (Debant et al., 1996). In *Drosophila*, Trio possesses exchange activity for Rac regulating axon guidance in the visual system and for the p21 activated kinase (Pak) in the CNS and for the repulsion of motor axons (Awasaki et al., 2000; Bateman et al., 2000; Hakeda-Suzuki et al., 2002; Liebl et al., 2000; Newsome et al., 2000b). In mushroom bodies, Trio controls both axonal and dendritic extension by regulating the activity of RhoA (Awasaki et al., 2000).

Guidance cues may also influence actin polymerization at the distal ends of actin filaments. The Arp2/3 complex promotes actin nucleation by members of the Wiskott-Aldrich Syndrome Protein (WASP) (Prehoda and Lim, 2002; Strasser et al., 2004). However, their physiological significance in axon guidance awaits further investigation.

Proteins binding to the actin-monomer-binding protein Profilin, such as Ena/VASP (enabled/vasodilator-stimulated phosphoprotein) proteins, are found at the leading edge of lamellipodia and filopodia (Nakagawa et al., 2001) and play important roles in axon outgrowth and guidance (Gitai et al., 2003; Lebrand et al., 2004). In the leading edge of filopodia, they promote the formation of long unbranched actin filaments, partly by protecting barbed ends from capping proteins (Sutherland and Way, 2002). The disassembly of actin filaments is controlled by Cofilin, a protein playing a fundamental role in extending and maintaining lamellipodial protrusions at the leading edge of migrating cells (Dawe et al., 2003). Cofilin is deactivated by LIM kinase1 (LIMK1) (Yang et al., 1998) and is dephosphorylated by the phosphoserine/ threonine phosphatase Slingshot (SSH) (Niwa et al., 2002). The LIMK1 pathway is activated by Rac/ Cdc42 and Rho effectors that act through Pak (Dan et al., 2001; Ohashi et al., 2000), depending on the presence of different Rac GEFs (Ng and Luo, 2004).

Through convergent and divergent signaling pathways, Rho GTPases in neurons control the dynamics of actin cytoskeleton and regulate axon guidance. This suggests that these components of the neuronal cytoskeleton are potential targets of signaling pathways downstream of guidance cues. Some of the guidance cues modulating actin cytoskeleton during the development of the nervous system are presented below.

1.1.3 Netrins

Netrins are a small family of secreted molecules with multifunctional roles in axon guidance, promoting axon outgrowth, guidance and neuronal branching in the developing nervous system (Kennedy et al., 1994; Serafini et al., 1994). Depending on the cellular context, they can act as chemoattractants or chemorepellents (Colamarino and Tessier-Lavigne, 1995; Kennedy et al., 1994; Serafini et al., 1994; Serafini et al., 1996). Members of the netrin family have been identified in *C. elegans* (Unc-6)

(Hedgecock et al., 1990), *Drosophila* (NetrinA and NetrinB) (Harris et al., 1996; Mitchell et al., 1996), mice (netrin-1, netrin-3, netrin-4, netrin-G1 and netrin-G2) (Kennedy et al., 1994; Serafini et al., 1994, Yin et al., 2000; Nakashiba et al., 2002), chicks (netrin-1 and netrin-2; Serafini et al., 1994) and humans (netrin-2-like, NTN2L; van Raay et al., 1997).

Netrins act through transmembrane receptors, such as members of the Deleted in Colorectal Cancer (DCC) and UNC5H families. DCC in vertebrates (Keino-Masu et al., 1996), UNC-40 in *C.elegans* (Chan et al., 1996) and Frazzled in *Drosophila* (Kolodziej et al., 1996) mediate netrin-induced growth cone attraction. DCC is a member of the immunoglobulin (Ig) superfamily receptors and contains three conserved motifs (P1, P2 and P3) within its cytoplasmic domain. P3 mediates the ligand-gated oligomerization of DCC proteins required for netrin-induced attraction (Stein and Tessier-Lavigne, 2001). The repulsive effects of netrin are mediated by members of the UNC-5 family, which are also conserved Ig superfamily receptors (Colamarino and Tessier-Lavigne, 1995; Hedgecock et al., 1990; Keleman and Dickson, 2001). Interactions between DCC and the DCC binding (DB) domain in the UNC-5 cytoplasmic region are responsible for long-range netrin-mediated repulsion, whereas short-range repulsion only requires UNC-5 (Hong et al., 1999; Keleman and Dickson, 2001).

In the vertebrate spinal cord and in the *Drosophila* ventral nerve cord, Netrin secreted from midline cells attracts commissural growth cones to the midline by binding to DCC or the *Drosophila* DCC ortholog, Frazzled, expressed on their axons (Harris et al., 1996; Keino-Masu et al., 1996; Kolodziej et al., 1996; Mitchell et al., 1996; Serafini et al., 1996). The precise spatial distribution of Netrin-A and Netrin-B, and not simply their presence, is required for proper formation of commissural and some longitudinal tracts. Frazzled indirectly regulates the guidance of specific axonal populations, possibly by capturing and presenting Netrin at various points along their trajectory

(Hiramoto et al., 2000). Interestingly, although netrins are considered to act as long-range chemoattractants, they provide local repulsive cues for commissural axons (Brankatschk and Dickson, 2006; Keleman and Dickson, 2001).

Recent evidence has begun to link Netrin-DCC signaling with the growth cone cytoskeleton. *In vitro* experiments have shown that DCC induces formation of filopodia by activating Cdc42 and Rac1 (Shekarabi and Kennedy, 2002). In *C. elegans,* Ena/UNC-34 is found to act genetically downstream of DCC/UNC40 to mediate growth cone attraction (Gitai et al., 2003). Furthermore, activation of Ena/VASP proteins is required for Netrin-DCC-induced filopodia formation in cultured neurons (Lebrand et al., 2004). Finally, in *Drosophila*, the Abelson tyrosine kinase (Abl) mediates phosphorylation of Frazzled and Trio, which interact genetically to mediate chemoattraction in commissural growth cones (Forsthoefel et al., 2005). Additional kinases that have been shown to act downstream of Netrin-DCC signaling include Fyn, Src and focal adhesion kinase (FAK), mediating signals that control remodeling of the actin cytoskeleton network within the growth cone and also promote neurite outgrowth (Li et al., 2004; Liu et al., 2004; Meriane et al., 2004; Ren et al., 2004).

1.1.4 Slits

Slits have been mainly characterized with respect to their role in orchestrating the navigation of axons at the midline of *Drosophila,* vertebrates and in *C.elegans* through repulsion (Kidd et al., 1999; Long et al., 2004; Simpson et al., 2000; Wang et al., 1999b; Zallen et al., 1998). They are large conserved secreted proteins with one member in *Drosophila* (Slit) and *C.elegans* (SLT-1) and three homologs (Slit1-3) in the mammalian nervous system (Brose et al., 1999; Marillat et al., 2002; Zallen et al., 1998).

Slit-induced chemorepulsion is mediated by Robo1, Robo2 and Robo3 receptors in *Drosophila*, Robo1, Robo2 and Rig-1 in vertebrates and SAX3/Robo in *C.elegans* (Brose et al., 1999; Kidd et al., 1999; Sabatier et al., 2004; Simpson et al., 2000; Yu et al., 2002; Zallen et al., 1998). Robos are members of the immunoglobulin (Ig) superfamily, containing an extracellular, a transmembrane and a cytoplasmic domain. In their extracellular domain, Robos contain five Ig-like repeats followed by three fibronectin type III repeats (Kidd et al., 1998). Conserved cytoplasmic CC motifs in their intracellular domain are required for Slit-mediated chemorepulsion and for silencing netrin-mediated chemoattraction (Bashaw and Goodman, 1999; Stein and Tessier-Lavigne, 2001). The presence of different types of CC motifs on each receptor subtype is considered to mediate distinct aspects of Robo-signaling (Bashaw and Goodman, 1999; Stein and Tessier-Lavigne, 2001; Yu et al., 2002).

Slit is expressed at the ventral midline, where it acts as a short-range repellent signaling through Robo to prevent ipsilaterally projecting axons from crossing the midline and commissural axons from recrossing. Commissural axons are repelled by Slit2 only after they have crossed the floor plate (Zou et al., 2000), due to their dynamic regulation of Robo expression. The level of Robo1 is low in growth cones of commissural axons as they approach and cross the midline and high in postcrossing and ipsilaterally projecting axons (Kidd et al., 1998), whereas Rig-1 is highly expressed in commissural axons before midline crossing and is downregulated after crossing. Rig-1 prevents commissural axons from sensing Slit in the floor plate through their cognate receptor Robo-1 as they grow towards the floor plate, allowing them to enter and cross to the contralateral side (Sabatier et al., 2004). In *Drosophila*, a type II transmembrane protein called Commissureless (Comm) regulates the intracellular trafficking of the Robo receptor from the cell surface by targeting it for lysosome degradation (Georgiou and Tear, 2002; Keleman et al., 2002; Keleman et al., 2005). Two other Slit receptors,

Robo2 and Robo3, specify the lateral positions of axons that run parallel to the midline, presumably in response to a long-range gradient of Slit activity diffusing away from the midline (Rajagopalan et al., 2000; Simpson et al., 2000). The change in the response of axons after they cross the midline is also partly due to silencing of Netrin-1 attraction by DCC interacting with Robo, which possibly alters the complement of adaptor proteins recruited by the activated DCC receptor (Stein and Tessier-Lavigne, 2001).

Knock-out studies have demonstrated that in addition to their role in midline axon guidance, Slit1 and Slit2 play redundant roles in the formation of the optic tracts and control the formation of the optic chiasm in mice (Erskine et al., 2000; Plump et al., 2002). Consistent with this, data from zebrafish have confirmed that members of the Robo receptors have an important role in axon guidance of the retinal ganglion cells (Fricke et al., 2001).

Considerable effort has been invested in connecting Robo signaling with regulators of the actin cytoskeleton machinery. Cdc42 downregulation has been shown to be required for Slit mediated repulsion in subventricular zone neurons (Wong et al., 2001), whereas in *Drosophila* and *C. elegans,* distinct conserved CC domains of Robo interact with Ena/UNC-34 and Abl kinase to mediate axon repulsion (Bashaw et al., 2000; Yu et al., 2002). Additional downstream components of Robo signaling include the adaptor protein Dreadlocks (Dock), the Rac effector, Pak, and the microtubule plus-end tracking proteins Orbit-MAST (Fan et al., 2003; Lee et al., 2004).

1.1.5 Semaphorins

Semaphorins (Semas) include both secreted and membrane-associated glycoproteins, and are divided into eight classes based on their structural similarities and origin of species (Semaphorin Nomenclature Committee, 1999). Semaphorins are characterized by a conserved 500 amino acid motif of cystein residues, called the Sema domain (Luo

et al., 1993). Semaphorins 1 and 2 are found in invertebrates, classes 3-7 represent vertebrate semaphorins and class 8 is a viral semaphorin (Kolodkin et al., 1993). Semaphorins mediate their responses by forming multimeric receptor complexes with two main families, the neuropilins and plexins (Winberg et al., 1998). Plexins comprise a large family of conserved transmembrane proteins and are essential signal transducing components of most semaphorin receptor complexes (reviewed in Tamagnone and Comoglio, 2000). Neuropilins are transmembrane proteins with short, conserved cytoplasmic tails but lack any identifiable signaling motifs and thus do not appear to confer ligand specificity or contribute to the semaphorin-induced repulsive signals (Nakamura et al., 1998). Invertebrate semaphorins, membrane-associated semaphorins in vertebrates and viral semaphorins have been shown to interact directly with plexins (Tamagnone et al., 1999; Winberg et al., 1998). Sema-3 is a secreted protein and utilizes neuropilin proteins as ligand-binding co-receptors, and together they assemble a semaphorin/ neuropilin/ plexin-signaling complex (He and Tessier-Lavigne, 1997; Raper, 2000).

In vitro experiments and genetic analyses of semaphorins in flies and mice suggests that they primarily act as short-range inhibitory cues in many areas of the brain, including the ventral midline in the spinal cord, the hippocampus, spinal motor axons and sensory ganglia (Zou et al., 2000; Cheng et al., 2001; Yaron et al., 2005; Huber et al., 2005).

However, there is additional evidence suggesting that semaphorins may also act as attractive cues. Sema3A can repel growth cones while it simultaneously stimulates the outgrowth of dendrites (Fenstermaker et al., 2004; Polleux et al., 2000) and Sema 3B exerts attractive and repulsive forces in distinct populations of tracts patterning the anterior commissure in mice through the Src/Fyn complex (Falk et al., 2005). In fact, the Rho family of GTPases appears to provide a critical link between semaphorin

receptors and the actin cytoskeleton. Rac1 is involved in Sema3A-induced growth cone collapse (Jin and Strittmatter, 1997), and GTP-dependent interaction between the cytoplasmic domain of vertebrate Plexin B1 and Rac1 inhibits Rac downstream signaling by sequestering Rac GTP, resulting in inhibition of Pak activation (Hu et al., 2001; Vikis et al., 2002). In contrast to vertebrate Plexin B1, which does not appear to directly interact with Rho (Vikis et al., 2002), *Drosophila* Plexin B sequesters Rac and directly binds RhoA, resulting in its activation (Hu et al., 2001).

1.1.6 Eph Receptors

Eph receptors form a large family of receptor tyrosine kinases (RTKs). In vertebrates, there are eight members of Eph-A receptors and five members of EphB receptors (Gale et al., 1996). In *Drosophila* and *C. elegans*, there is one Eph receptor and one and three members of ephrin ligands, respectively (Chin-Sang et al., 1999; George et al., 1998; Scully et al., 1999). Class-A ephrins are GPI-anchored proteins and activate EphA receptors, whereas class B ephrin ligands contain a transmembrane domain and activate EphB receptors. An exception to this rule is the EphA4 receptor, which interacts with both ephrin-As and ephrin-Bs, and the EphB2 receptor that can be activated by ephrin-A5 (Gale et al., 1996; Himanen et al., 2004). In their extracellular domain, Eph receptors contain a ligand-binding domain, a cysteine-rich region, and two fibronectin-like repeats, while the cytoplasmic domain contains a pair of conserved tyrosine residues, a classical protein tyrosine kinase (PTK) domain, a sterile-α-motif (SAM) and a PDZ domain-binding motif (Huot, 2004; Kullander and Klein, 2002). Ligand binding induces forward signaling via the receptor, but ephrins also activate reverse signaling (Bruckner et al., 1997; Davy et al., 2004).

The ephrin-Eph receptor system regulates many cellular functions that depend upon cytoskeletal remodeling, such as axon guidance and synaptic plasticity. The

influence of ephrin-Eph activation on cell behavior differs depending on the cell type. It is generally associated with repulsion of neighboring cells or of cellular processes. However, in some cases, Eph-ephrin activation leads to increased adhesion or attraction (reviewed in Wilkinson, 2001; Pasquale, 2005).

Ephrins are best known for their role in regulating topographic map formation in the retinotectal system of vertebrates. The anterior posterior targeting of retinal ganglion cell (RGC) axons is regulated by a graded distribution of EphAs and ephrin-As in the retina and tectum, where axons terminate. RGC axons expressing high levels of EphA (EphA3 in chick, EphA5 in mice) project to the anterior tectum where there are low levels of ephrin-A2 and ephrin-A5, whereas axons with low levels of EphA target to more posterior regions with higher levels of ephrin-A repellents (Cheng et al., 1995; Drescher et al., 1997). Differences in the sensitivity of RGC axons to the repulsive effects of ephrin-As depends on relative levels of EphA on these axons and bias their success in targeting the tectum (Frisen et al., 1998; Feldheim et al., 2000; Brown et al., 2000). In the dorso-ventral axis, RGC axons express EphB2 in a high ventral to low dorsal gradient, whereas in the tectum ephrin-B1 and ephrin-B2 are expressed in a high dorsal to low ventral gradient (Braisted et al., 1997). As RGC axons expressing the highest levels of EphBs connect with areas of the tectum with the highest levels of ephrin-B ligands, it appears that Eph-ephrin interactions mediate attractive interactions between RGC axons and tectal cells (Brainsted et al., 1997). Importantly, ephrin/EphB interactions along the lateral-medial tectal axis regulate the formation of a dorso-ventral topographic map through both forward and reverse signaling (Hindges et al., 2002; Mann et al., 2002). Finally, members of the EphB family and their membrane ligands ephrin-Bs have been implicated in sorting RGC axons at the optic chiasm expressing ephrin-B, by preventing EphB RGC axons from projecting in the contralateral side of the brain (Nakagawa et al., 2000).

Activation of Eph receptors by ephrins leads to induction of signals regulating cytoskeletal rearrangements, neurite retraction and growth cone collapse. These are mediated primarily by RhoA activation (Wahl et al., 2000; Shamah et al., 2001; Knöll and Drescher, 2004; Harbott and Nobes, 2005). Ephs can associate with Abl tyrosine kinase, (Yu et al., 2001), which has been shown to mediate an ephrin-A-induced repulsive response *in vitro* (Harbott and Nobes, 2005). Furthermore, some ephrins can be phosphorylated in the conserved C-terminal cytoplasmic domain. Tyrosine phosphorylation of ephrin-B appears to mediate ephrin-B reverse signaling through the recruitment of the SH2/SH3 adaptor protein Grb4. This leads to upregulation of FAK catalytic activity, redistribution of the focal adhesion marker paxillin, and disassembly of F-actin-containing stress fibers (Cowan and Henkemeyer, 2001). In reverse signaling, activation of ephrin-A2 or A5 by one of their receptors, EphA3, results in integrin-dependent increased adhesion (Huai and Drescher, 2001). These data provide a biochemical pathway whereby cytoskeletal regulators are recruited to Eph-ephrin bidirectional signaling complexes.

1.1.7 Morphogens

Morphogens are secreted proteins produced by a restricted group of cells that induce distinct cellular responses and specify cell fates by regulating differential gene expression in a concentration-dependent manner. Morphogens have been implicated in many developmental processes, such as the organization of the major body axes, limb development and patterning of the nervous system (reviewed in Jessell, 2000; Ashe and Briscoe, 2006). During vertebrate CNS development, the best examples of signaling molecules acting as morphogens are possibly provided by the graded function of Wnt in patterning the neural plate along the anterioposterior axis (Wilson and Houart, 2004) and the antagonistic function of bone morphogenetic proteins (BMPs) and Sonic

Hedgehog (Shh) to specify neuronal identity along the dorsoventral axis of the entire neural tube (Liem et al., 2000; Briscoe et al., 2001). Moreover, high levels of the fibroblast growth factor 8 (FGF8) gradient along the longitudinal axis of the chick embryo maintain cells in the posterior of the embryo in an undifferentiated state while cells located far enough from the source are able to differentiate (Vasiliauskas and Stern, 2001). Recent studies propose that in addition to these roles, diffusible factors are also involved in axon guidance.

In the chick visual system, high levels of Shh repress the outgrowth of RGC axons, whereas low levels promote their growth (Trousse et al., 2001; Kolpak et al., 2005). In the floor plate, Shh signaling attracts commissural axons towards the midline independently of Netrin-1-mediated chemoattraction, via Smoothened (Charron et al., 2003), whereas BMP7 and BMP6 expressed by the roof plate are potential dorsal repellent cues from commissural axons (Augsburger et al., 1999). Following exit from the midline, Shh directs commissural axons rostrally along the longitudinal axis of the spinal cord, using a different receptor, Hedgehog interacting protein (Hip) (Bourikas et al., 2005). These data suggest that depending on its concentration or the receptor used for the activation of downstream effectors, Shh signaling exerts different effects on growth cones.

Wnt4 expressed in the floor plate attracts postcrossing commissural axons rostrally (Lyuksyutova et al., 2003). Mutant mice for the Wnt receptor Frizzled3 (Fz3) display anterior posterior guidance defects after midline crossing, suggesting that Wnt signaling guides commissural axons along the anterior posterior axis of the spinal cord through activation of Fz3 (Lyuksyutova et al., 2003). In addition, Wnt3 expressed in the chick optic tectum regulates descending corticospinal axon tracts and retinal axon outgrowth along the dorso-ventral axis through its receptor Ryk (Schmitt et al., 2006).

1.1.8 Cell Adhesion Receptors

Cell adhesion receptors, including Ig cell adhesion molecules (CAMs), cadherins, as well as integrins and proteoglycans regulate axon guidance through interactions with ligands present on neighboring cells or in the extracellular matrix (ECM).

CAMs contain Ig and fibronectin type III domains and mediate Ca^{2+}-independent homophilic and heterophilic interactions between cells (reviewed in Walsh and Doherty, 1997). The best-characterized Ig CAMs in the vertebrate nervous system are neural CAMs (NCAMs) and their close relative L1. Both molecules are abundantly expressed in the nervous system and have been linked to neurite outgrowth (Beggs et al., 1994; Ignelzi et al., 1994; Williams et al., 1994; Paratcha et al., 2003). In chick, two Ig-containing CAMS, axonin-1 expressed on commissural axons and Nr-CAM on the floor plate, interact and render the floor plate permissive for commissural axons to enter (Stoeckli and Landmesser, 1995). Another recently discovered CAM protein, the Down syndrome cell adhesion molecule (Dscam), has been shown to regulate axon guidance in the *Drosophila* embryonic CNS and target selection of olfactory receptor neuron (ORN) axons in the antennal lobe (Schmucker et al., 2000; Hummel et al., 2003). Through alternative splicing, Dscam can potentially generate 38,016 different isoforms (Hummel et al., 2003). In fact, different combinations of Dscam isoforms are expressed in different ORNs and target neurons endowing them with a unique molecular identity (Schmucker et al., 2000). Dscam exhibits *in vitro* isoform-specific homophilic binding. It has been proposed that it mediates repulsion of neurites when high levels of the same isoform are present or weak adhesion when different but similar isoforms are expressed (Wojtowicz et al., 2004). Dscam interacts with the SH3/SH2 adaptor protein Dreadlocks (Dock) and Pak, and thus can potentially signal to the actin cytoskeleton (Schmucker et al., 2000).

Cadherins are transmembrane proteins that promote calcium-dependent intracellular adhesion mainly between cells containing the same type of receptor (reviewed in Gumbiner, 2005), although heterophilic interactions between isoforms have also been reported (Shimoyama et al., 2000; Ting et al., 2005). Classical cadherins (E-cadherin, N-cadherin, P-cadherin and VE-cadherin) contain a single-pass transmembrane domain, five cadherin repeats in the ectodomain and a highly conserved cytoplasmic region (Gumbiner, 2000). Their cytoplasmic tails are indirectly linked to the cytoskeleton through association with a group of conserved cytoplasmic proteins, the catenins, which bind to actin filaments and trigger remodeling of the actin cytoskeleton through RhoA and Rac activation (Laplante et al., 2004; Gavard et al., 2004). Other cadherins, such as T-Cadherin, contain similar ectodomains but are attached to the plasma membrane through GPI anchors (Ranscht and Dours-Zimmermann, 1991). Protocadherins contain more than five cadherin repeats and have cytoplasmic domains structurally distinct from those of classical cadherins (Sano et al., 1993).

N-cadherin is expressed in the nervous system in both vertebrates and invertebrates (Iwai et al., 1997; Clandinin and Zipursky, 2002), where it plays important roles in axon guidance and synapse formation and plasticity (reviewed in Ranscht, 2000; Gumbiner, 2005). In *Xenopus*, *N-Cadherin* is required for axonal growth of RGC axons (Riehl et al., 1996), whereas in *Drosophila* it regulates target specificity of photoreceptor axons (Lee et al., 2001) and formation of ORN axon projections in the antennal lobe (Zhu and Luo, 2004; Hummel and Zipursky, 2004).

Extracellular matrix molecules (ECMs), such as integrins, have been shown to control the response of growth cones to guidance cues. Integrins are a large family of heterodimeric cell-surface receptors, composed of non-covalently associated α and β subunits that provide a physical link between ECM and the cytoskeleton (Hynes, 2002).

They are activated by laminins. These are heterotrimers that exhibit growth- promoting or inhibiting effects depending on the combination of isoforms expressed in a given cell type (Miner et al., 1997). In *Xenopus*, laminin-1 causes retinal axons to change their response to Netrin-signaling from attraction to repulsion (Hopker et al., 1999), and modifies the ephrin-A5-induced repulsion to attraction (Weinl et al., 2003). In *C. elegans*, *laminin* is required for commissural axon guidance (Huang et al., 2003), whereas in *Drosophila*, *laminin* mutants exhibit defects in pathfinding of ocellar pioneer axons (Garcia-Alonso et al., 1996). Similarly in zebrafish, *laminin* is required for RGC axon guidance and the formation of several CNS axon tracts (Paulus and Halloran, 2006).

Heparan sulphate proteoglycans (HSPGs) are a group of extracellular and cell surface proteins that bear long chains of differentially modified sugars and seem to influence Hh, FGF and Wg signaling (Bornemann et al., 2004; Kirkpatrick et al., 2004; Carrasco et al., 2005; Norton et al., 2005). HSPGs, such as Syndecan and Dally and Dally-like, have also been implicated in the regulation of axonal pathfinding in the *Drosophila* and *C. elegans* midline by regulating the distribution of Slit (Johnson et al., 2004; Steigemann et al., 2004; Rhiner et al., 2005). Additionally, *syndecan* mutants exhibit disruptions in the projection pattern of photoreceptor axons in *Drosophila* and mutations in *Exostosin* (*EXT*), a glycosyltransferase involved in HSPG biosynthesis, cause defects in the sorting of dorsal RGC axons in the optic tract and their pathfinding in the tectum (Rawson et al., 2005; Lee et al., 2004). Chondroitin sulphate proteoglycans (CSPGs) are a heterogeneous group of ECMs that appear to influence the behavior of the growth cones during development, and importantly, following CNS injury (Bovolenta and Fernaud-Espinosa, 2000; Morgenstern et al., 2002; Holt and Dickson, 2005). They have been implicated in guiding RGC axons in the optic chiasm and target recognition of the tectum (Chung et al., 2000). Both HSPGs and CSPGs on

the surface of growth cones interact with Sema5A receptors (Kantor et al., 2004). CSPGs function as bound localized extrinsic cues that convert Sema5A from an attractive to an inhibitory guidance cue, whereas axonal HSPGs are required for Sema5A-mediated attraction (Irie et al., 2002; Kantor et al., 2004). These findings suggest that the growth cone may modulate its behavior depending on the presence of different types of sulphated proteoglycans in the environment.

1.1.9 Modulation of Axon Guidance Cues

The establishment of correct neuronal connections is crucial for proper functioning of the nervous system. To reach their proper targets, axons rely upon the expression of highly conserved families of attractive and repulsive guidance molecules. These are used to generate an astonishingly varied set of neuronal circuits. However, the complexity with which molecules and receptors from different families interact in signaling to create more complicated responses is not well understood. This complexity lies in the potential of most of these cues to act as both attractants and repellents or to interact with each other in different combinations. During the past ten years, modulation of growth cone responses to axon guidance cues has additionally been attributed to the role of Ca^{2+} and of the second messenger cAMP in regulating the intracellular levels of Ca^{2+} and subsequently changing the response of growth cones to several axon guidance cues, such as netrin and semaphorin (Ming et al., 1997; Song et al., 1998; Hong et al., 2000; Ming et al., 2001; Shewan et al., 2002;) as well as to mechanisms regulating local protein synthesis (Campell and Holt, 2001; Brittis et al., 2002; Brunet et al., 2005). These findings suggest that the responses of growth cones to guidance cues can be modulated depending on the presence of intrinsic as well as extrinsic factors. As the growth cone response to different sets of guidance cues is regulated by quite a complex mechanism, *in vivo* analysis of axon guidance models and identification of additional

novel factors with more restrictive expression and more specific function is a fundamental task.

1.2 The visual system of *Drosophila*

The adult visual system of *Drosophila* consists of the compound eye and the optic lobe. The *Drosophila* compound eye consists of approximately 800 identical units, called ommatidia (Figure 2A). Each contains 8 photoreceptor cells (R-cells, R1-R8) (Figure 2B), as well as 12 accessory cells including bristle, pigment and cone cells. R-cells can be divided into three main categories based on their spectral sensitivity and target layer specificity (Wolff and Ready, 1993). R1-R6 cells, also called outer photoreceptors, are involved in motion detection and dim light vision. They express Rhodopsin 1 (Rh1) (O'Tousa et al., 1985), a light sensing protein, which accumulates in the microvillar structures that capture light, the rhabdomeres. R1-R6 rhabdomeres span the whole depth of the retina. The two inner photoreceptors, R7 and R8 respond to ultraviolet and green light, respectively, and are involved in color discrimination (reviewed in Cook and Desplan, 2001). The R7 rhabdomere spans only the distal half of the retina whereas the R8 rhabdomere is found in the proximal half. Expression of different rhodopsins divides the ommatidia in two distinct subtypes: pale ommatidia (~30% of total) express Rh3 in R7 and Rh5 in R8, while yellow ommatidia (~70%) express Rh4 in R7 and Rh6 in R8 (Zuker et al., 1985; Chou et al., 1996; Montell et al., 1997; Papatsenko et al., 1997). Outer photoreceptors terminate in the first optic ganglion called the lamina, whereas the inner photoreceptors terminate in two distinct sub-layers within the second optic ganglion, the medulla (reviewed in Meinertzhagen and Hanson, 1993). The adult compound eye and the optic lobe develop from two separate precursor populations found in the eye imaginal disc and the optic lobe primordium (Meinertzhagen and Hanson, 1993).

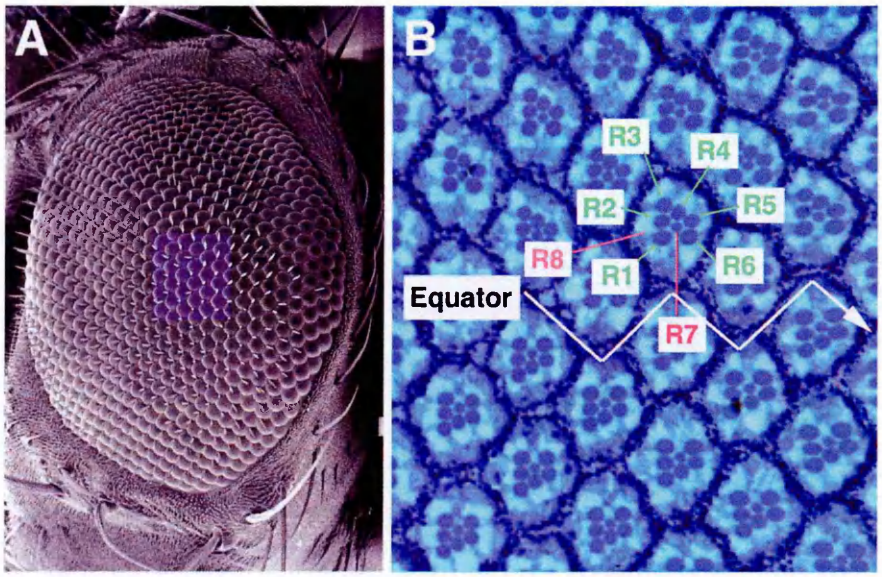

Figure 2. The Fly Compound Eye.

The *Drosophila* eye consists of approximately 800 ommatidia (A), each of which contains 8 photoreceptor cells (R-cells, R1-R8). (B) R1-R6 cells form a trapezoid and are called outer photoreceptors. R7 and R8 are in the center and are called inner photoreceptors. Since R8 is found below R7, only one of each can be seen in a given transverse section of the eye. (Eq equator). Kindly provided by I. Salecker.

1.2.1 Differentiation of Photoreceptors

R-cells in the *Drosophila* compound eye develop in a highly stereotypic and repetitive pattern within the eye imaginal disc. The latter arises during early larval development from a contiguous group of cells that form the eye-antenna imaginal disc (Meinertzhagen and Hanson, 1993). These cells commit to either eye or antennal fate through the combined action of Notch, and epidermal growth factor receptor (EGFR), Hedgehog (Hh) and Wingless (Wg) signaling (Kumar and Moses, 2001). During the later half of the 2nd instar larval stage, Notch upregulation in the posterior part of the disc results in the restrictive expression of the eye selector gene *eyeless* (*ey*) in the eye portion of the disc (Kumar and Moses, 2001). From this stage onward, seven key regulators required for the specification of the compound eye (Gehring et al., 1998) are

coexpressed within the presumptive eye imaginal disc (Kumar and Moses, 2001). During the 3rd instar larval stage, Hh expression at the posterior region of the eye imaginal disc induces the expression of Decapentaplegic (Dpp), a member of the transforming growth factor-β/bone morphogenetic protein (TGFβ/BMP) family of secreted proteins (Tabata and Kornberg, 1994), in anteriorly adjacent cells and initiates a wave of morphogenesis that traverses the eye imaginal disc from posterior to anterior. The front of this wave is marked by an apical constriction of the imaginal epithelium, called the morphogenetic furrow (MF) (Ready, 1976). As cells enter the MF, they synchronize and arrest in the G1 phase of the cell cycle and either move apically to assemble into preclusters and initiate ommatidial recruitment, or remain undifferentiated at the basal part of the disc (see Figure 2 for equator). A continuous supply of Hh and Dpp produced by newly born cells is required for the propagation of the MF across the retinal epithelium (Heberlein and Moses, 1995). The MF reaches the anterior end of the disc by early pupal development (Meinertzhagen and Hanson, 1993).

Hh and Dpp regulate the expression of a number of molecules associated with neuronal determination and differentiation, such as the proneural bHLH factor, *atonal* (*ato*) (Jarman et al., 1994). Broad expression of Ato is first observed in a continuous stripe ahead of the MF in response to Hh and Dpp proteins diffusing from the more posterior portion of the eye disc, and marks the start of neurogenesis (Greenwood and Struhl, 1999; Curtiss and Mlodzik, 2000). Soon after, its expression becomes restricted to evenly spaced single cells that become R8 founder neurons by Notch-mediated lateral inhibition (Baker et al., 1996). R8 cells are the first photoreceptor neurons to differentiate in each ommatidium. Their differentiation is dependent upon the expression not only of Atonal, but also of its bHLH heterodimer partner Daughterless (da) and the downstream effector zinc finger transcription factor Senseless (Sens) (Jarman et al., 1995; Nolo et al., 2000).

Following R8 selection, Ato-positive R8 cells expressing the EGFR-like ligand Spitz, sequentially recruit other photoreceptors in pairs of R2/R5 and R3/R4 from surrounding undifferentiated cells to form preclusters of R-cells (Tio and Moses, 1997). EGFR is activated in R8 as well as in the remaining R-cells of the precluster, and is additionally required for the spacing between the precluster "intermediate groups" but not for R8 specification (Yang and Baker, 2001). This is mainly because Senseless blocks the activation of EGFR in R8 by repressing the expression of *pointed*, a nuclear effector of EGFR signaling (Frankfort and Mardon, 2004). Following R3 and R4 cell fate determination, preclusters rotate 90° towards the dorsoventral midline, the equator, with R3 facing away from it, and acquire opposite chirality in the dorsal and ventral halves of the eye imaginal disc. This is reflected in the asymmetric arrangement of R3 and R4 in mature ommatidia, ensuring ommatidial polarity in the adult compound eye, which is important for accurate vision (Wolff and Ready, 1993, Figure 1).

Immediately posterior to the precluster, a second mitotic wave gives rise to the remaining three photoreceptor cells in a sequential order, R1 and R6, and finally R7 (Wolff and Ready, 1993). R7 are the last of R-cells to be recruited in the ommatidial cluster, and require in addition to EGFR signaling, activation of Notch (Tomlinson and Struhl, 2001) and Sevenless (Sev) receptor signaling (Tomlinson et al., 1987). Sev is an RTK expressed in R1, R3, R4, R6 and R7. Its ligand, Bride of sevenless (boss) expressed in R8 cells, activates the receptor only in R7 to specify their fate (Reinke and Zipursky, 1988), as the remaining Sev-positive R-cells express the zinc-finger transcription factor Seven-up which makes them ignore the Boss-Sevenless signal (Mlodzik et al., 1990).

1.2.2 R-cell Target Selection in the two Optic Ganglia

The *Drosophila* optic lobe consists of three ganglia, the lamina, medulla and lobula complex, that arise from cell populations found within the outer and the inner proliferation centers (OPC and IPC, respectively). OPC and IPC are separated by a groove called the lamina furrow (Figure 3A). Progeny of the OPC give rise to lamina and outer medulla neurons, whereas progeny of the IPC contribute to the inner medulla, lobula and lobula plate (Meinertzhagen and Hanson, 1993). During the 3rd instar larval stage, differentiating R-cells in the eye disc extend axons and project through the optic stalk into the optic lobe in a sequential order that follows the posterior (p) to anterior (a) order of their differentiation in the eye imaginal disc (Meinertzhagen and Hanson, 1993). In this way, R-cells in adjacent ommatidia extend axons next to each other forming a topographic map in the visual system of *Drosophila.*

Apart from the sequential order along the anterior-posterior axis, R-cells axons are thought to project in the optic lobe in the order of their recruitment in each ommatidium. R8 may act as pioneer neurons, as their axons project first. The initial direction of R-cell axonal outgrowth toward the posterior of the eye imaginal disc and through the optic stalk is provided by subretinal glia, whose migration at the posterior region of the disc appears to be regulated by Hh signaling (Hummel et al., 2002). Subsequently, R1-R6 and finally R7 axons choose their targets in the optic lobe (Meinertzhagen and Hanson, 1993). R1-R6 axons terminate in the lamina inbetween two rows of glial cells, the epithelial and marginal glia (Perez and Steller, 1996a). R7 and R8 axons project through the lamina and terminate in the medulla (Figure 3A). In the adult visual system, R1-R6 axons together with five postsynaptic lamina neurons (L1-L5) are organized into synaptic modules called cartridges (Figure 3B), while R8 and R7 axons innervate two distinct sub-layers of the medulla, called M3 and M6,

respectively. R7 and R8 terminals connect with target neurons in radially oriented modules, called columns (Meinertzhagen and Hanson, 1993; Figure 3B).

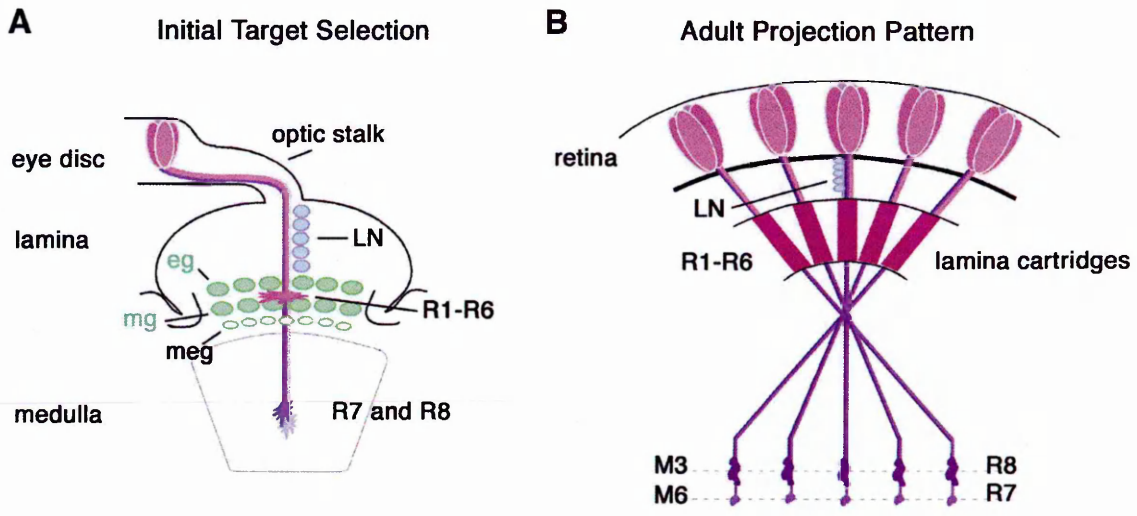

Figure 3. Target Selection in the *Drosophila* Visual System.
(A) During 3rd instar larval stage, R-cells assemble into clusters in the eye imaginal disc and extend axons through the optic stalk into the optic lobe. R1-R6 axons terminate in the lamina along columns of lamina neurons (LN) and between two rows of glial cells, the epithelial (eg) and marginal (mg) glia. R7 and R8 axons extend through the lamina and terminate in the medulla. (meg, medulla glia).
(B) In the adult, the initial projection pattern is reorganized. R1-R6 axons form functional units with lamina neurons (LNs), called the lamina cartridges. R7 axons terminate in the M6 layer in the medulla, whereas R8 are in the more superficial M3 layer.

This highly coordinated process through which the optic lobe is innervated is also required for establishing a retinotopic map in the visual system. Positional cues provided by the eye or the target, such as Eph and Wnt4 receptor signaling, have also been shown to regulate the spatial arrangement of R-cell axons in the projection field along the dorso-ventral axis, independently of retinal neighbors (Dearborn et al., 2002; Sato et al., 2006). Furthermore, proteins such as the *Drosophila* homolog of Nck, Dreadlocks and the GEF Trio recruit Pak and are required for maintaining the spatial arrangement of R-cell axons by regulating the actin-cytoskeleton machinery (Garrity et

al., 1996; Hing et al., 1999; Newsome et al., 2000b). These findings suggest that the formation of topographic map involves complex bidirectional interactions between R-cell axons and between these afferents and target cells.

1.2.3 Development of the Target

Different populations of cells in the optic lobe give rise to the future anatomically distinct information processing centers (lamina, medulla and lobula complex) within the optic lobe. These precursors lie adjacent to each other but do not intermingle (Meinertzhagen and Hanson, 1993). The compartmentalization of the optic lobe is partly controlled by Slit/Robo signaling and is required for brain morphogenesis and the proper function of the visual system (Tayler et al., 2004).

Proliferation, differentiation, as well as migration of target cells rely on signals provided by incoming R-cell afferents progressively innervating the optic lobe. One of these cues, Hh, is transferred along R8 axons and is both necessary and sufficient for lamina precursor cells (LPCs) to enter S-phase and to undergo cell division at the lamina furrow (Huang and Kunes, 1996). Hh also induces the onset of expression of the early neuronal differentiation marker, Dachshund (Dac) (Huang and Kunes, 1996; Figure 4). The resulting lamina neurons assemble lamina columns in close association with R-cell axon bundles. The transcription factor Single minded (Sim) has been proposed to be involved in this recruitment process (Umetsu et al., 2006). In parallel, Dac induces the expression of the EGFR in the LPCs (Chotard et al., 2005). Its ligand, Spitz, expressed along R-cell axons, activates EGFR in the target and triggers the maturation and further differentiation of lamina neurons by inducing the expression of the late neuronal differentiation marker Elav (Huang et al., 1998; Figure 4).

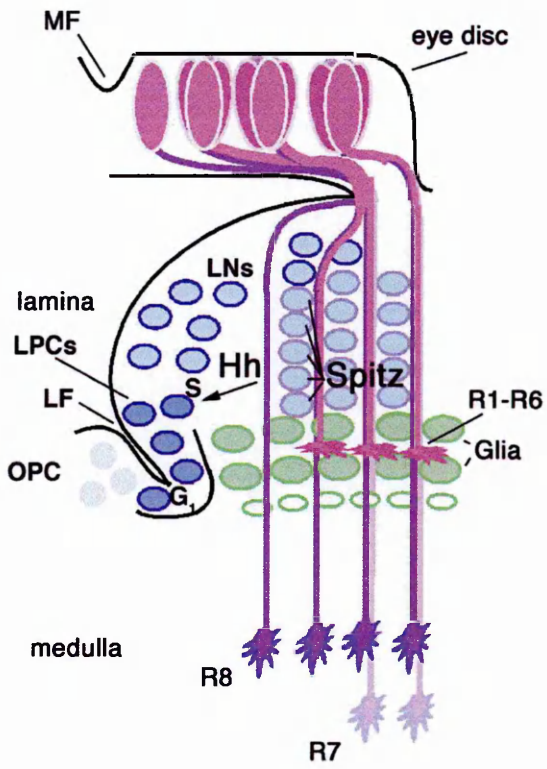

Figure 4. Development of Lamina Neurons is Induced by Hh and Spitz Anterograde Signaling.
Differentiating R-cells extend to the optic lobe and secrete Hh, which induces lamina precursor cells (LPCs) at the lamina furrow (LF) to leave G_1 and enter the S phase of the cell cycle. Hh also induces initial differentiation of lamina neurons (LNs) and their assembly into columns. Subsequently, Spitz activates EGFR in the target, inducing the further maturation of lamina neurons. (MF, morphogenetic furrow and OPC, outer proliferation center).

Apart from lamina neurons, R-cell axons entering the optic lobe encounter different types of glial cells. Lineage analysis has revealed that lamina glia are derived from different precursors than those of lamina neurons. The former are found in glial precursor cell (GPC) areas, located at the most dorso-ventral edges of the R-cell projection field on the surface of the optic lobe (Winberg et al., 1992; Perez and Steller, 1996; Chotard et al., 2005). Entry of R-cell axons in the target field induces differentiation and migration of epithelial and marginal glia to their appropriate positions in the lamina (Perez and Steller, 1996). Although the molecular mechanisms through which this is accomplished are not known, it is believed that glial cell migration from the GPC area may be directed towards the target field by scaffold axons from neurons at the dorsal and ventral margins of the medulla (Dearborn and Kunes, 2004).

1.2.4. Glial Cells Act as Intermediate Targets for R1-R6 Initial Target Selection

The presence of epithelial and marginal glia in the target field prior to innervation by R1-R6 axons suggested that they might provide these axons with guidance cues. Furthermore, the fact that R1-R6 axons selectively stop at the lamina prior to making connections with their postsynaptic partners (Meinertzhagen, 2000), suggested that lamina glia play the role of intermediate targets for these axons (Perez and Steller, 1996). On the contrary, the proliferation, differentiation and migration of lamina neurons to their characteristic positions rely on retinal innervation, therefore, it is unlikely that these cells provide incoming R-cell axons with positional information. Indeed, in the absence of Hh signaling, R1-R6 target selection in the lamina occurs normally (Poeck et al., 2001).

Following these observations, analysis of *nonstop* and *jab1/csn5* mutants, whose protein products are involved in protein degradation, showed that the failure of R1-R6 axons to terminate in the lamina and their mistargeting in the medulla was due to defects in epithelial and marginal glial cell migration (Poeck et al., 2001, Suh et al., 2002). Additionally, as *jab1/csn5* is required in R-cells whereas *nonstop* is required in glia, these findings suggested that the differentiation and migration of epithelial and marginal glia is partially regulated by cues provided by R-cell afferents entering the target field as well as by cues affecting glia in a cell-autonomous fashion (Poeck et al., 2001, Suh et al., 2002). The latter was confirmed with the mutant analysis of two closely related transcription factors with glial promoting activity in the embryo (Jones et al., 1995), *glial cells missing* (*gcm*) and *glial cells missing 2* (*gcm2*), which are required redundantly for the formation of glial cells in the lamina and subsequently for the correct targeting of R1-R6 growth cones there (Chotard et al., 2005). These data confirmed previous observations about the origin of epithelial and marginal glia in the

lamina, and proposed that these glia provide a "stop" signal to R1-R6 growth cones in the lamina.

Although the molecular nature of this signal is not known, several factors have been shown to regulate the ability of R-cells responding to it. One of them, Brakeless (Bks), a transcription factor expressed in all R-cells, specifically regulates R1-R6 target layer selection by repressing the transcription factor Runt in these cells (Kaminker et al., 2002). In *bks* mutant animals, R2 and R5 misexpress Runt, causing all R1-R6 axons to fail to terminate in the lamina and misproject into the medulla, together with R7 and R8 (Rao et al., 2000; Senti et al., 2000; Kaminker et al., 2002). These findings suggest that Bks and Runt are examples of molecular labels on R-cells that enable them to follow or dismiss the guidance cues provided by the lamina glia.

Other factors that regulate R1-R6 target layer selection in the lamina include the protein tyrosine phosphatase (PTP) receptors Lar, PTP69D, and Off-track and two RTKs, the insulin receptor (InR) and the Eph receptor (Clandinin et al., 2001; Garrity et al., 1999; Gafferty et al., 2004; Song et al., 2003; Dearborn et al., 2002). Downstream components of the phosphotyrosine signaling cascade, such as Dock, regulate R1-R6 target layer selection by recruiting downstream effectors to tyrosine-phosphorylated proteins (Garrity et al., 1996). An example of such a protein is the *Drosophila* homolog of Nck-interacting kinase, Misshapen (Msn). Msn and Bifocal, a putative cytoskeletal regulator, rearrange the actin-cytoskeleton of R-cell growth cones and regulate R1-R6 target layer selection in the lamina (Ruan et al., 2002; Babu et al., 2005).

1.2.5 R-cell Target Selection during Later Stages of Development - Neural Superposition

Following the completion of retinal innervation into the optic lobe, the eye imaginal disc develops into a complex compound eye and R-cell axon projections undergo a

major reorganization to accommodate the functional requirements of the adult animal. In several insects with compound eyes, R-cell axons form different patterns of connections to represent images of the external environment in the brain and achieve photon capture and spatial resolution. For example, in each ommatidium of the apposition eye, R-cells have fused rhabdomeres, and therefore receive similar input through the lens. A different mechanism is employed by superposition eyes, in which the rhabdomeres in each ommatidium are separated by an extracellular space of 1-2 μm, allowing individual receptive structures underneath each lens (reviewed in Land, 1997). The *Drosophila* eye is a characteristic neural superposition eye (Kirschfeld, 1967). Due to the curvature of the adult eye and the geometric arrangement of R-cells in each ommatidium, the angle between the axes of neighbouring rhabdomeres of one ommatidium equals the angle between two neighboring ommatidia (Kirschfeld, 1967; Figure 5A). As a consequence, particular sets of R1-R6 in six adjacent ommatidia receive the same input from the optical environment (Figure 5B). However, lamina neurons, the postsynaptic partners of R1-R6, receive information derived from one point of the visual environment only. This is achieved by a complex pattern of connections, in which the axons of R1-R6 cells that "see" the same point in space, following initial target layer selection in the lamina, converge into and connect with lamina neurons in a lamina cartridge unit. In this way, each unit is innervated by a complete set of R1-R6 axons from six different ommatidia that lie adjacent to each other (Figure 5C) (Kirschfeld, 1967). By superimposing synaptic inputs from multiple R-cells that receive input from the same point in space, the sensitivity of the eye to visible light is enhanced.

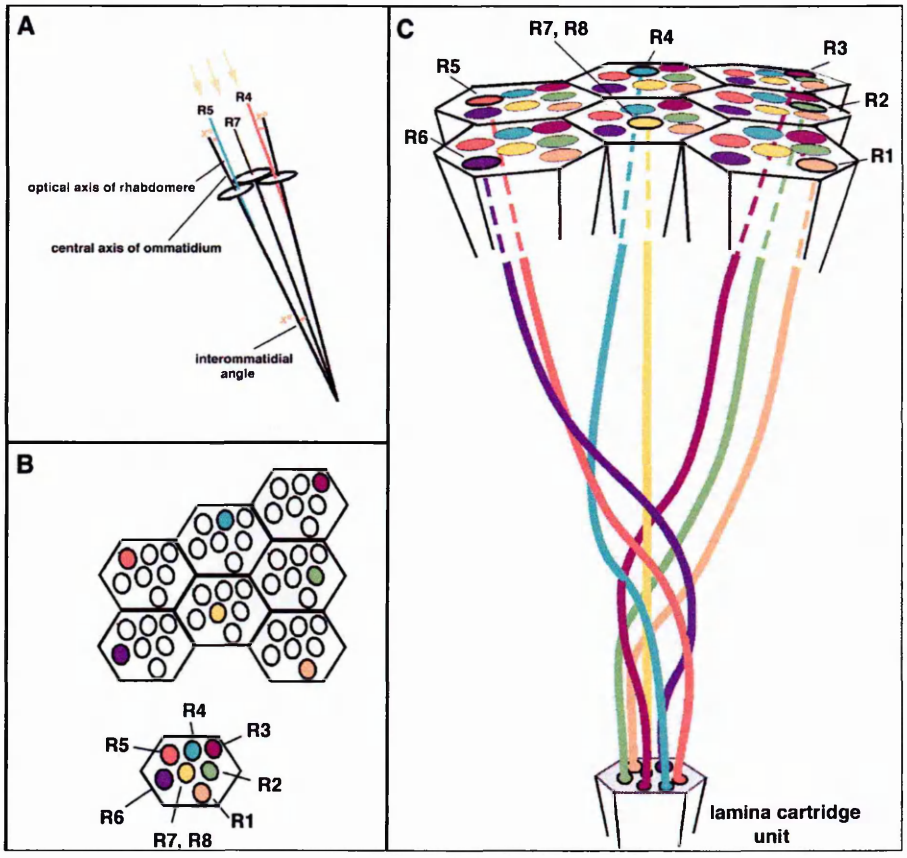

Figure 5. Neural Superposition Eye.

(A) Due to the geometrical arrangement of R-cells within an ommatidium and the curvature of the *Drosophila* eye, the interommatidial angle equals the angle between the optical axes of particular rhabdomeres in adjacent ommatidia. Particular sets of individual R-cells in adjacent ommatidia "see" the same point in space (B) by converging input for this information to lamina neurons (LN) in one lamina cartridge unit (C). The pattern of selected R-cells innervating each cartridge is the same as the pattern they have in each ommatidium but inverted by 180° (B). Adapted from Clandinin and Zipursky, 2000.

As a result of such an arrangement, R-cells in each ommatidium see different angular positions of the visual field, with the exception of R7 and R8, which look at the same point. To yield such a complex pattern of neuronal connections, around 30 hours of pupal development, R1-R6 cell axons from each ommatidium begin to defasciculate from their original R-cell bundle and its associated column of lamina neurons and project across the surface of the lamina towards their postsynaptic partners in a precise and invariant pattern (reviewed in Clandinin and Zipursky, 2002) (Figure 6, 30 hours).

R1-R6 axons reach their respective target cells in neighboring columns within 10-12 hours, and lamina cartridge units assemble (Figure 6, 43 hours).

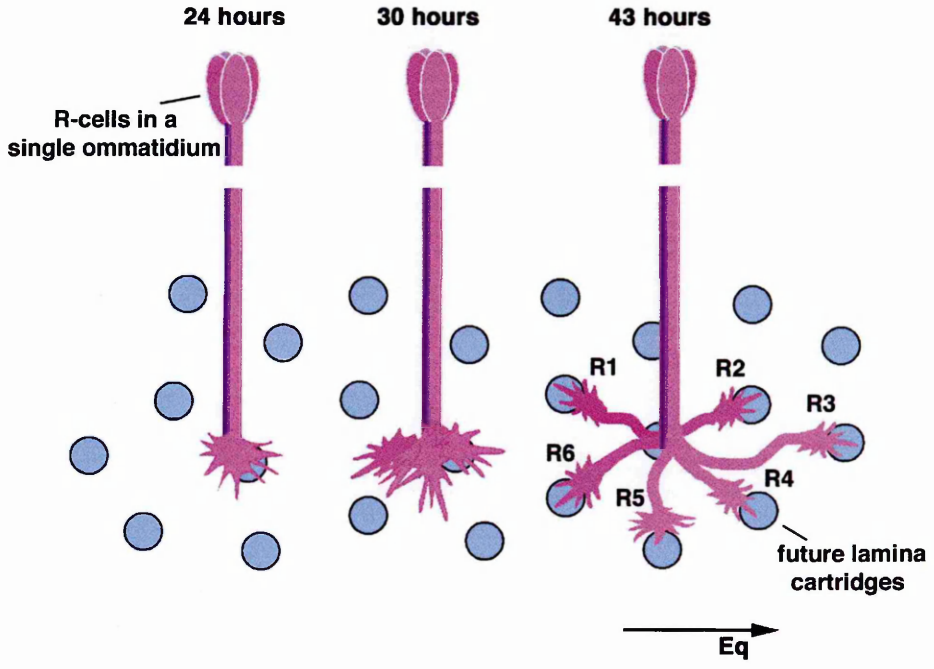

Figure 6. Defasciculation of R1-R6 During Development.
During development R-cell axons from each ommatidial cluster enter the target field as one bundle. Around 30 hours of pupal development, R1-R6 growth cones start to defasciculate from the ommatidial bundle and extend towards their postsynaptic partners, the lamina neurons. The defasciculation process is completed around 43 hours of pupal development. The projection pattern of R1-R6 axons within the lamina is stereotypic with R3 axons always extending to a target cartridge towards the equator (Eq).

1.2.6 R1-R6 Selection of Postsynaptic Partners in the Lamina

The projection pattern of each of the R1-R6 cell axons is invariant and is always oriented with respect to the dorsoventral midline of the eye, with R3 axons extending towards the equator (Figure 6). As a consequence, individual R1-R6 projection patterns form mirror images with respect to the equator, similar to the chirality observed in the ommatidia but rotated by 180° (reviewed in Clandinin and Zipursky, 2002). Experiments that affect the polarity in the eye have demonstrated that the orientation of

R1-R6 axon projections along the dorsoventral axis of the lamina is largely determined by the orientation of their cell bodies (Clandinin and Zipursky, 2000).

As more evidence is accumulating, it becomes clear that interactions between R-cell afferents are required for target specificity. The importance of direct contacts between specific growth cones was initially demonstrated in mutations for genes that transform some of the outer R-cells into either non-neural cone cells (*phyllopod*) or R7 cells (*lozenge* and *seven-up*) (Clandinin and Zipursky, 2000). Analysis of these mutants revealed that although defasciculation of R1-R6 axons does not necessarily require a full R-cell complement, R3 and R4 axons seem to play a dominant role in controling target specificity for R1, R2, R5 and R6 growth cones, whereas removal of R1 and R6 has no effect on the trajectories of R3 and R4 (Clandinin and Zipursky, 2000).

The importance of specific interactions between R-cell growth cones is further supported by the presence of cell surface receptors and adhesion molecules mediating these interactions. Two of these molecules, the receptor tyrosine phosphatase Lar and the classical cadherin, N-Cadherin (Cad-N), are involved in similar steps in R-cell targeting during the defasciculation process. Lar and Cad-N are widely expressed in all R-cell axons and also in lamina, medulla and lobula complex target neurons during pupal development. However, in both mutants, R1-R6 axons terminate correctly in the lamina, but fail to extend outward from the original bundle toward their postsynaptic partners (Clandinin et al., 2001; Lee et al., 2001). These findings suggest that Lar and Cad-N are cell-autonomously required in R-cell axons to regulate their polarity prior to their extension from the ommatidial bundle. Interestingly, Cad-N not only mediates interactions between R-cell afferents, but also between R-cell growth cones and target neurons. Close examination of animals bearing mutant lamina neurons showed that R1-R6 cells fail to extend towards columns of lamina neurons lacking Cad-N, suggesting that it may be mediating homotypic interactions between R-cell afferents and

postsynaptic units in the target cartridge (Prakash et al., 2005). Furthermore, although isoform diversity is not required for R1-R6 cell target choice (Prakash et al., 2005), a recently identified allele of *Cad-N*, *Cad-N*^{18Astop}, was shown to have a later function in R1-R6 target specificity, raising the possibility that individual isoforms may regulate distinct aspects of interactions between R-cell axons and different target cells due to differences in their expression levels (Nern et al., 2005).

Recently, the protocadherin Flamingo (Fmi) (Wu and Maniatis, 2001) was also shown to be required for R1-R6 axons to select appropriate targets in the lamina (Lee et al., 2003b). Several genetic studies have implicated Fmi in the regulation of planar cell polarity as well as dendritic patterning (Usui et al., 1999; Gao et al., 2000). In the visual system, Fmi has a dynamic expression pattern in R-cell axons and in the target as it is only expressed until early to mid pupal development (Lee et al., 2003b). *fmi* mosaic animals, similarly to *Cad-N* mosaics, do not exhibit any R-cell targeting defects during third instar larval stage. However, defasciculation of R1-R6 axons is defective, as axons extend to inappropriate targets during pupal stages, resulting in irregular cartridges containing variable numbers of presynaptic components (Lee et al., 2003b). This phenotype is not a consequence of disrupted planar polarity of R-cells in the eye, as mutations in genes, such as *frizzled* and *spiny legs*, required for the establishment of ommatidial polarity together with Fmi (Feiguin et al., 2001), do not exhibit any defects in R-cell projection pattern formation (Clandinin and Zipursky, 2000). The fact that *fmi* mutant R1-R6 growth cones acquire extensive filopodia as they grow out from the ommatidial bundle makes this a different phenotype from the one observed in *Cad-N* and *Lar* mosaic animals, in which there is no or little outgrowth. Although Fmi appears to regulate a different later step in R1-R6 target selection, synapse formation occurs normally, as suggested by the presence of output synapses in mutant R-cell axons and

lamina neurons (Lee et al., 2003b). Taken together, these data support the view that Flamingo mediates interactions between R1-R6 afferents regulating target specificity.

1.2.7 R7 and R8 Target Layer Specificity and Topographic Map Formation in the Medulla

In the adult, R7 and R8 axons from each ommatidium project through the lamina into the medulla and terminate in distinct sub-layers within the medulla neuropil. R7 axons form synapses with processes of target neurons that project in the M6 layer, whereas R8 innervate the more superficial M3 layer (Meinertzhagen and Hanson, 1993). The precise positions of individual sets of R7 and R8 axons in the medulla ensure that, as in the case of cartridges in the lamina, adjacent points in space are represented in neighboring columns, forming a topographic map of the visual environment (reviewed in Mast et al., 2005). Apart from Dock and Trio (Garrity et al., 1996; Hing et al., 1999; Newsome et al., 2000b), the two cell adhesion molecules Fmi and Cad-N have also been shown to be required for topographic map formation in the medulla. Fmi has also been proposed to facilitate competitive interactions between adjacent R8 axons to separate them from one other in an orderly fashion as soon as they enter the optic lobe (Lee et al., 2003b; Senti et al., 2003). During this stage, R8 growth cones occupy a superficial layer of the medulla (Ting et al., 2005; Shinza-Kameda et al., 2006). A few hours later, R7 axons from the same ommatidium follow this trajectory and extend past R8 growth cones to terminate in a deeper temporary layer within the medulla (Ting et al., 2005). Following the separation of the two temporary layers, during the second stage of R7 and R8 target selection (around mid-pupal development), both R7 and R8 growth cones extend further into the medulla through combined active migration and displacement by ingrowing lamina and medulla processes (Clandinin et al., 2001; Ting et al., 2005). Eventually, R7 and R8 axons reach their recipient layers and assume their adult configuration.

Recent work has identified three cell-surface proteins necessary for R7 target layer specificity: PTP69D, Lar, and Cad-N (Newsome et al., 2000a; Clandinin et al., 2001, Lee et al., 2001; Ting et al., 2005; Nern et al., 2005). When the function of *Ptp69D*, *Lar* and *Cad-N* was removed from R7 cells, their axons were found to inappropriately terminate in the R8 recipient layer in the adult. In *Cad-N* and *Lar* mosaics, R7 terminals initially reach their temporary layer, but soon after retract into the R8 recipient layer (Clandinin et al., 2001; Maurel-Zaffran et al., 2001; Ting et al., 2005). Yet again, $Cad\text{-}N^{18Astop}$ mutants exhibit a later onset phenotype in R7 targeting, raising the possibility that isoforms containing alternative exon 18A may be involved in distinct steps of R7 target layer specificity (Nern et al., 2005).

Two cell adhesion molecules have been implicated in R8 target layer specificity, Fmi and Capricious (Caps). In both mosaic animals in which the function of the genes has been selectively removed from the eye, initial target selection of R8 in the medulla appears normal. However, in the adult, R8 terminals appear highly disorganized and are frequently found either in more superficial layers than M3 or in the R7 recipient layer (Senti et al., 2003; Shinza-Kameda et al., 2006). In addition to their inhibitory role in interactions between R8 afferents, Fmi and Caps also appear to positively regulate homotypic interactions between R8 terminals and the target. In comparison with the role of Cad-N in regulating R7 target layer selection, Fmi and Caps may also regulate distinct R8 targeting decisions in the medulla through their homotypic cell adhesion properties. Although their expression pattern is somewhat less broad both spatially and temporally compared to N-Cadherin, it is found in both photoreceptor axons and cells in the target (Lee et al., 2003; Shinza-Kameda et al., 2006). It is expected that additional determinants of target layer specificity for R7 and R8 exist.

1.3 Anaplastic Lymphoma Kinase

1.3.1 Receptor Tyrosine Kinases

Receptor tyrosine kinases (RTKs) belong to a large family of receptor proteins that control many distinct functions of living cells. In the nervous system, this includes the regulation of neuronal proliferation, differentiation, and survival, as well the formation of functional neural circuits (reviewed in Wilkinson, 2001).

RTKs regulate signal transduction cascades through the phosphorylation and activation of downstream targets inside the cell. They are endowed with intrinsic protein tyrosine kinase activity, facilitating the transfer of the γ phosphate of ATP to hydroxyl groups of tyrosines on target proteins (reviewed in Schlessinger et al, 2000). RTKs are composed of three domains: an extracellular ligand-binding domain, a single hydrophobic transmembrane domain and a cytoplasmic catalytic domain. In response to binding to their ligands, RTKs dimerize and rapidly autophosphorylate. This both activates catalytic activity and generates phosphorylated tyrosine residues that mediate specific binding of cytoplasmic adaptor proteins containing, for instance, Src homology-2 (SH2) and protein tyrosine-binding (PTB) domains (Schlessinger, 2000). Serving as a platform for the recognition and recruitment of specific signaling protein complexes, the activation of RTKs has been linked to several signaling pathways, such as the mitogen activated protein kinase (MAPK), phospholipase C-γ (PLC-γ) and the phosphoinositol-3-phosphate kinase (PI-3K) pathway. The activation of signaling pathways involving these molecules leads to changes in gene expression and changes in the phenotypic state of the cell (Schlessinger et al, 2000).

1.3.2 Oncogenic Potential of RTKs

In resting untransformed cells, RPTK activity is tightly regulated by extracellular ligand stimulation. However, when RTKs are constitutively activated by point mutations, gene

amplification, or chromosomal rearrangement of the corresponding genes, these receptors develop oncogenic potential (reviewed in Blume-Jensen and Hunter, 2001). Chromosomal rearrangements often produce chimeric genes encoding novel amino-terminal sequences derived from an unrelated locus fused to the catalytic domain of the PTK. This is believed to produce conformational changes normally generated upon ligand binding, resulting in constitutive activation of the tyrosine kinase catalytic domain or abnormal intracellular localization. One shared feature of various amino-terminal fusion partners of such truncated PTKs is their ability to mediate the dimerization (or oligomerization) of the chimeric proteins in which they are found (Blume-Jensen and Hunter, 2001).

There are many well-documented cases of chromosomal rearrangements giving rise to chimeric proteins with oncogenic potential, where the transforming capacity of the proteins they encode is activated, contributing to the generation of human tumors. An example of constitutive activation of an RTK through this mechanism is seen in RET receptor. Under normal conditions, RET is activated in response to ligand stimulation by G-protein coupled receptor (GPCR) endothelin receptor B (EDNRB), regulating differentiation and survival in the enteric nervous system (Barlow et al., 2003). However, fusion of the intracellular domain of RET with the N-terminal region of activating genes capable of ligand-independent dimerization, leads to constitutive activation of the catalytic domain of the receptor in thyroid follicular cells resulting in papillary thyroid carcinomas (PTC) (Santoro et al., 2004).

1.3.3 Anaplastic lymphoma kinase (Alk)

Based on the homology of the RTK domain, mammalian Alk is a receptor tyrosine kinase of the insulin receptor subfamily with closest homology to the leukocyte

tyrosine kinase (Ltk) (Ben-Neriah and Bauskin, 1988; Krolewski and Dalla-Favera, 1991; Iwahara et al., 1997; Morris et al., 1997).

Alk has a specific expression pattern in the vertebrate nervous system, such as the thalamus, hypothalamus, midbrain, olfactory bulb, selected cranial and dorsal root ganglia and in the enteric nervous system (Iwahara et al., 1997; Morris et al., 1997). Interestingly, Alk is also expressed in the superior colliculi, which is a center for processing visual information in mice and humans (Iwahara et al., 1997; Morris et al., 1997). Although highest expression of *Alk* mRNA has been detected in the neonatal brain, its function in the developing nervous system is not known (Iwahara et al., 1997).

The molecular weight of the mouse and human Alk proteins is about 180kDa (1621 and 1619 amino acids long, respectively). Mammalian Alk contains a large extracellular domain, a hydrophobic transmembrane domain and a cytoplasmic tyrosine kinase domain. The extracellular domain of murine Alk bears a highly hydrophobic region that is likely to serve as a secretory signal sequence, a series of consensus N-linked glycosylation sites and an EGF-like cysteine-rich region that is also found in Ltk. It further contains a low-density lipoprotein a domain (LDLa) and two MAM domains (named after mephrins, A-5 protein and receptor protein tyrosine phosphatase μ) (Iwahara et al., 1997; Morris et al., 1997, Figure 7). The MAM domains are thought to mediate cell-cell interactions (Beckmann and Bork 1993). The NPXY motif within the juxtamembrane segment and several potential phosphotyrosine residues in the carboxy-terminal domain of Alk are believed to serve as binding sites for substrates with SH2 and PTB domains, such as the insulin receptor substrate (IRS-1) (van der Geer and Pawson, 1995; Morris et al., 1997; Iwahara et al., 1997). The putative kinase domain of the murine Alk possesses paired tyrosine residues characteristic of the major autophosphorylation site of the insulin receptor subfamily and shows an extraordinarily high degree of similarity with that of human Alk (98%) (Morris et al., 1994; Fujimoto et

al., 1996), murine Ltk (~70%) and IR subfamily members (~40%) (Iwahara et al., 1997; Morris et al., 1997). However, the fact that the proximal amino-terminal sequence in Alk shows no homology to any known proteins and the high degree of similarity between Alk and Ltk primary structure suggests that they form a novel subfamily of orphan RTK receptors (Figure 7).

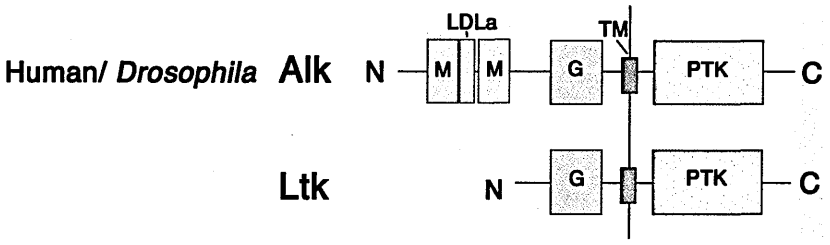

Figure 7. Molecular Structure of Alk and its Closest Homolog Ltk.
The receptor tyrosine kinase Alk contains an extracellular domain, a single transmembrane domain and a cytoplasmic catalytic domain. The extracellular domain of Alk consists of two MAM domains (M), a type a LDL receptor-repeat motif (LDLa) and a glycine-rich region (G). Ltk does not possess the MAM domains or the LDL receptor motifs, yet it contains the glycine-rich region and shows high homology (70%) in the catalytic protein kinase domain (PTK) with Alk. (TM, transmembrane domain).

1.3.3.1 Oncogenic Properties of Alk

Alk was first identified as a result of the aberrant presence of the chimeric nucleophosmin-Alk protein (NPM-Alk) in patients with a specific type of non-Hodgkin's lymphoma (Morris et al., 1994, Shiota et al., 1995). Around 80% of all Alk positive anaplastic large cell lymphomas (ALCLs) express the NPM-Alk chimeric protein in abundance, whereas 15-25% bear Alk fusion proteins with partners other than NPM (Stein et al., 2000; Pulford et al., 1999). The *NPM-Alk* fusion gene is generated by a 2;5 chromosomal translocation [t(2;5)(p23;q35)] and is believed to be the causative agent of human ALCLs. It contains the portion of the *Alk* gene in chromosome 2 encoding the entire cytoplasmic region, including the catalytic domain, fused to the 5'

end of the *NPM* gene on chromosome 5 containing the active promoter (Morris et al., 1994; Fujimoto et al., 1996). The molecular mass of the resultant chimeric protein is approximately 80kDa ($p80^{npm\text{-}alk}$) (Morris et al., 1994; Shiota et al., 1995).

NPM is a highly conserved nucleolar phosphoprotein that is ubiquitously expressed. It contains a bipartite nuclear localization signal (NLS) and shuttles between the nucleus and the cytoplasm (Michaud and Goldfarb, 1991; Borer et al., 1989). It normally undergoes self-oligomerization and it has been involved in ribosomal protein assembly and transport outside the nucleus (Chan and Chan, 1995), as well as in the regulation of centrosome duplication (Okuda et al., 2000).

Through the chromosome translocation, the NPM gene contributes an active promoter to drive the synthesis of the fusion protein in lymphoma cells resulting in oncogenic transformation (Fujimoto et al., 1996; Bischof et al., 1997; Bai et al., 1998). Presence of NPM fusion proteins has been reported in other types of myeloid leukemias where it constitutively activates proteins, such as the myeloid leukemia factor 1 (MILF1) and retinoic acid (RA) (Yoneda- Kato et al., 1996; Redner et al., 1996). Fusion proteins with NPM have nuclear/ nucleolar and cytoplasmic localization, mirroring that of normal NPM (Yoneda- Kato et al., 1996; Redner et al., 1996).

Although Alk expression is normally restricted to neural tissues, fusion with the NPM promoter following the t(2;5) translocation results in ectopic expression of chimeric NPM-Alk in T lymphocytes (Iwahara et al., 1997). The NPM portion present in the chimeric NPM-Alk protein contains the oligomerization motif that enables it to form homodimers, resulting in constitutive activation of Alk tyrosine kinase, as well as heterodimers with wild type NPM (Bischof et al., 1997; Mason et al., 1998). However, it does not contain the nuclear localization signal. Thereby, heterodimers are allowed to enter the nucleus and nucleolus, whereas homodimers remain in the cytoplasm of transformed cells (Bischof et al., 1997). This indicates that the NPM portion of the

chimeric protein is only required for the formation of kinase-active oligomers in fusion proteins. Importantly, NPM trafficking signals direct the activated catalytic PTK domain of Alk present in the chimeric protein from the cell membrane to the cytoplasm and nucleus (Iwahara et al., 1997). Cytoplasm-restricted NPM-Alk is sufficient to cause transformation (Bischof et al., 1997; Mason et al., 1998). Additionally, a variety of other oligomerization domain-containing proteins can replace NPM and the resulting Alk fusion variants are exclusively found in the cytoplasm of the transfected cells, leading to their transformation (Bischof et al., 1997; Mason et al., 1998). These findings support that the oncogenic effect of NPM-Alk in ALCL is a consequence of misexpression of Alk in lymphocytes and its constitutive activation in the inappropriate cell compartment, such as the nucleus and cytoplasm.

1.3.3.2 Mechanisms of NPM-Alk-Mediated Oncogenicity

The transforming potential of NPM-Alk leading to oncogenicity has been established by *in vitro* studies (Fujimoto et al., 1996; Bischof et al., 1997; Kuefer et al., 1997; Chiarle et al., 2003). Efforts to elucidate the mechanism through which dysregulation of proliferation in cells expressing the chimeric protein results in their transformation have revealed a putative role for PLC-γ (Bai et al., 1998). NPM-Alk and PLC-γ associate *in vivo* and NPM-Alk appears to be required for the activation of the catalytic domain of PLC-γ (Bai et al., 1998). Removal of the PLC-γ binding site abolishes the growth of NPM-Alk-transfected cells, supporting the importance of PLC-γ in mediating the growth-promoting capabilities of the chimeric Alk protein (Bai et al., 1998). NPM-Alk-mediated proliferation has also been linked to other substrates, such as Src-family kinases, and in particular $pp60^{c\text{-}src}$, STAT3 and STAT5, which are members of the signal transducer and activator of transcription proteins (STAT) signal transduction protein family (Nieborowska-Skorska et al., 2001; Zamo et al., 2002; Cussac et al., 2004).

Disrupted interaction or direct inhibition of these substrates results in decreased proliferation of NPM-Alk transfected cell lines, suggesting that they mediate NPM-Alk-induced oncogenicity.

NPM-Alk has additionally been shown to interact with the PI-3K/Akt anti-apoptotic pathway (Bai et al., 2000). NPM-Alk and PI-3K interaction is mainly mediated by the C-terminal SH2 domain of PI-3K regulatory subunit (p85). However, it has also been suggested that adaptor proteins, such as SHC, Gab2 or GrkL may function as intermediates (Bai et al., 1998; 2000). In different cell lines, blocking the activation of PI-3K prevents NPM-Alk-mediated mitogenicity (Bai et al., 2000; Slupianek et al., 2001). Interestingly, phosphorylation of the p85 subunit is comparable in both Alk positive and negative ALCL cell lines, suggesting that there might be additional PTKs capable of activating PI-3K in ALCL (Dirks et al., 2002).

Although verification of the significance of the signaling molecules mediating mitogenicity and anti-apoptotic effects in NPM-Alk-positive cell lines still remains to be demonstrated in an *in vivo* model for ALCL, the identification of activated Alk fusion proteins in ALCL has proved invaluable for the diagnosis of ALCL and also for understanding the pathogenesis of the disease that could lead to progress regarding possible therapeutic approaches (Turturro et al., 2002; Chiarle et al., 2005).

1.3.3.3. Alk Function in Vertebrates

Although there is evidence for the role of Alk in cancer, its normal function in the nervous system has not been addressed *in vivo*, however, constitutively active forms of Alk have been used in *in vitro* studies. For their generation, two approaches have been described: 1) replacement of the extracellular domain of Alk for the mouse IgG 2b Fc domain, resulting in dimerization of the protein in the absence of ligand (Souttou et al., 2001) and 2) generation of an antibody that recognizes the extracellular domain of Alk

and mimics the binding of cognate agonists (Motegi et al., 2004). Using either approach, these independent studies revealed that Alk promotes neurite outgrowth and in some cases, DNA synthesis. Use of PLC-γ, PI-3K and MAPK inhibitors in cells transfected with a constitutive active form of Alk, revealed that both mitogenic and neuritogenic properties are MAPK-dependent (Souttou et al., 2001; Motegi et al., 2004).

1.3.3.4 Potential Ligands for Alk: Pleiotrophin and Midkine

The presence of an EGF receptor motif in the extracellular domain of Alk initially suggested that the protein may activate itself through dimerization caused by direct receptor-receptor interactions (Ogiso et al., 2002). However, two heparin-binding factors, pleiotrophin (PTN) and midkine (MK) have been proposed to act as possible ligands for Alk in humans. (Stoica et al., 2001; Stoica et al., 2002). PTN and MK share 50% amino acid homology (Muramatsu et al., 2002) and have similar three-dimensional structures (Iwasaki et al., 1997). MK and PTN promote neurite outgrowth and nerve cell migration, and have been proposed to play a neuroprotective and an angiogenic role (reviewed in Kadomatsu and Muramatsu, 2004). In mice and rats, PTN is expressed in the developing nervous system, in the thalamus, midbrain, as well as in the mesoderm of rat. The distribution of PTN in the nervous system is similar to that of Alk, with strong expression during fetal development but decreasing in the adult (Silos-Santiago et al., 1996). PTN is also expressed in the CA1 region of the rat hippocampus, and appears to be involved in LTP induction (Amet et al., 2001). MK is a retinoic acid responsive heparan-sulphate proteoglycan. Its expression in the embryo starts earlier than PTN and is restricted to the ventral part of the ventricular zone whereas PTN covers the dorsal half (Fan et al., 2000). It shows strong expression during mid-gestation and, similarly to PTN, is down regulated at birth (O'Brien et al., 1996).

PTN and MK were identified as possible ligands for the receptor Alk using receptor binding assays (Stoica et al., 2001; Stoica et al., 2002). Furthermore, PTN- and MK-induced activation of Alk results in phosphorylation of the adaptor molecules IRS-1 and Shc and subsequently the phosphorylation of PLC-γ, PI-3K and ERK (Stoica et al., 2001; Stoica et al., 2002). Further *in vitro* analysis demonstrated that PTN promotes mitogenesis requiring both PI-3K and MAPK pathways. However, PTN-induced survival appears to be mediated specifically through the MAPK pathway (Bowden et al., 2002).

Apart from activating Alk, PTN and MK may also activate additional receptors, such as the receptor protein tyrosine phosphatase β/ζ (RPTPβ/ζ) (Maeda and Noda, 1998) and the LDL receptor-related protein (LRP) (Muramatsu et al., 2000). Although their identification as possible ligands for Alk revealed some of the downstream effectors of Alk signaling, their role has not been yet demonstrated *in vivo*. Concomitant with this, the normal function of Alk in the nervous system is not known. Although it has been suggested that Alk may be involved in angiogenesis (Stoica et al., 2001), it remains to be verified whether PTN mediates its angiogenic effects through Alk or by its other receptor proteins.

1.3.4 *Drosophila* Alk and its Activating Ligand Jelly belly

Evidence for the normal *in vivo* function of Alk derives from its *Drosophila* homolog, which has been identified by Ruth Palmer and colleagues using degenerate PCR (Loren et al., 2001). The *Alk* locus was mapped to region 53 on the second chromosome and comprises eight exons encoding a 200kDa RTK protein. The kinase domain of *Drosophila* Alk shares 85% homology with human Alk (hAlk) and contains several sequence motifs conserved among PTKs (Loren et al., 2001).

The recently identified activating ligand for *Drosophila* Alk, Jelly belly (Jeb) was identified in a screen for genes whose transcription is regulated by the homeodomain protein Tinman (Tin) (Weiss et al., 2001). Tin, a member of the NK family of homeodomain proteins, plays an important role in the development of the embryonic heart and visceral mesoderm (Azpiazu and Frasch, 1993). The *jeb* locus is mapped to 48E9 of the right arm of the second chromosome and consists of two exons and one large intron (Weiss et al., 2001). The predicted Jeb protein contains a secretory signal peptide and an LDL receptor repeat motif, which seems to be similar to the same motifs of two vertebrate proteins, Sco-spondin and enterokinase (Weiss et al., 2001; Figure 8). *jeb* function seems to be partially regulated by alternative splicing. Three isoforms have been characterized, with two found in the early embryo and a larger third variant found later in embryogenesis (Weiss et al., 2001).

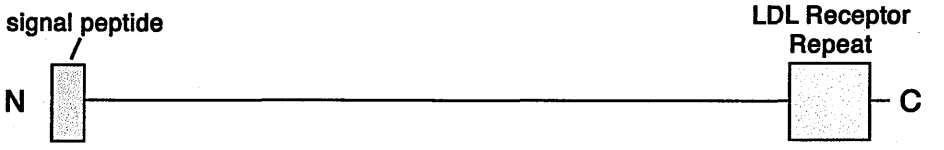

Figure 8. Jeb Structure.
The predicted protein is approximately 560 amino acids long. The first 20 amino acids are hydrophobic and contain a secretory signal (signal peptide), whereas a type A LDL Receptor repeat is located in the carboxy-terminal region.

Binding assays and epistasis analysis demonstrated that Jeb binds to Alk and that it acts as the activating ligand for this orphan receptor in the visceral mesoderm (Lee et al., 2003; Englund et al. 2003). In fact, the PTK activity of Alk is not only required for the binding and signal transduction response to Jeb, but also for the uptake of Jeb into the cells and the subsequent degradation of the ligand-receptor complex in the visceral mesoderm (Englund et al., 2003).

1.3.4.1 Development of Visceral Musculature in *Drosophila*

The visceral musculature in *Drosophila* arises through the fusion of multiple myoblasts, so that each muscle consists of two different myoblast cell types: one muscle founder cell, giving each future muscle its unique identity, and several fusion competent myoblasts (FCMs) (reviewed in Dworak and Sink, 2002). Hh, Dpp and Tin induce visceral mesoderm by activating the expression of two transcription factors Bagpipe (Bap) and Biniou (Bin) (Azpiazu et al., 1996). The combined actions of these signals generate segmental clusters of visceral mesoderm precursors in the dorsal mesoderm. During germband retraction (embryonic stage 12), FCMs are assembled into clusters while founder cells are at pre-defined positions along the epidermis. Soon after, FCMs migrate and fuse with the founder cells (stage 13). Following fusion, the newly formed myotubules contact the epidermis attachment sites and subsequently spread out dorsally and ventrally to encircle the entire gut (Dworak and Sink, 2002). The cell adhesion molecule Dumbfounded (Duf) (also known as Kirre) is expressed across the membrane of muscle founder cells before fusion with FCMs takes place and is downregulated at its completion (Ruiz-Gomez et al., 2000; Strünkelnberg et al., 2001). Duf mediates this by recognizing an Ig transmembrane protein named Sticks and Stones (Sns), present on migrating FCMs (Bour et al., 2000). Sns and Duf/Kirre or its paralog Irregular ChiasmC-roughest (IrreC-rst) mediate in *trans* heterotypic cell adhesive interactions between these two types of cells (Strünkelnberg et al., 2001; Galletta et al., 2004). This engagement is required for the translocation of the multidomain protein Rolling pebbles (Rols) from the cytoplasm to the Duf sites, anchored to its intracellular domain through ankyrin repeats. Translocation of Rols to the fusion sites is then sufficient to initiate the first round of fusion and through positive feedback it enables more rounds to follow (Menon et al., 2005).

1.3.4.2 Expression of Alk and Jeb in the Visceral Mesoderm

In contrast to nervous system-restricted expression in vertebrates, *Drosophila* Alk is also expressed in the visceral mesoderm during embryonic development. Alk protein is first detected at germband extension (stage 10 of embryonic development) in two Alk-positive cell groups per segment in the metameric clusters, before the fusion of the visceral mesoderm precursors from each segment (Loren et al., 2001). During the germband retraction stage, the clusters fuse into a continuous band. At the end of germband retraction, Alk is expressed in muscle founder cells forming a broad waved band of visceral mesoderm (Figure 9). Interestingly, from stage 13 of embryonic development onwards, Alk is expressed within the developing brain and ventral nerve cord, where it persists through larval stages (Loren et al., 2001).

jeb mRNA is first detected at stage 8 in somatic mesoderm precursors, and subsequently in two roughly parallel continuous bands in the ventral mesoderm, in somatic precursor cells, as well as in dorsally located Alk-expressing muscle founder cells (Weiss et al., 2001). As there is clear co-localization of Alk and Jeb at the sites of contact between these cells, it seems that *jeb* is transcribed in the somatic mesoderm cells, and then secreted and specifically taken up by the visceral mesoderm cells through Alk (Englund et al., 2003; Figure 9). Additional evidence for Jeb secretion has come from the observation that it is detected more abundantly in culture medium than inside the Jeb-producing cells (Weiss et al., 2001). The punctate pattern of Jeb in the receiving cells is suggestive of receptor-mediated endocytosis as a mechanism for Jeb accumulation in visceral mesoderm cells. This was verified with the use of a temperature-sensitive allele of *shibire* encoding a dynamin-related GTPase required for microtubule-mediated endocytosis. It revealed that *shibire*-mediated endocytosis is required for Jeb to accumulate in the visceral mesoderm (Weiss et al, 2001).

1.3.4.3 Alk and Jeb Function in *Drosophila*

Alk and *jeb* homozygous mutant embryos lack a functional midgut, cannot ingest food and die during the 1st instar larval stage (Englund et al., 2003; Loren et al., 2003). The onset of *Alk* and *Jeb* mutant phenotypes is at stage 11 of embryonic development, highlighted by the absence of organized columns of muscle founder cells. Myocyte enhancer factor 2 (Mef2), produced in all muscle lineages of the *Drosophila* embryo, and the anti-myosin-heavy-chain (MHC), normally expressed in the thin layer of gut mesoderm, are both absent from *Alk* and *Jeb* homozygous mutant animals (Englund et al., 2003). Moreover, the immunoglobulin-domain adhesion molecule Fasciclin III (FasIII), which is a marker for differentiated visceral mesoderm, and Duf, normally expressed in the muscle founder cells regulating the muscle fusion process (Ruiz-Gomez et al., 2000), are both absent from the visceral mesoderm of *Alk* and *jeb* mutants (Englund et al. 2003). Similarly, the *Drosophila* homolog of the T-box transcription factor 1 (TBX1), org-1, that is initially expressed in all visceral mesoderm precursors prior to being restricted to founder cells, is absent from *jeb* mutants (Lee et al., 2003). Expression of activated Alk in *jeb* homozygous mutant background is able to rescue the expression of these markers and restore midgut morphogenesis, thereby confirming that Jeb is the activating ligand for the receptor Alk (Lee et al., 2003).

Localized activation of the Ras/MAPK pathway in somatic muscle lineage is required for muscle founder cell specification. ERK activation is specifically observed in muscle founder cells and not in FCMs (Gabay et al., 1997). In the absence of Alk signaling, muscle progenitors fail to differentiate into visceral mesoderm precursors (Lee et al., 2003). In *Alk* and *jeb* mutants, diphospho-ERK is absent from the visceral precursors, suggesting that the secreted molecule Jeb and the receptor Alk are critical for ERK activation in the muscle founder cells (Englund et al., 2003). Furthermore, Jeb inhibits the expression of the immunoglobulin protein Sticks and Stones (Sns) (Lee et

al., 2003), required for somatic muscle determination (Bour et al., 2000), thereby further supporting the role of Jeb as a positive regulator of visceral musculature cell fate. Somatic muscle patterning is normal in both *Alk* and *Jeb* mutant animals (Loren et al., 2003; Englund et al., 2003; Lee et al., 2003). Taken together, these data suggest that Alk and its activating ligand Jeb are required for visceral mesoderm development through a mechanism that involves the MAPK pathway (Figure 9).

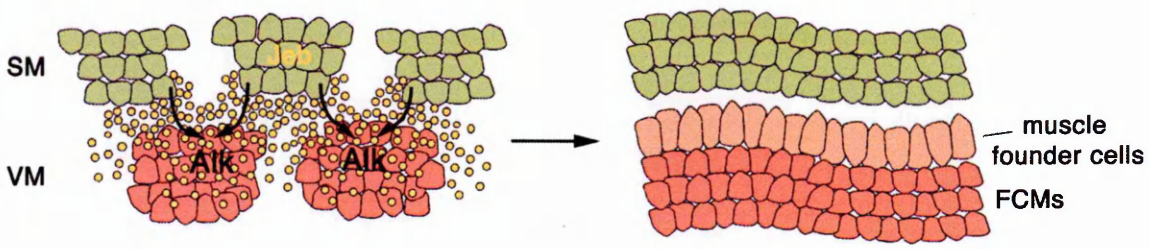

Figure 9. *Alk* and *jeb* are Required for Visceral Mesoderm Development.
Jeb, produced by somatic mesoderm cells (SM), is secreted and uptaken by visceral mesoderm precursors (VM) expressing Alk (red). This leads to the activation of the receptor Alk, which induces the differentiation of muscle founder cells (orange) and fusion competent myoblasts (FCMs) (red). Adapted from Freeman and Doe, 2001 and Freeman, 2003.

Many interesting questions arise from these findings. These include the identification of downstream effectors of Alk signaling or possible alternative ligands for Alk regulating differentiation in the visceral mesoderm of *Drosophila*. Additionally, as Alk is expressed in both vertebrate and nervous system in *Drosophila*, it raises the possibility that this orphan tyrosine kinase receptor is required for the development and normal function of the nervous system through activation by Jeb or another ligand.

1.4 Aims of the work presented in this thesis

Guidance of neuronal axons occurs in a step-wise fashion, and in the visual system of *Drosophila* R-cell axons projecting into the target optic lobe encounter glia and neurons along their trajectory. R-cells and their axons are easily visualized and genetically manipulated, and therefore provide a favorable system to study how target specificity is accomplished. A number of genetic screens have focused on factors required autonomously on R-cells for correct targeting in the synaptic layers of the optic lobe, and have demonstrated that epithelial and marginal glia in the lamina play an active role for the R1-R6 target layer specificity during initial target selection (Poeck et al., 2001). Until recently, it was not possible to systematically address the role of target-required factors in the regulation of R-cell projection pattern formation.

In the first part of my thesis, I focused on addressing which cues are provided by epithelial and marginal glia as well as by target neurons to R-cell axons during initial target selection, and the molecular mechanisms regulating the differentiation and migration of these target cells. To achieve this task, the lab established the ELF system (*ey-Gal80; lama-Gal4; UAS-FLP* system) (Chotard et al., 2005). Using this system, I participated in an FLP-FRT system-based genetic screen, from which we expected to isolate genes regulating initial target selection in the visual system of *Drosophila.*

In the second part of my project, I focused on elucidating the role of Alk and its activating ligand Jeb in the developing visual system of *Drosophila.* To address this, I determined their expression pattern during late larval and pupal development and used mosaic analysis by removing their function specifically from the areas they are expressed in.

2. Materials and Methods

2.1 Genetics

The genotypes of the flies used for this thesis are described in table 1. All flies were raised at room temperature (25°C) on standard cornmeal/agar food.

Genotypes	Source/Reference
wild type Oregon R	Lab Stock
y w^{1118}	Lab Stock
y w; Cyo/ Gla Bc	Lab Stock
w; FRT40A	Lab Stock
w; FRT42D	Lab Stock
w; FRT42D $Alk^{1/8/9}$/ Gla Bc	Ruth H. Palmer (Loren et al., 2003)
w; FRT42D $jeb^{l(2)SH0422}$/ Gla Bc	(P{lacW} l(2) $SH0422^{SH0422}$), Steven X. Hou (Oh et al., 2003)
w; FRT42D jeb^{weli}/ Gla Bc	Anne Holz (Stute et al., 2004)
PKA-C1 [H2]/ Cyo	Bloomington Drosophila Stock Center
ey-FLP; FRT42D PCNA/ Cyo Kr-GFP	eyeless enhancer provided by Barry Dickson (Newsome et al., 2000a) – lab Stock
$ey^{3.5kb}$-FLP; FRT42D cycE/ Cyo Kr-GFP	Lab Stock
y w ey-Gal80; Ub-GFP cycE FRT40A/ Cyo; lama Gal4 UAS FLP mδ	(ELF, 2L), lab Stock
y w ey-Gal80; FRT42D UbGFP PCNA/ Cyo; lama Gal4 UAS FLP mδ	(ELF, 2R stock), lab Stock (Chotard et al., 2005)
$elav^{C155}$ Gal4 UAS-cd8GFP hs-FLP^{122}; FRT42D tubP-Gal80/ Cyo Kr-GFP	Tom Clandinin (Lee et al., 2003b)
w; Rh1-lacZ	Lab Stock
w; Rh4-lacZ	Lab Stock
hs-FLP; cn bw/ Cyo; Rh6-lacZ/ TM2	Frank Pichaud (Cook et al., 2003)
w; ato-τ-myc/ Tm6B	DNA provided by Barry Dickson (Senti et al., 2003)
w; FRT42D ALK^{1}/ Gla Bc; Rh1-lacZ/ Tm6B	Lab Stock

w; FRT42D ALK^{1}/ Gla Bc; Rh4-lacZ/ Tm6B	Lab Stock
w; FRT42D ALK^{1}/ Gla Bc; Rh6-lacZ/ Tm6B	Lab Stock
w; FRT42D ALK^{1}/ Gla Bc; ato-τ-myc	Lab Stock
w; FRT42D jeb$^{l(2)SH0422}$/ Gla Bc; Rh4-lacZ/ Tm6B	Lab Stock
w; FRT42D jeb$^{l(2)SH0422}$/ Gla Bc; Rh6-lacZ/ Tm6B	Lab Stock

Table 1. Fly Stocks.

2.2 Histology

2.2.1 Staging and Dissection of Pupae

White pupae were placed in grapefruit agar plates and staged at 17, 24, 40, 43, 50, 55, 60 and 75 hours at 25°C. Pupation in *Drosophila* lasts approximately 100 hours at 25°C. Instead of using adult flies, in all experiments pupae were dissected just before hatching (~95-100 hours). Following staging, pupae were collected and placed on double-sticky tape to confer stability during dissection. Initially, the cap of the pupal case was removed, and then by cutting from anterior to posterior, the pupal case was opened up to reveal the pupa inside. Heads of pupae were placed into a drop of phosphate buffer saline solution (PBS) and the brains were dissected out.

2.2.2 Immunohistochemistry

3rd instar larval or pupal brains were dissected in PBS and fixed in PLP buffer {8% paraformaldehyde (PFA) and L-lysine-HCl, $Na_2HPO_4{\cdot}7H_20$, phosphate buffer (PB)} for one hour at room temperature. They were then washed three times in PBT (PBS and 0.5% Triton X-100) for 15 minutes. Brains were pre-incubated in solution consisting of 10% normal goat serum (NGS) (SIGMA) and 90% PBT and then incubated in primary antibodies at 4°C overnight on a shaker. Primary antibodies are shown in Table 2. All

antibodies were diluted in 90% PBT- 10% NGS. After 15 minute washes in PBT, brains were incubated in secondary antibodies for 2 1/2 hours at room temperature.

Primary Antibodies	Dilution	Origin
Mouse mAb24B10	1:75	DSHB (Zipursky et al., 1984)
Mouse anti-Highwire	1:10	DSHB (Wan et al., 2000)
Guinea pig anti-Alk	1:1,000	Ruth Palmer (Englund et al., 2003)
Guinea pig anti-Jeb	1:5,000	Ruth Palmer (Englund et al., 2003)
Guinea pig anti-Senseless	1:1,000	Hugo Bellen (Nolo et al., 2000)
Rabbit activated anti-Caspase	1:75	Cell Signalling Technology
Mouse anti-Dachshund	1:25	DSHB (Mardon et al., 1994)
Rat anti-Elav	1:12	DSHB (O'Neil et al., 1994)
Rabbit anti-Repo	1:500	(Halter et al., 1995)
Rabbit anti-βGal	1:120,000	Cappel
Rat anti-DN-Cadherin	1:10	DSHB (Iwai et al., 1997)
Mouse anti-Flamingo	1:20	DSHB (Usui et al., 1999)
Rabbit anti-Myc	1:500	Santa Cruz Laboratories

Table 2. Primary Antibodies.

HRP-conjugated goat anti-mouse (1:200 BioRad) secondary antibody was developed with 3-3' diaminobenzidine (DAB)/ H_2O_2. The rest of the secondary antibodies used for immunofluorescence are shown in Table 3.

Secondary Antibodies	Fragments	Dilution	Origin
Cy3-conjugated anti-mouse	$F(ab)_2$'	1:400	Jackson Immunoresearch Laboratories
Cy3-conjugated anti-rat	$F(ab)_2$'	1:400	Jackson Immunoresearch Laboratories
FITC-conjugated anti-guinea pig	$F(ab)_2$'	1:200	Jackson Immunoresearch Laboratories
Cy5-conjugated anti-rabbit	$F(ab)_2$'	1:200	Jackson Immunoresearch Laboratories
Cy5-conjugated anti-guinea pig	$F(ab)_2$'	1:200	Jackson Immunoresearch Laboratories

Table 3. Secondary Antibodies.

For immuno-fluorescence staining, brains were washed twice in PBT and twice in PBS before embedding in Vectashield (Vector labs). DAB stained samples were embedded in 70% glycerol/30% PBS solution.

Brains stained with fluorescent dyes were oriented and mounted using a GFP microscope (LEICA MZFLIII) and images were visualized using a laser-scanning confocal microscope (BioRad/ Zeiss Radiance 2100). For electron microscopy, samples were prepared as described by Salecker and Boeckh (1995).

2.2.3 DiI Injections

DiI crystals (Molecular Probes) were crushed between two glass slides, and stored covered with aluminium foil at 4°C. White pupae were picked and placed in grapefruit/agar plates at 25°C and staged. 43 hours later, the brains were dissected in PBS and fixed in 4% PFA (Polysciences, Inc) (diluted in 0.1M PB) for 2 days at 4°C. After fixation, the brains were placed into a drop of PBS and pulled towards the end of the drop. 5 very small crystals were picked with the help of a micromanipulator and

positioned at the border between the pigmented and unpigmented pupal retina. The samples were stored in plenty of PBS and the DiI was left to diffuse overnight at 4°C. DiI-labeled axons were visualized under a GFP microscope (LEICA MZFLIII) and images of the individual labeled ommatidia and their underlying cartridges were taken using a laser scanning confocal microscope.

2.3 Molecular Biology

2.3.1 Genomic DNA Extraction

20 flies of control and mutant genotypes were anaesthetized, collected and frozen at -80°C for 5 minutes. They were then homogenized in 200 µl of Grind Buffer (11.6 ml 0.5 M EDTA, 1.6 ml 5.0M NaCl, 2.4 ml 1.0M Tris-HCl pH=8.0, 1.0 ml 1.0M Tris-Base pH=9.2, 2.5 ml 20% SDS, 59.9 ml sterile H_2O, 20 ml 1.0M sucrose), with 6.5 µl sterile H_2O/ EtOH (1:5). Using the Grind Buffer, the mixture was diluted to a 400 µl final volume and was incubated at 65°C for 30 minutes. 1/5 of volume of 5.0M KAc was added. Samples were incubated on ice for 15 minutes and were spun at 13,000 rpm for 15 minutes. The supernatant containing genomic DNA was removed and purified by phenol/chloroform extraction. The samples were spun at 13,000 rpm for 10 minutes and the upper phase containing genomic DNA was removed. 1:1 volume of chloroform was then added and the mixture was spun at 13,000 rpm for another 10 minutes. The supernatant was carefully removed and the sample was washed with 1 ml of 70% EtOH. Following a 10-minute spin at 13,000 rpm the supernatant was discarded and the pellet was left to dry at room temperature. Finally, the pellet was resuspended in 150 µl of sterile water. To determine the genomic DNA concentration, 1 µl from each sample was used for spectrophotometric analysis.

2.3.2 Amplification of *PKA-C1* Coding Region for DNA Sequencing

To sequence the fragment of interest, genomic DNA was prepared from adult flies heterozygous for the *PKA-C1* allele (*2-26*) over the *Gla Bc* balancer. The *PKA-C1* gene was amplified in three different PCR reactions that together covered the entire *PKA-C1* coding region. Primers 1 and 3 were forward, and primers 2 and 4 were reverse.

Primer 1: 5'-GACGATCAGGCCCAAGTGTC-3'

Primer 2: 3'-GGAGTTCCACTGCCTGAAGC-5'

Primer 3: 5'-TCGAGTACCTGCACTACTTG-3'

Primer 4: 3'-CGCAGTAGCGGATACAATTG-5'

Genomic DNA (50 ng) was amplified by PCR using different sets of primers in a total volume of 50 µl of buffer solution containing 10mM dNTP mixture, 15mM $MgCl_2$, 0.75 units of high fidelity *Taq* DNA polymerase (Roche). Each reaction was performed for 1 minute under the following conditions: 94°C for denaturation, 55°C for annealing and 72°C for elongation. The PCR products were analysed by electrophoresis on 1% agarose gels, and stained with ethidium bromide.

2.3.3 Modifying *ey-FLP* to Generate Mosaic Clones in the Eye Disc

The cDNA of the FLP recombinase together with a *heat shock protein* (*hsp*) trailer was excised from the pBD 924-7 vector (kindly provided by Barry Dickson; Newsome et al., 2000a) and was cloned into a pCaSpeR4 vector at the sites of Asp718 and EcoRI. Subsequently, an *eyeless*$^{3.5kb}$ enhancer fragment containing the *hs* minimal promoter was isolated from the ey-tTA vector (kindly provided by Bruno Bello; Bello et al., 1998), using XbaI and Asp718 enzymes (Roche), and was incorporated into the FLP-containing pCaSpeR4 vector (Figure 10). The *ey* $^{3.5kb}$*-FLP* transgene-containing vector (final concentration 500 ng/µl) as well as the transposase DNA (turbo Δ2-3) (kindly provided by J.P. Vincent) were diluted in PBSA and distilled H_2O. This mixture

was injected in *y* w^{1118} hosts by P-element-mediated transformation using standard methods (Roberts, 1998).

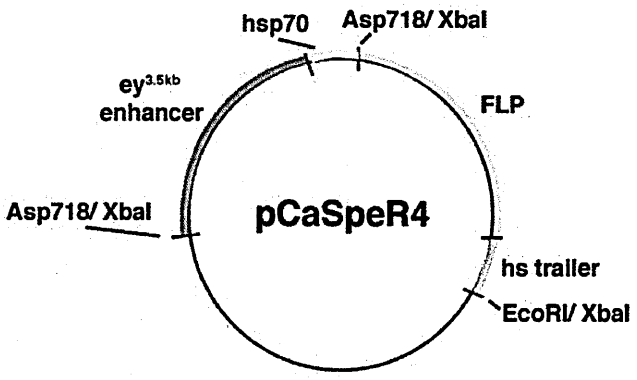

Figure 10. Construct for *ey*$^{3.5}$- *FLP*.

2.3.4 Inverse PCR for Sequencing the *jeb*$^{l(2)SH0422}$ Allele

Following genomic DNA extraction from the line P{lacW} l(2) SH0422^{SH0422}, 10 µl of the gDNA was digested with the enzyme HinPI at 37°C for 2.5 hours in a mix containing RNase A (100 µg/ml) and buffer A (Roche). The digestion mix was then heated at 65°C for 20 minutes for inactivation of the enzyme. 10 µl of the digested DNA was subjected to ligation at 4°C overnight in a final volume of 400 µl with 1600 U of T4 DNA ligase (NUB) and the respective buffer (Promega). Subsequently, 40 µl of 3M NaAc and 1 ml of 100% EtOH were added to the ligation mix and the solution was left on ice for 15 minutes. Following a 20 minute centrifugation at 13,000 rpm, the supernatant was removed and the pellet was washed with 1 ml of 100% EtOH. A second centrifugation of 15 minutes at 10,000 rpm followed and the supernatant was discarded. The pellet was left to air-dry at room temperature for 10 minutes and was then resuspended in 150 µl of sterile water.

The ligated genomic DNA was used as a matrix in the following PCR reaction. The primers used were chosen to match the sequence at the 5' and 3' end of the P-element flanking region:

Primer 1 (Plac4): 5'-ACT GTG CGT TAG GTC CTG TTC ATT GTT-3'

Primer 2 (Plac1): 5'-CAC CCA AGG CTC TGC TCC CAC AAT-3'

The PCR mix contained 10 µl of ligated gDNA, 1 µl of 10mM dNTPs, 1.2 µl of Primer 1, 1 µl of Primer 2, 0.8 µl of Taq polymerase 3.5U/µl and the respective buffer (Roche, Expand High Fidelity PCR system) in a final volume of 50 µl. The reaction was performed as followed: first denaturation step at 94°C for 1 minute, then 30 cycles with 15 seconds at 94°C for denaturation, 2 minutes at 60°C for annealing and 2 minutes at 72°C for degradation. The last cycle includes 15 seconds of denaturation at 94°C, 2 minutes of annealing at 60°C and 7 minutes for elongation at 72°C, which terminates the reaction. The corresponding PCR product was purified using the QIAquick PCR purification kit (QIAGEN), then analysed by electrophoresis on 1% agarose gel and stained with ethidium bromide. The PCR product was sequenced using the primer: (Spi, PlacW): 5'-ACA CAA CCT TTC CTC TCA ACA A-3'

3. Genetic Screen for Target Area-Required Factors Regulating Axon Guidance in the Visual System of *Drosophila*

3.1 The ELF System

In the developing visual system of *Drosophila* around late 3rd instar larval stage, R-cell axons project into the optic lobe and terminate in their respective temporary layers. R1-R6 axons terminate in the lamina inbetween the epithelial and marginal glia, whereas R7 and R8 axons project through the lamina and terminate in the medulla. Along their trajectory in the target, R-cell axons encounter neurons and glia. Epithelial and marginal glia have been shown to play the role of intermediate targets for R1-R6 axons and provide them with a stop signal at the lamina (Poeck et al., 2001), whereas other types of glia, such as medulla neuropil glia, form boundaries between the medulla and the lobula complex, preventing the intermingling of cell populations between the two (Tayler et al., 2004; Fan et al., 2005). To address the role of target glia in the regulation of R-cell projection pattern formation as well as to study the molecular mechanisms required for their formation and migration to their characteristic positions, the lab established an FLP/FRT system-based genetic approach, called the ELF (*yw ey-Gal80; Ub-GFP cycE FRT40A/ FRT40A; lama-Gal4 UAS-FLP mδ/ +)* system.

The *lamina ancestor* (*lama*) gene was identified in a screen for genes expressed in the R-cell axon target field using P-element enhancer trap lines (Perez and Steller, 1996b). *lama-lacZ* is expressed in precursors of lamina glia from the 1st instar larval stage, whereas in precursors of lamina neurons the onset of expression coincides with the innervation of the target by R-cell axons. For our purposes, the *lacZ* P element (Perez and Steller, 1996b) was replaced by a *Gal4* enhancer trap line inserted in the *lama* locus (Chotard et al., 2005). The *lama-Gal4* enhancer is expressed in the optic lobe from first instar larval stage onwards. During the 3rd instar larval stage, its activity is detected in the target, as well as in some differentiated R-cells and in wing imaginal

discs (Chotard et al., 2005). By recombining the *lama-Gal4* driver with a *UAS-FLP* transgene and an *FRT40A* chromosome carrying the clonal marker green fluorescent protein (GFP) under the control of a Ubiquitin (Ub) promoter, somatic clones visualized by the absence of GFP were generated in the target as well as in the eye imaginal disc. To increase the size of the somatic clones, a cell lethal mutation (*cyclin E)* was also recombined to the *FRT40A* chromosome (Figures 11A-C). Mitotic recombination events in the eye were specifically suppressed using the transgene expressing the Gal4 antagonist, *Gal80* (Lee and Luo, 1999), under the control of a 3.5kb eye-specific enhancer element from the *eyeless* (*ey*) gene (Bello et al., 1998; Chotard et al., 2005). In the presence of this *ey-Gal80* transgene, clone formation in the eye is suppressed, whereas clone formation in the optic lobe is not affected (Figures 11E-G). In the case of mutant *FRT* chromosomes, this system allows the generation of mosaic animals, in which wild type heterozygous R-cell axons innervate a target area containing large homozygous mutant clones of glial cells, lamina and medulla neurons, and their precursors (Chotard et al., 2005). In the optic lobe, large clones of marginal and medulla glia can consistently be made homozygous mutant (80%), whereas the frequency of recombination events in target neurons in the lamina and medulla is more variable (Figures 11E-G).

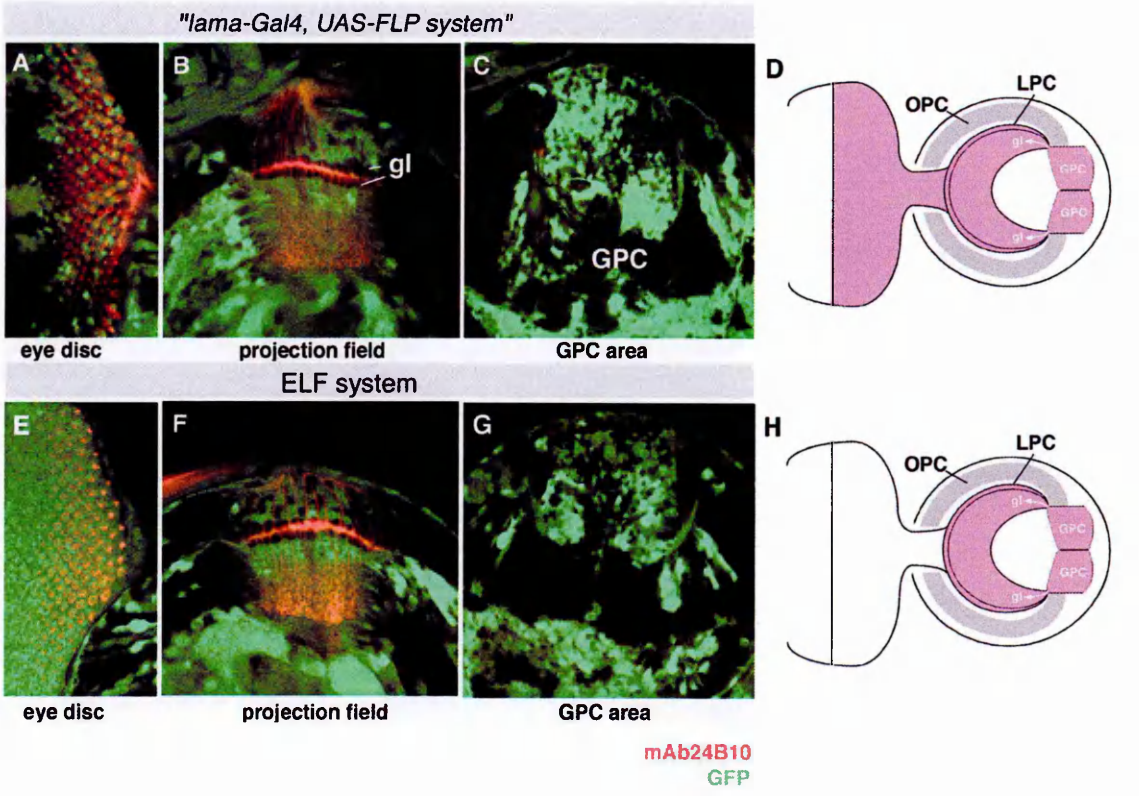

Figure 11. Genetic Tools to Create Mosaic Clones in the Target Area.
(A, B, C) Genotype: *yw; Ub-GFP cycE FRT40A/ FRT40A; lama-Gal4 UAS-FLP mδ/+.*
Large somatic clones are generated in glial cells and lamina target neurons in the projection field and the glial precursor cell (GPC) area. Some clones are also induced in the eye imaginal disc. Somatic clones are visualized by the absence of GFP. (D) Scheme highlighting the areas of mitotic recombination in the *"lama-Gal4 UAS-FLP"* system.
(E, F, G) Genotype: *yw ey-Gal80; Ub-GFP cycE FRT40A/ FRT40A; lama-Gal4 UAS-FLP mδ/+.*
Large somatic clones are restricted to the projection field in both lamina neurons and glia, as well as in the GPC area. (H) Scheme highlighting the areas of mitotic recombination in the ELF system. From Chotard et al., 2005.

3.2 Screen on the Left Arm of the Second Chromosome

With the use of the ELF system I participated in a genetic screen for the left arm of the second chromosome (2L). This work was conducted as a collaborative effort in the whole laboratory with C. Chotard, W. Leung and I. Salecker.

Male flies containing *FRT* recombination sites on the left arm of the second chromosome were treated with ethane methane sulphonate (EMS) and crossed en masse to females carrying a double balanced chromosome (*Gla Bc/ Cyo hs-hid*). The *Cyo*

balancer chromosome contained a *hs-hid* transgene, driving the expression of the proapoptotic gene (*head involution defective; hid)* (White et al., 1994) under the control of a heat-shock promoter. Heat-shock of early 3rd instar larvae for 1 hour at 37° allowed us to establish stocks that carried only one balancer chromosome (*Gla Bc*). We recovered 2,279 individual balanced *FRT* lines carrying lethal mutations. Only lethal lines were tested, whereas viable lines were not kept. This was done for two reasons. Firstly, most axon guidance molecules isolated from screens in *Drosophila* are lethal. Secondly, at the next step of the screen involving mapping genes of our mutant candidates, it would not be possible to subject viable lines to complementation tests with known deficiencies, thus making their identification more difficult. Lethal lines were crossed with the *"lama-Gal4 UAS-FLP* system", driving recombination in both R-cells and target area. Using this system in the first round of the screen, we isolated genes required in the target and in the eye. 3rd instar larval eye-brain complexes were dissected and labeled with the R-cell specific marker mAb24B10 to assess the R-cell projection pattern. 1,739 mutant lines did not show any defects in the assembly of R-cells in the eye imaginal disc or in the R-cell projection pattern in the target, suggesting that the function of the genes involved is not required in either during 3rd instar larval stage. However, 509 mutant lines showed strong projection defects in the target area. Most of them (n= 429) also displayed a "rough" eye phenotype, i.e., disorganized patterns of assembling R-cell clusters in the developing eye disc. The remaining candidates (n= 80) had normal eye phenotypes. To distinguish between projection defects that arise as a consequence of gene requirement in the target or in R-cells, we re-tested these lines with the ELF system. *3rd* instar larva eye-brain complexes were processed as before and the R-cell projection pattern was assessed using mAb24B10 labeling. In the final step, 50 mutant lines were identified with strong projection pattern defects (Figure 12).

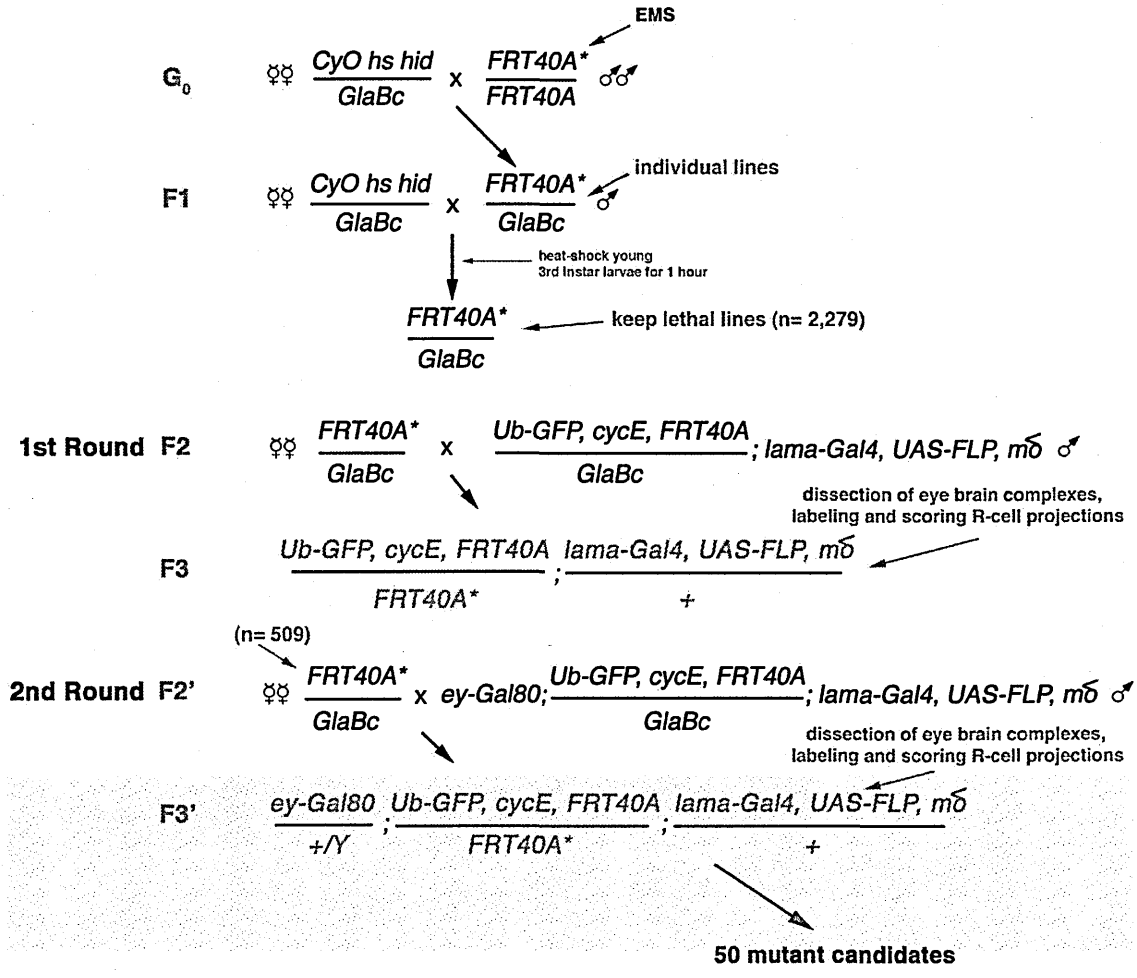

Figure 12. Screen Scheme.

Flies containing FRT recombination sites on the left arm of the second chromosome were treated with EMS. 2,279 individual lines carrying lethal mutations were recovered and tested with the "*lama-Gal4 UAS-FLP* system" in the first round. Eye-brain complexes were dissected, and labelled with the R-cell specific marker mAb24B10. Mutant lines with R-cell projection defects (n=509) included some that affected genes required only in the target and some required in both target and eye. These were further analyzed with the ELF system in the second round to distinguish between eye and target area-required genes. In this step 50 mutant candidates were obtained with requirement exclusively in the target. Full genotypes are shown.

3.2.1 Mutant Candidates

Due to the design of our screen, we expect to isolate mutants in which genes encoding regulators of proliferation and differentiation or migration of glial cells have been affected. The fact that, in addition to glial cells, recombination events also occur in target neurons raises the possibility that some mutations lie in genes required for the

differentiation or proliferation of neurons. Candidate genes regulating cell cycle or migration can be recognized by the presence or absence of GFP-negative clones in the projection field or in the GPC area. In the cases where the above processes are normal, the remaining mutants are expected to yield axon guidance molecules, such as diffusible proteins and cell adhesion molecules.

The mutant candidates isolated from our screen have been placed into four general categories according to their phenotype. In some cases photoreceptor axons formed thick bundles ("bundling" phenotype, Figure 13B). One possibility for such a phenotype could be that the gene causing such a phenotype may encode a cell surface molecule regulating fasciculation, such as members of the Ig CAM family, or a factor creating an inhibitory environment that pulls axons together. Less often, we observed projection patterns, in which one set of axons at the dorsal or ventral margin of the projection field crossed over toward the opposite side. Factors responsible for this "straying" phenotype (Figure 13C) may be involved in dorsoventral patterning of the R-cell target field (Sato et al., 2006). Another group of mutant candidates exhibited targeting defects, in which R1-R6 axons failed to terminate in lamina and extended towards the medulla (Figures 13D-F). Similar phenotypes have been described in mutations that cause abnormal glial differentiation and migration in the lamina and in compartment boundaries (Poeck et al., 2001; Tayler et al., 2004). Finally, the last group includes mutants in which the size of the projection field and the pattern of R-cell projections were disrupted (Figures 13G, H, I). The presence of an abnormal sized projection field suggests that the gene involved may regulate the normal development and/or migration of target cells. Since we did not observe any "rough" eye phenotype in the lines tested with the ELF system, retrograde signaling from the target to the R-cells does not seem to regulate eye development during third instar larval stage.

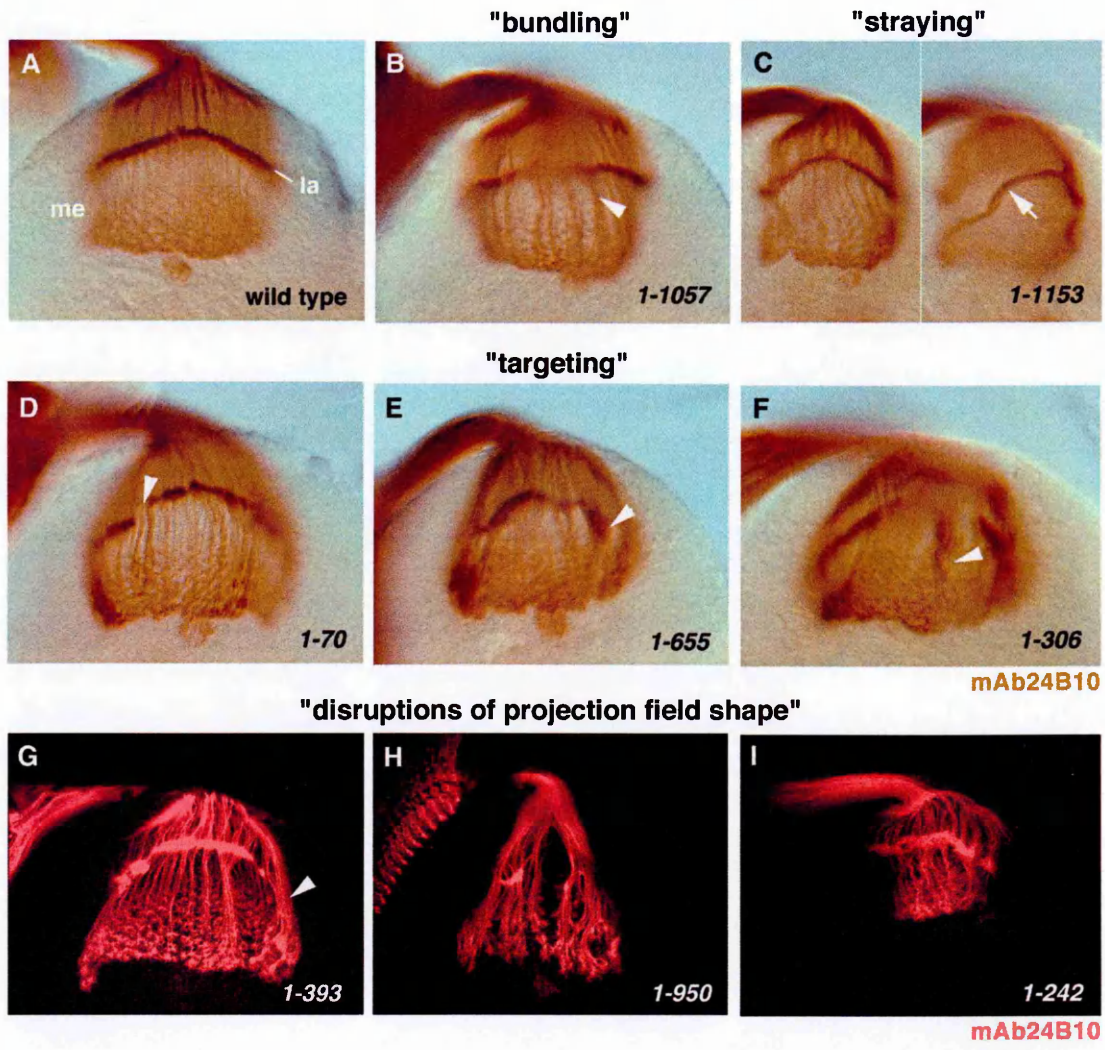

Figure 13. Examples of Mutant Candidates Isolated from the Screen using the ELF System.

(A-I) R-cell axons in wild type and mosaic animals visualized using mAb24B10. Eye disc development is normal in all lines (data not shown).

(A) In wild type, R1-R6 axons stop in the lamina (la) forming the lamina plexus and R7 and R8 axons project into the medulla (me) forming staggered rows of evenly distributed growth cones.

(B) In line *1-1057*, R-cell axons form bundles (arrowhead) in the projection field (bundling phenotype).

(C) In line *1-1153*, a ventrally located axon bundle projects dorsally in a different plane from the projection field (arrow) (straying phenotype).

(D, E, F) In lines *1-70*, *1-655* and *1-306*, the lamina plexus is disrupted. Arrowheads point at gaps (in line 1-70) and thicker axon bundles (lines *1-655* and *1-306*) (targeting phenotype).

(G, H, I) In lines *1-393*, *1-950* and *1-242*, the projection field is smaller and R-cell projection pattern is severely disrupted. Moreover, thick axon bundles are present (arrowhead).

Figure kindly provided by I. Salecker.

3.2.2 First Identified Mutant Candidate

When tested with the *"lama Gal4 UAS FLP* system", the mutant line 2-26 exhibited strong projection pattern defects with disrupted lamina plexus and thicker bundles in the medulla (Figure 14B'). Due to generation of somatic clones in the eye, the assembly of R-cells in the eye imaginal disc was also severely disrupted (Figure 14B). Using the ELF system, the phenotype was restricted to the projection field, which showed a narrowed lamina, indicating possible defects in the formation of target lamina neurons, whereas the arrangement of ommatidial clusters in the eye disc was normal (Figure 14C'). As the *lama-Gal4* driver induces mitotic recombination not only in the visual system, but also in the wing disc, *2-26* mosaic animals exhibited defects in the anterior wing compartment, such as an additional wing tissue and ectopic veins (Figure 14E). These phenotypes are characteristic of a Hedgehog (Hh) signaling defect and have also been observed in Protein Kinase A (PKA) mutants (Wang et al., 1999). PKA belongs to the family of cAMP- dependent serine/ threonine protein kinases. It is composed of two regulatory, cyclic-AMP-binding subunits (~45kD) and two catalytic subunits (~38kD) (reviewed in Garnegie and Scott, 2003). The locus of the first catalytic subunit (*PKA-C1*) lies on the left arm of the second chromosome, which is the target chromosome arm of our screen. Complementation tests with a null allele of *PKA*, $PKA\text{-}C1^{H1}$, demonstrated that the *2-26* is indeed an allele of *PKA-C1* (I. Salecker, unpublished observations).

To map the mutation in *2-26*, genomic DNA from adult heterozygous flies (*2-26 FRT40A/ Gla Bc*) was subjected to sequencing analysis. As controls, I used genomic DNA from a line carrying wild type *FRT* chromosomes and a second line carrying a different mutation (*2-4*), balanced over a *Gla Bc* chromosome. In both control experiments the electropherogram revealed a normal sequence for the *PKA-C1* subunit.

However, sequencing results for the *2-26* line uncovered a point mutation in position 86 in the PTK domain, where the substitution of a cytosine molecule by a thymine converted the amino acid glutamine into a stop codon, causing a truncation of the kinase domain (Figure 14F).

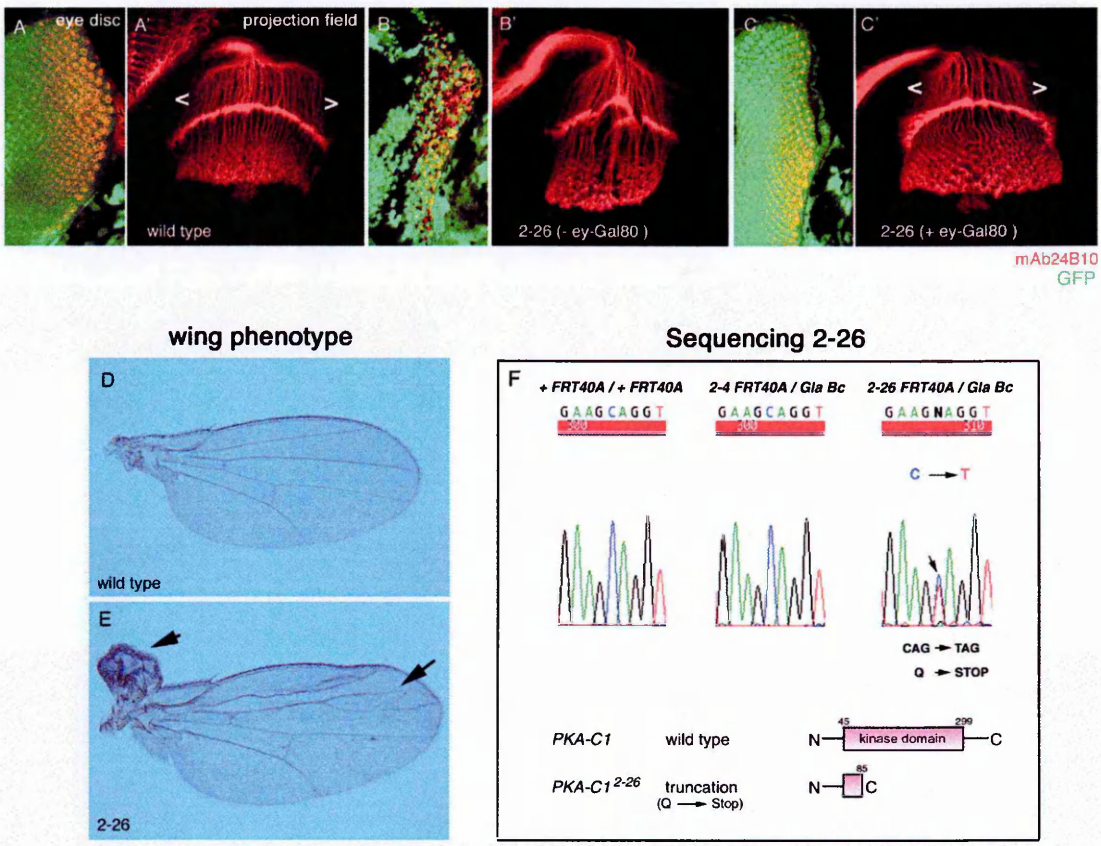

Figure 14. Identification of PKA in the Axon Guidance Screen using the ELF system.

(A, A') Wild type: *yw ey-Gal80; Ub-GFP cycE FRT40A/ FRT40A; lama-Gal4 UAS-FLP mδ/ +.*

(B, B', E) *2-26* mosaic: *Ub-GFP cycE FRT40A/ FRT40A 2-26; lama-Gal4 UAS-FLP mδ/ +.* Somatic clones visualized by a *Ubiquitin*-GFP transgene (green) are generated in both the eye disc and the target. (B, B') The eye has a rough phenotype and R-cells show projection defects in the target. R-cells and their axons are labelled with mAb24B10 (red). (E) Wing disc has a small ectopic distal wing and an additional vein (arrows in E), which are indicative of the Hh signaling pathway.

(C, C') *2-26 ELF* mosaic: *yw ey-Gal80; Ub-GFP cycE FRT40A/ FRT40A 2-26; lama-Gal4 UAS-FLP mδ/ +.* Somatic clones are restricted in the target area. The eye disc is normal but the projection field in the lamina is narrower than usual (brackets).

(D) Wild type: OregonR.

(F) Electropherogram of sequencing results demonstrates that *2-26* line carries a point mutation causing truncation in the kinase domain of PKA. Figure kindly provided by I. Salecker.

3.3 The ELF system During Pupal Development

To address whether the ELF system can be used to analyze gene function in the target area during later stages of development, I examined clone formation throughout pupal development, using a wild type FRT chromosome.

During 3rd instar larval stage, cells that have undergone mitotic recombination in the lamina and medulla are found adjacent to each other (Figures 15A, B). At 24 hours of pupal development, clones in medulla target neurons become dispersed and mix with heterozygous cells in a "salt and pepper" pattern (Figure 15B). This suggests that migration and reorganization of target cells in the medulla occurs during pupal development. Cells remain scattered until late pupal stages (Figures 15C, D, F). The presence of somatic clones in the adult indicates that the ELF system can be used for analysis of later stages of development.

In parallel to the examination of clone formation, the reorganization of R-cell projection pattern throughout pupal development was also followed. During the 3rd instar larval stage, R8 axons are the first to extend into the optic lobe and terminate in the medulla. R7 are the last photoreceptors to differentiate, and thus project into the target area later than all the other R cells. R7 terminals extend alongside R8 axons and terminate deeper just below R8 terminals, embedded within the medulla neuropil (Figure 15A). By 24 hours of pupal development all of the R7 axons have entered the projection field. The oldest R7 terminals are clearly separated from the R8 in two layers, whereas the youngest R7 are still in close proximity to the R8 terminals (Figure 15B, B'). The separation of R7 and R8 is, in part, due to the intercalation of processes from lamina and medulla neurons (Clandinin and Zipursky, 2002; Ting et al., 2005). R7 axons terminate in a temporary layer within the medulla neuropil, whereas R8 terminals are found at the distal border of the medulla neuropil (Figure 15B, B'). At 40 hours of pupal development, the medulla has completed the rotation with respect to the lamina

and the optic chiasm has formed (Meinertzhagen and Hanson, 1993). R8 terminals still remain at the distal border of the neuropil and the distance between the two temporary layers of R7 and R8 increases (Ting et al., 2005, Figure 15 C, C'). By 60 hours, R8 axons have entered the medulla neuropil and have reached their future recipient M3 layer (Figure 15D, D'). In the adult, R7 and R8 terminals have reached their recipient layers and assumed their final form (Figure 15E, E') (Meinertzhagen and Hanson, 1993).

The presence of somatic clones during pupal development and in adult mosaic animals carrying the ELF system, suggests that it could be used to study the function of genes required during the reorganization of neuronal connections in the optic lobe or even for the maintenance of the final connections in the adult. Our observations together with the findings of two additional groups (Ting et al., 2005; Shinza-Kameda et al., 2006) have revealed a two-step mechanism for the medulla neuropil innervation by R7 and R8 axons during pupal development. An interesting task for analysis will be to identify the molecular mechanisms employed by R7 and especially R8 during this active process.

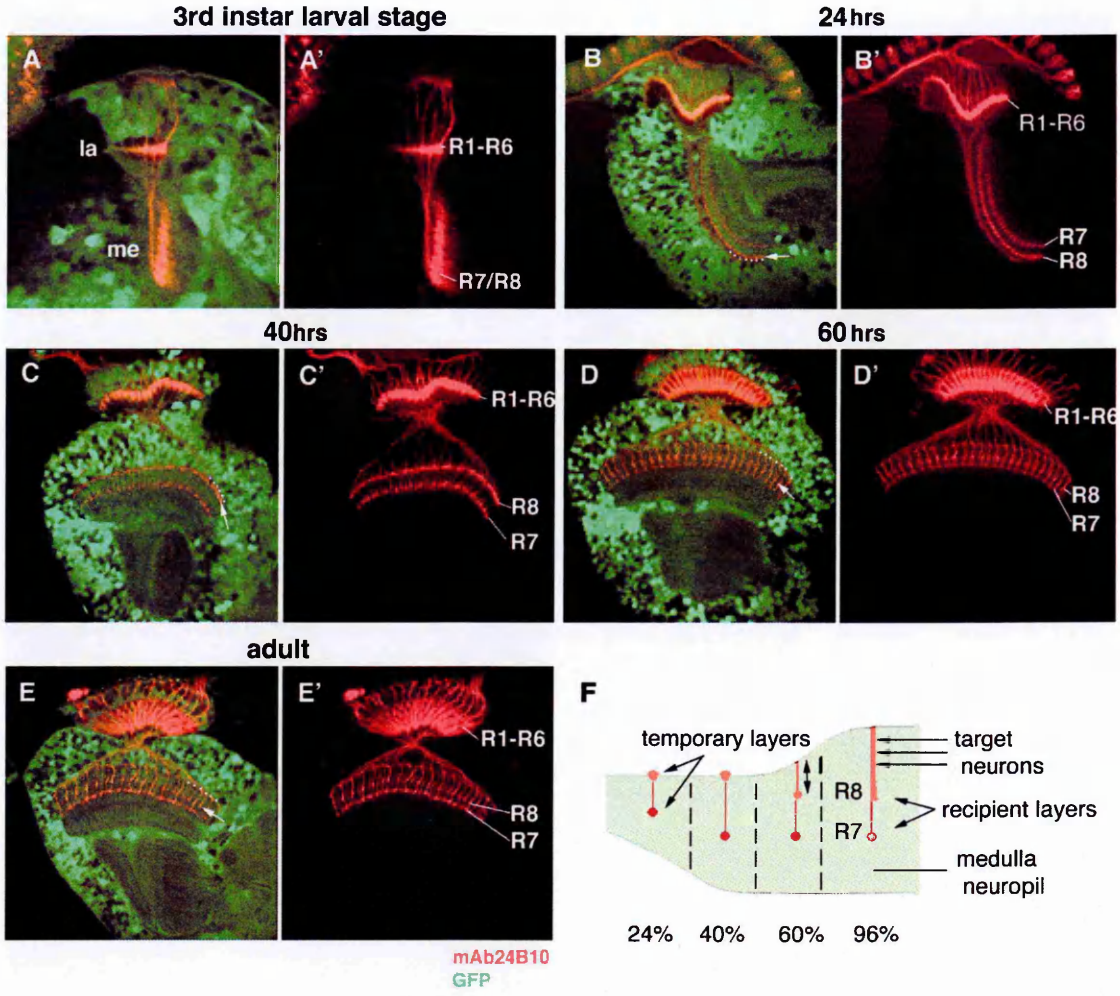

Figure 15. Target Mosaic Analysis during Pupal Development using the ELF system.

(A- E') Genotype: *yw ey-Gal80; Ub-GFP PCNA FRT42D/ FRT42D; lama-Gal4 UAS-FLP mδ/ +.* With the ELF system we can efficiently generate somatic clones in the optic lobe during pupal development, but not in the eye. The *Ubiquitin-GFP* transgene serves as a clonal marker (green). R-cell axons are labeled with mAb24B10 (red). Cells that undergo mitotic recombination are GFP-negative. During 3rd instar larval stage large compact clones of target cells are formed (A, A'). (B, C, D, E) During pupal development cells become scattered within the lamina (la) and medulla (me). The distal border of the medulla neuropil is marked by a dotted line. R8 terminals have entered the neuropil by 60 hours of pupal development (D, D').

(F) Schematic representation illustrating the changes of R8 projections during pupal development. At 24 hours of pupal development, R7 and R8 layers are separated in their temporary layers. R7 terminals lie within the medulla neuropil whereas R8 are in the distal border. At 40 hours, the distance between R7 and R8 layers increases. R8 invade the neuropil by 60 hours. In adults, R7 and R8 terminals are found in their recipient layers.

3.4 Discussion

3.4.1 ELF is a Novel Genetic Tool to Generate Target Mosaic Animals

To systematically address the molecular mechanisms regulating axon guidance in the visual system of *Drosophila*, focusing on the requirement of factors expressed in target cells, the lab established the ELF system (Chotard et al., 2005). With this genetic tool, we can generate mutant mosaic animals with wild type heterozygous R-cells whose axons project into a mutant target area. Since the onset of recombination events in the target occurs during early larval stage (Chotard et al., 2005), the ELF system can potentially be used to study early events in the development of the optic lobe prior to retinal innervation or subsequent steps following R8 axon polarization towards the optic stalk. More importantly, as clones are present during the development of the visual system from late larval to adult stages, this tool can be used to address what kind of cues are provided by target cells to incoming R-cell afferents for their initial target selection and for guiding them towards their postsynaptic partners. Concomitant with this, this tool can be used to also identify cell-autonomous factors required for the normal development and migration of target cells. To answer these questions, I participated in a large-scale mutagenesis screen for the chromosome arm 2L using the ELF system, focusing on cues required in target cells for the formation of R-cell projection pattern during initial target selection (3rd instar larval stage). Although for our purposes we kept mutant lines with projection defects during late larval stage, this screen strategy could also be used to identify target-derived factors required during selection of final targets by R-cell axons or formation and maintenance of synapses between R-cell axons and target cells during later stages of development.

3.4.2 Requirement of *Protein Kinase A* in the Lamina

From our mutagenesis screen we isolated 50 mutant candidates affecting factors required in the target for the initial R-cell projection pattern. In search for allelic groups within our mutant candidates, each of them was crossed to the remaining 49 (C. Chotard, W. Leung and I. Salecker, unpublished observations). Some of the lines failed to complement each other when crossed together, revealing eight allelic groups. Deficiency mapping of isolated mutants is in progress.

One of our mutants (*2-26*) was found to carry a mutation in the first catalytic subunit of *PKA* (*PKA-C1*). PKA is a serine/threonine protein kinase involved in synapse formation and plasticity (Munno et al., 2003; Yamamoto et al., 2005) as well as in differentiation of RGCs in *zebrafish* in cooperation with the Hh signaling pathway (Masai et al., 2005). In the eye imaginal disc of *Drosophila*, two forms of Cubitus interruptus (Ci), a zinc finger transcription factor of the Gli family, control the expression of Hh target genes. The full-length form of Ci is activating Hh signaling, whereas the proteolytically cleaved form is a repressor (reviewed in Lum and Beachy, 2004). Phosphorylation of Ci by PKA targets Ci for proteolytic processing to antagonize Hh signaling (Wang et al., 1999).

Subsequent characterization of *PKA-C1 ELF* mosaic animals with neuron- and glia-specific markers revealed that lamina neurons extended more dorsally and ventrally within the optic lobe when compared to wild type. Our findings show that PKA has a cell-autonomous requirement in lamina neurons, which confirms its role in lamina neurogenesis (Huang et al., 1998). In addition, small ectopic clones of neurons were found in the most dorsal and ventral regions of the GPC areas (I. Salecker, unpublished observations), known to give rise to glial cells and proximal medulla neurons, but not lamina neurons (Chotard et al., 2005), suggesting that PKA may also play a role in preventing neurogenesis outside the lamina and in GPC areas.

The fact that the first identified mutant of the screen yielded a component of the Hh signaling pathway, which is expected to act in the target, validates our genetic strategy. Using this screen strategy, the identification of novel factors playing a role in the visual system of *Drosophila* will prove very valuable for improving our understanding concerning the interactions between photoreceptor axons and cells in the target during initial target selection.

4. The Role of Alk in the Visual System of *Drosophila*

Anaplastic lymphoma kinase (Alk) is a receptor protein kinase with neuritogenic and mitogenic properties *in vitro* and a specific expression pattern in vertebrate nervous system. The normal function of the protein has been demonstrated by the *in vivo* analysis of the *Drosophila* homolog of Alk and its activating ligand Jeb in the developing visceral mesoderm (Englund et al., 2003; Lee et al., 2003). In these studies it was also shown that both proteins are expressed in the developing nervous system from embryonic stage 11 onwards (Loren et al., 2001; Weiss et al., 2001). To address whether these molecules are required for the development of the nervous system, their expression pattern in the developing visual system was determined. Alk expression was detected using an anti-Alk antibody against the aminoterminal domain of the receptor, whereas the anti-Jeb antibody has been generated against amino acids 41 through 355 of the secreted protein (both kindly provided by Ruth Palmer, Englund et al., 2003). R-cells and their axons were labeled with mAb24B10.

4.1 Alk and Jeb Expression Pattern During Optic Lobe Development

During the 3rd instar larval stage, Alk is strongly expressed in the target area, and particularly in the medulla and lobula neuropils. It is also expressed in the lamina, albeit at lower levels. Alk expression is not detected in R-cells in the eye imaginal disc or in lamina glial cells (Figures 16A-B'). During pupal development, Alk expression increases in the medulla neuropil and remains strong in the adult. In the lamina, Alk increases within the developing lamina cartridges from mid-pupal development onwards, concomitant with the formation of elaborate lamina neuron dendrites (Figures 16C-F').

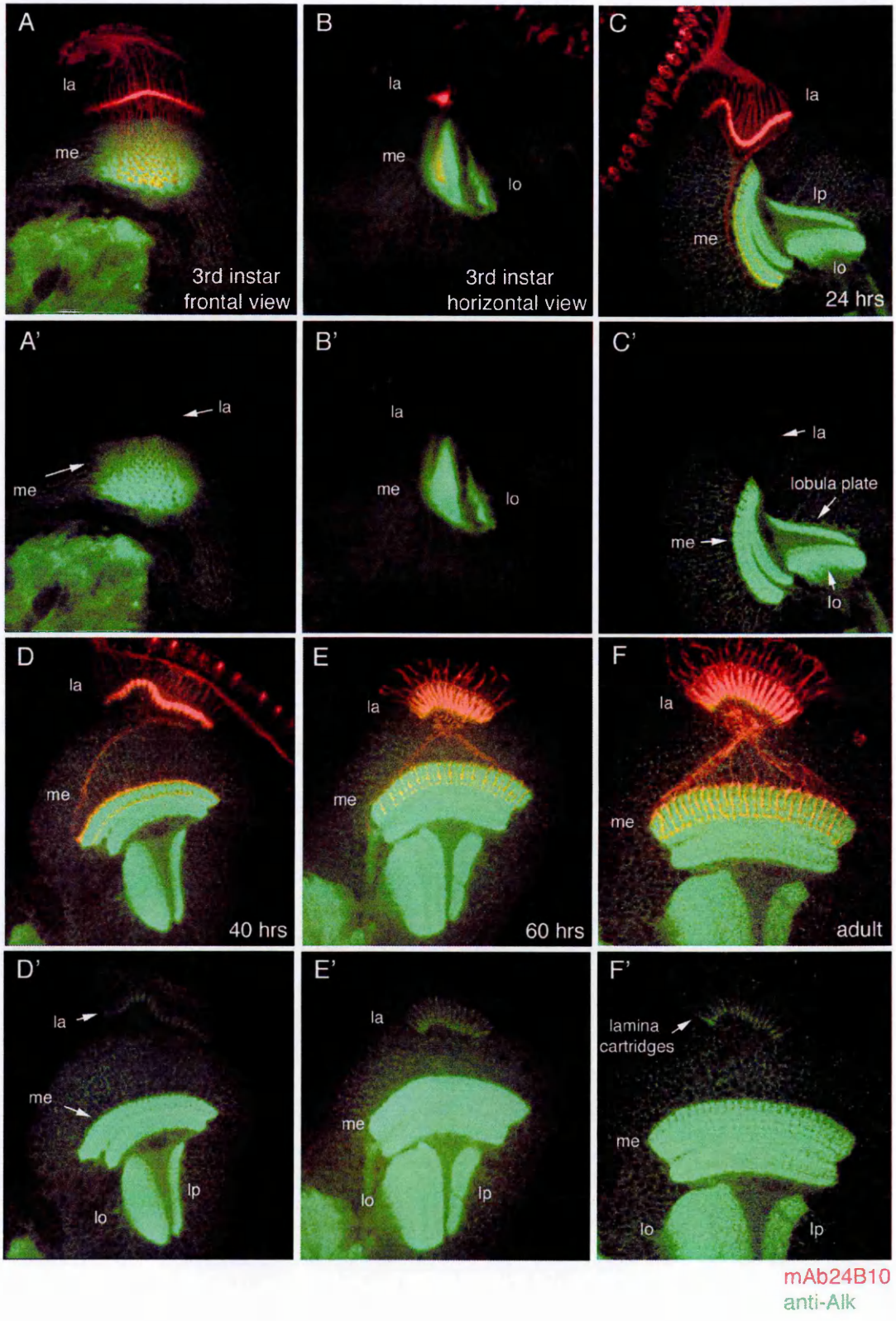

Figure 16. Alk Expression Pattern During Pupal Development.

(A-B') Alk (green) is strongly expressed in the medulla (me) and lobula (lo) and at lower levels in the lamina (la) during 3rd instar larval stage. R-cells are visualized with mAb24B10 (red).

(C-F') Alk expression pattern at 24, 40, 60 hours of pupal development and in adults. Strong Alk expression (green) is detected in the medulla neuropil, as well as the lobula and lobula plate (lp). Alk expression also increases in the lamina from 40 hours onward (arrow in F').

Jeb is expressed in a complementary pattern of Alk in the visual system of *Drosophila* during early developmental stages. During 3rd instar larval stage, Jeb is expressed in the photoreceptors in the eye imaginal disc and along R-cell axons. It is strongly detected in the R1-R6 growth cones forming the lamina plexus, and along the R7 and R8 axon shafts and their growth cones in the medulla (Figures 17A-B'). At 24 hours of pupal development, strong expression persists in R1-R6 terminals in the lamina and becomes refined to the R7 and R8 growth cones in the medulla. Jeb protein is also detected in the lobula and lobula plate (Figures 17C, C'). Around 40 hours of pupal development, Jeb is expressed in R7 and R8 growth cones in a more punctate pattern, suggesting that it may be secreted (Figures 17D, D'). From 60 hours onwards, Jeb is down-regulated in R-cell terminals and is up-regulated in lamina, medulla, and higher-order target neurons, albeit only at low levels (Figures 17E-F'). Jeb expression appears to localize more strongly in the R8 recipient layer at 60 hours (Figure 17 E, E').

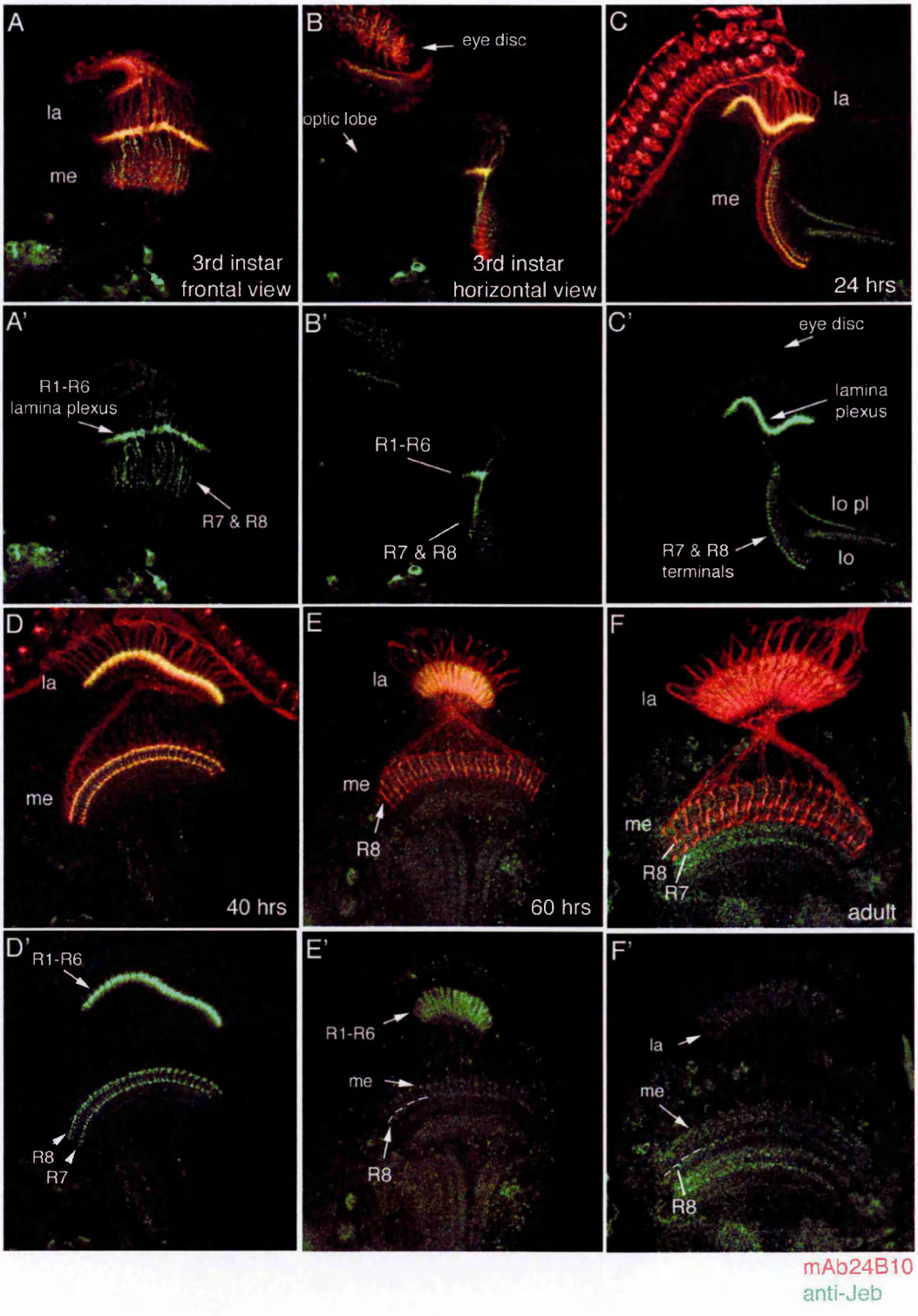

Figure 17. Jelly belly Expression Pattern.

(A-B') During 3rd instar larval stage, Jeb (green) is expressed in the R-cells in the eye disc (arrow). It is also strongly detected in R1-R6 growth cones in the lamina (la) and along the R7 and R8 axon shafts in the medulla (me). R-cells are labeled with mAb24B10 (red).

(C-D') 24 and 40 hours of pupal development. Jeb expression becomes refined to the R1-R6 growth cones in the lamina and the R7 and R8 terminals in the medulla.

(E-F') During the second half of pupal development (from 60 hours to adult), Jeb expression is downregulated in R-cell axons but slightly increases in lamina and medulla neurons.

These findings reveal a highly dynamic and initially complementary expression pattern for Jeb in R-cells and Alk in the target neurons during a time when major reorganization of R-cell axons takes place to establish the adult R-cell projection pattern. This raises the possibility that, similarly to the visceral mesoderm, these two proteins form a ligand/receptor system that could be important for R-cell projection pattern formation. In particular, Jeb provided by R cells and the receptor Alk in target neurons during pupal development could elicit responses that may regulate specific steps in the navigation of R-cell axons towards their postsynaptic partners.

4.2 Loss-of-Function Analysis of *Alk*

4.2.1 *Alk* Alleles

Most animals homozygous for *Alk* mutations usually die during embryonic development and none progresses past 1st instar larval stage (Loren et al., 2003). However, R-cell projection pattern formation occurs from the 3rd instar larval stage onwards. To address the function of *Alk* in the visual system during larval and pupal stages, we generated *Alk* mosaic animals using three alleles (kindly provided by Ruth Palmer, Loren et al., 2003, Figure 18). Wild type Alk consists of two MAM domains, an LDLa receptor repeat motif, a glycine-rich region, a transmembrane domain and a tyrosine kinase domain. In the Alk^{1} allele, a stop codon introduced after the first MAM domain of the receptor produces a truncated protein. The Alk^{8} allele arises from a splice-donor-site mutation after the transmembrane domain that also results in a truncated protein lacking the RTK catalytic domain. Finally, in the Alk^{9} allele, the substitution of glutamate for lysine in position 1244 within the conserved PTK domain of the receptor produces a protein with a non-functional catalytic domain. The "kinase inactive" mutant alleles allow us to test whether the PTK activity of the receptor is essential for the *in vivo* action of Alk in the

optic lobe, as it has already been demonstrated in the developing visceral mesoderm in *Drosophila* (Englund et al., 2003).

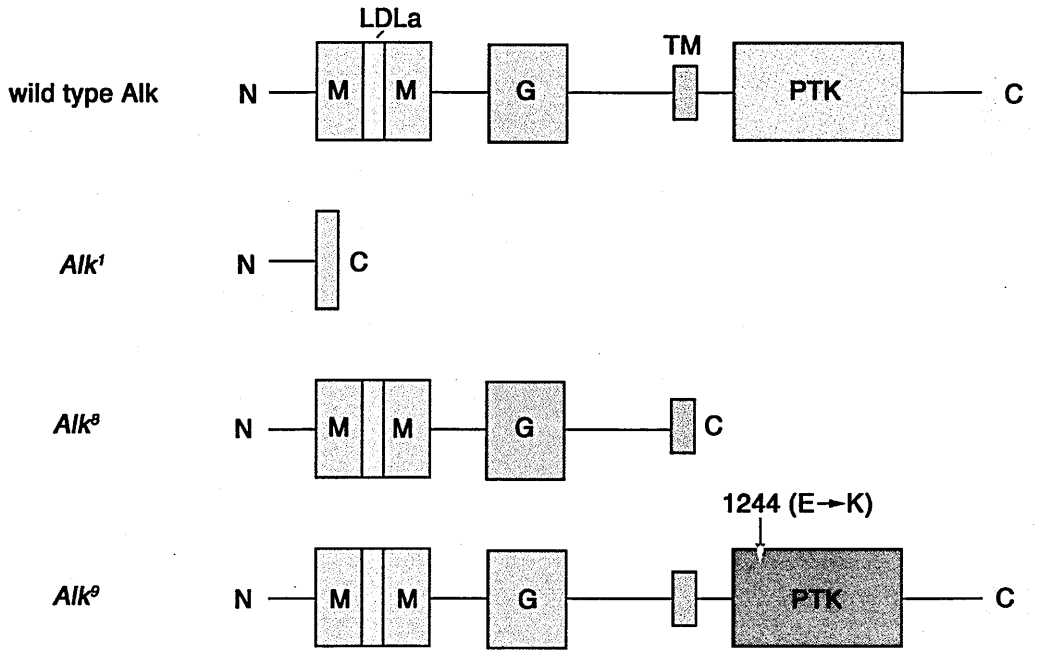

Figure 18. Wild type and Mutant *Alk* Alleles.
Wild type Alk consists of two MAM domains (M), an LDLa receptor motif, a glycine-rich region (G), a transmembrane domain (TM) and a cytoplasmic catalytic protein tyrosine kinase domain (PTK). Alk^1 allele has a truncation after the first MAM domain, Alk^8 allele lacks the PTK domain, whereas Alk^9 allele carries a point mutation in the PTK domain. Adapted from Loren et al., 2003.

4.2.2 *Alk* is not Required for Initial R-cell Target Selection During 3rd Instar Laval Stage

Since immunolabeling revealed that Alk is strongly expressed in the target during 3rd instar and pupal development, the ELF system was used to generate homozygous mutant cells expressing the Alk^1 allele in the lamina and medulla. The R-cell projection pattern was assessed using the R-cell specific marker mAb24B10. As the gene encoding the *Drosophila Alk* lies on the right arm of the second chromosome, a recombinant FRT42D chromosome was used carrying a *Ubiquitin-GFP* transgene and the cell lethal mutation *PCNA* to enhance clone formation.

By generating *Alk*^{1} *ELF* mosaic animals, *Alk* function was removed from a large portion of lamina and medulla neurons, as well as epithelial and marginal glia. In these animals, projection pattern defects are not observed for either R1-R6 axons in the lamina or R7 and R8 axons in the medulla during 3rd instar larval stage. As in wild type, R1-R6 axons form a normal lamina plexus and R7 and R8 axons form regular staggered rows in the medulla in *Alk*^{1} target mosaic animals (n=9, Figures 19A-B').

These data suggest that *Alk* is not required in the target during initial target selection of R-cell axons.

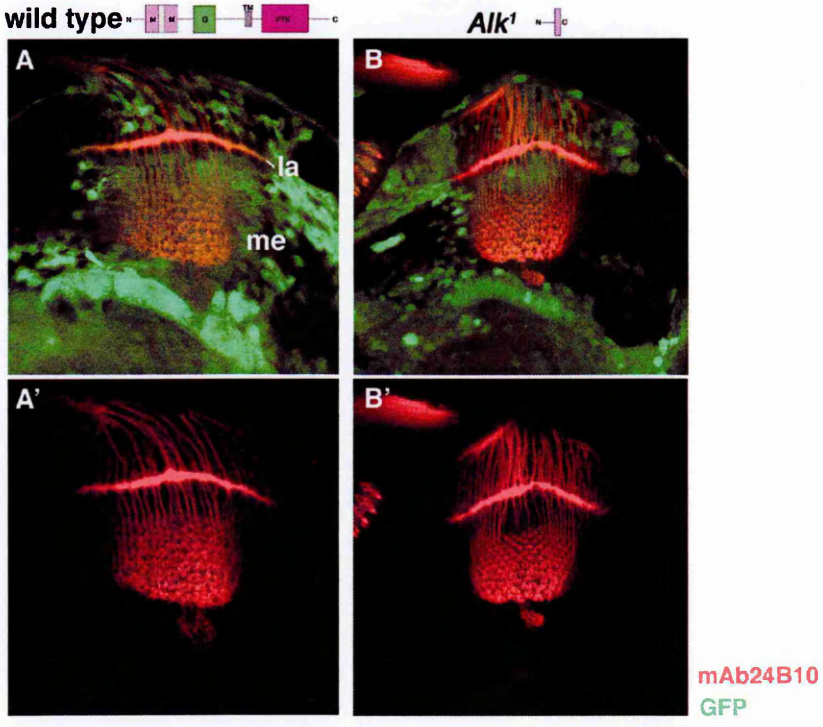

Figure 19. *Alk* is Not Required in Target Neurons for R-cell Projection Pattern Formation During Larval Development.

(A/A') Wild type: *yw ey-Gal80; Ub-GFP PCNA FRT42D/ FRT42D; lama-Gal4 UAS-FLP m δ/ +.* Kindly provided by I.Salecker.

(B, B') *Alk*^{1} *ELF* mosaic: *yw ey-Gal80; Ub-GFP PCNA FRT42D/ FRT42D Alk*^{1}*; lama-Gal4 UAS-FLP mδ/ +.* In *Alk*^{1} target mosaic animals R1-R6 axons terminate normally in the lamina and form a continuous lamina plexus (la), whereas R7 and R8 axons are arranged in regular staggered rows in the medulla (me), as in wild type animals. Somatic clones are visualized using a *Ubiquitin- GFP* transgene (green) and R-cell axons are labeled with mAb24B10 (red).

4.2.3 *Alk* is Not Required in the Eye

Although Alk is not expressed in the eye, it could regulate the differentiation of R-cells or play a role in later steps of ommatidial assembly in the compound eye through retrograde signaling. To assess whether Alk is required in the eye, Alk^{1} eye mosaic animals were generated using the "$ey^{3.5kb}$-*FLP* system". Using the eyeless$^{3.5kb}$ enhancer, I was able to drive mitotic recombination in a large portion of R-cells, while keeping target cells in the optic lobe in a heterozygous wild type state. The *Ubiquitin-GFP* transgene was used to mark wild type and heterozygous cells, and the *cyclin E* transgene was used to increase the size of somatic clones that do not express GFP (Figure 20).

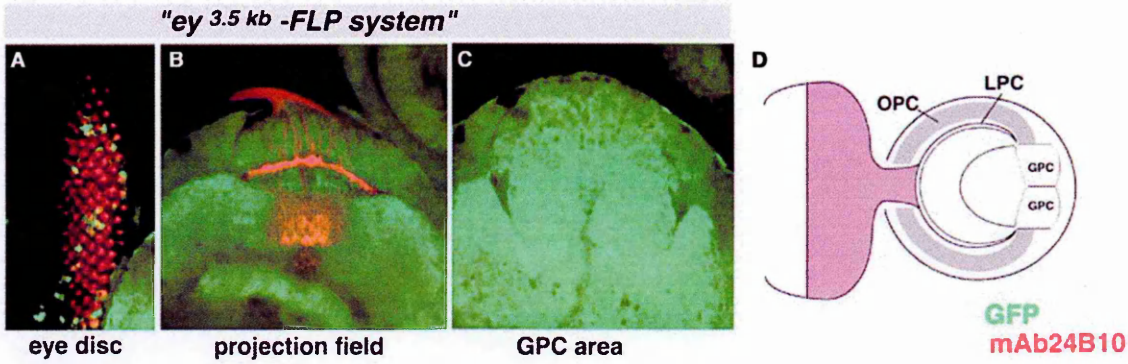

Figure 20. Modification of the "*ey-FLP* system".
(A, B, C) *yw ey$^{3.5}$-FLP; Ub-GFP cycE FRT42D/ FRT40A*. Somatic clones are visualized by the absence of GFP (green). R-cells and their axons are labelled with mAb24B10 (red). The majority of R-cells in the eye have undergone mitotic recombination, whereas in the target area there are no clones.
(D) Schematic representation of clone formation in the eye (purple).
Figure kindly provided by I. Salecker.

Removing *Alk* function from the eye using the Alk^{1} allele produces a phenotype that is indistinguishable from wild type adult animals, indicating that Alk is not required in R-cells for the formation of R-cell projection pattern (Figures 21A, A').

4.2.4 *Alk* is Required for R-cell Projection Pattern Formation in the Adult

Next, to address whether *Alk* is required in the target for R-cell projection pattern during later stages, the R-cell projection pattern of adult Alk^1, Alk^8 and Alk^9 target mosaic animals was assessed by mAb24B10 immunolabeling (Alk^1 *ELF* mosaic: n=64, Alk^8: n=30, Alk^9: n=37, Figures 21B-D'). All adult *Alk* target mosaic animals exhibit an irregular R-cell projection pattern in the medulla and thickened terminals. R8 terminals appear to be absent from their recipient layer M3, suggesting that they might terminate either in a more superficial or in a deeper layer of the medulla. In other cases, R8 terminals are observed to defasciculate from the original bundle with the R7 axons, and instead cross over to adjacent columns (Figures 21B-D'). As this abnormal phenotype is evident with all three *Alk* alleles used, including the "kinase dead" alleles, these findings suggest that Alk kinase activity is required for its *in vivo* function in the optic lobe.

Since mutant cells are scattered during late pupal stages, I determined the approximate percentage of mutant (GFP-negative) versus total amount of cells (n=25 for Alk^1, n=15 for Alk^8 and n=15 for Alk^9 target mosaic animals) focusing in the medulla. Numbers of mutant cells were determined using single optical sections. Percentages of mutant lamina neurons were not assessed in these samples, as they have been described not to regulate target layer selection of R7 and R8 (Ting et al., 2005). Analysis of the samples revealed that homozygous mutant medulla neurons in these animals range between 15%-55%. In most samples (64%), the size of the clones correlated with the severity of the phenotype in the medulla. The strength of the phenotype, however, sometimes varied, possibly due to the specific neural types that have undergone mitotic recombination and are homozygous mutant for *Alk* using the ELF system.

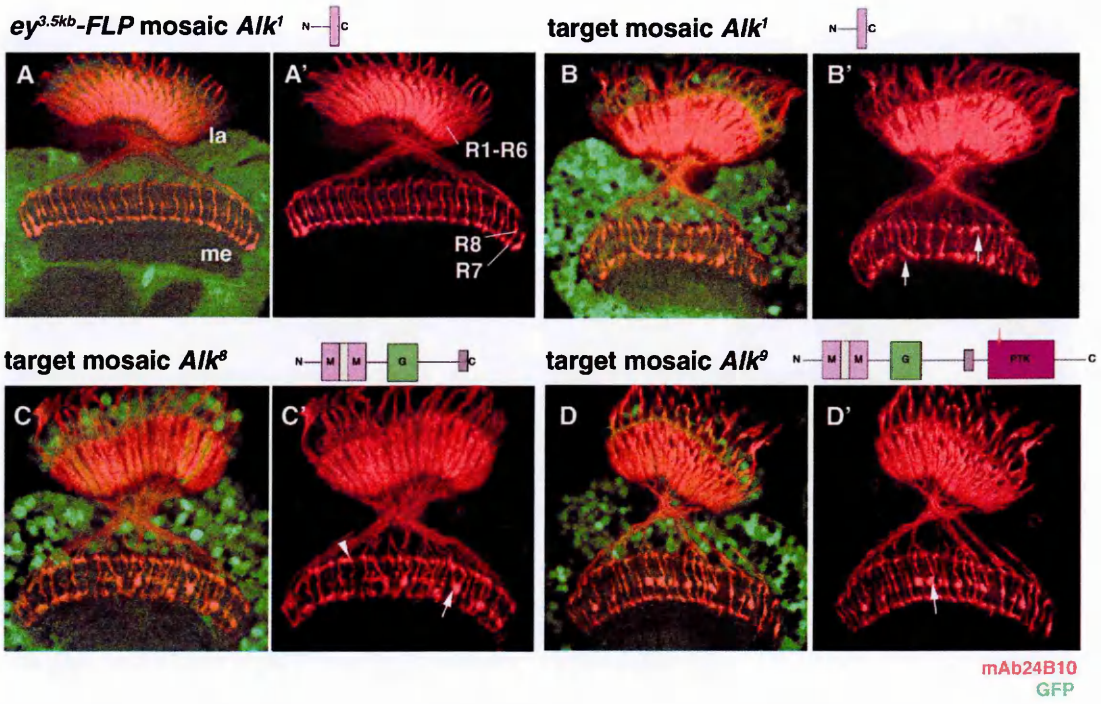

Figure 21. *Alk* is Required in Target Neurons for R-cell Projection Pattern Formation in the Adult.

(A, A') *Alk*^{1} eye mosaic *ey*$^{3.5}$*-FLP; Ub-GFP PCNA FRT42D/ FRT42D Alk*^{1}. R-cell axons are labeled with mAb24B10 (red). Somatic clones are visualized by the absence of the *Ubiquitin-GFP* transgene (green). Consistent with its expression pattern, removing *Alk* function from R-cells does not cause R-cell projection defects.

(B-D') *Alk ELF* mosaic: *yw ey-Gal80; Ub-GFP PCNA FRT42D/ FRT42D Alk*^{1,8,9}*; lama-Gal4 UAS-FLP mδ/ +. Alk* target mosaic animals show non-cell-autonomous projection defects in the medulla. R8 axons have thickened terminals and appear to stall at the distal part of the medulla (arrowhead) or fasciculate with R8 or R7 axons in adjacent columns (arrows).

4.2.5 *Alk* Regulates R8 Target Layer Specificity

Since 24B10 staining did not allow us to assess targeting defects of different R-cell subtypes, we tested their projection pattern in the lamina and medulla using specific markers for each group. To assess the R8 projection pattern, a population of R8 was labeled using *Rh6-lacZ*, a transgene expressing β-galactosidase under the control of the rhodopsin promoter Rh6 (Cook et al., 2003).

In *Alk*^{1} *ELF* mosaic animals we observed that R8 terminals failed to terminate in the target layer M3 and in their original column (n=9). Instead, some R8 axons stopped

at the distal border of the medulla neuropil (30/103, n=9), where they are normally located at 40 hours of pupal development, or failed to terminate in their recipient layer and misprojected to the R7 layer in Alk^1 target mosaic animals (3/103, n=9) (Figures 22B, B').

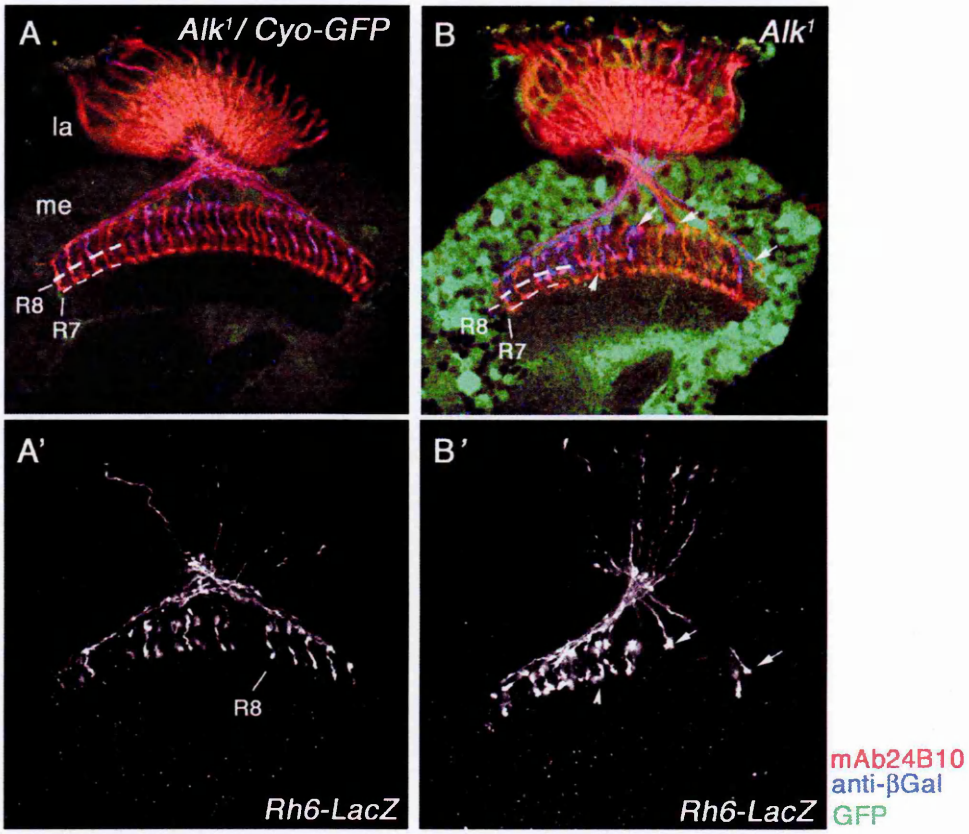

Figure 22. *Alk* is Required in Target Neurons for R8 Targeting.

(A, A') Control heterozygous animals: *yw ey-Gal80; FRT42D Alk¹ / CyO Kr-GFP; lama-Gal4 UAS-FLP/ Rh6-lacZ.*

(B, B') *Alk¹ ELF* animals: *yw ey-Gal80; UbGFP PCNA FRT42D/ FRT42D Alk¹; lama-Gal4 UAS-FLP/ Rh6-lacZ.* All R-cell axons are labelled with mAb24B10 (red). A subgroup of R8 axons is labeled using an *Rh6-lacZ* transgene (blue). In controls, R8 axons terminate in a superficial sublayer above the R7 axons in the medulla (me). (la, lamina). In *Alk¹* target mosaic animals, R8 axons extend to an adjacent column (arrowhead) or stall at the distal border of the medulla neuropil (arrows).

4.2.6 R7 Target Layer Specificity is Normal in *Alk ELF* Mosaic Animals

In *Alk ELF* animals stained with mAb24B10, R7 axons seemed to terminate correctly in their recipient M6 layer and also stay in their correct column. To verify this observation, I used a *lacZ* reporter driven by the R7-specific rhodopsin (Rh4) promoter (Figures 23A-B').

Indeed, R7 terminals are positioned correctly in Alk^1 mosaic animals apart from a very small percentage of R7 terminals (1.6%, 6/373 R7 terminals, n=15) that appear to shift to an adjacent column in the M6 layer (Figures 23B, B'). In samples where this subtle R7 targeting phenotype was observed, the R8 phenotype is very strong, and thus the R7 mistargeting may be a secondary effect as a consequence of the R8 targeting defects.

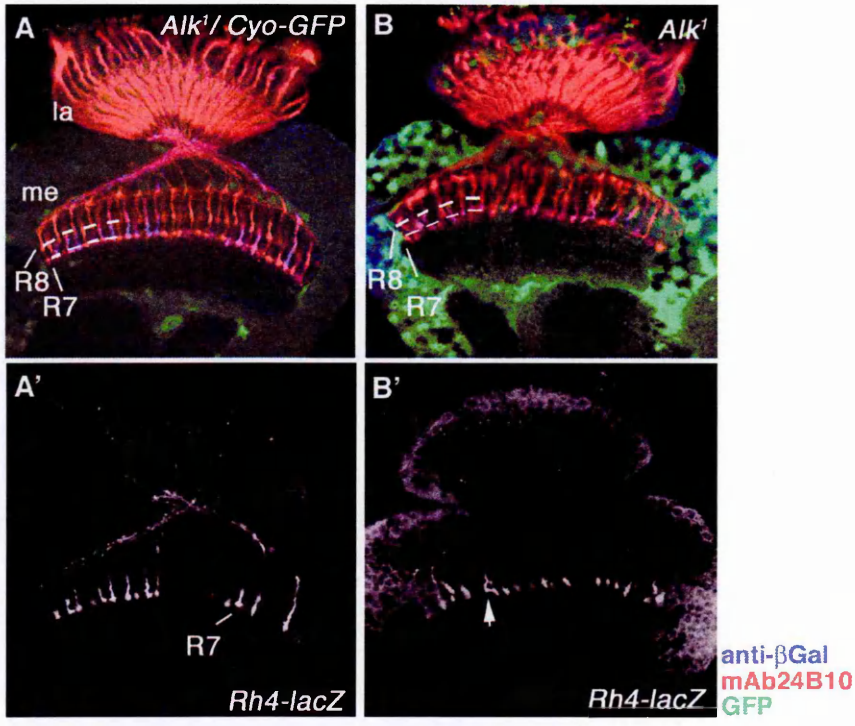

Figure 23. *Alk* is Not Required for R7 Target Layer Specificity.

(A, A') Control heterozygous animals: *yw ey-Gal80; FRT42D Alk^1/ CyO Kr-GFP; lama-Gal4 UAS-FLP/ Rh4-lacZ.*

(B, B') *Alk^1* target mosaic animals: *yw ey-Gal80; Ub-GFP PCNA FRT42D/ FRT42D Alk^1; lama-Gal4 UAS-FLP/ Rh4-lacZ.*

All R-cell axons are labeled with mAb24B10. A subgroup of R7 axons is labeled using an *Rh4-lacZ* transgene (blue). Somatic clones are visualized by the absence of GFP. In controls, R7

axons terminate below the R8 axons in the medulla (me). (la, lamina). In Alk^1 target mosaic animals, almost all R7 axons terminate correctly in their recipient layer. Very rarely, they shift to an adjacent column (arrow).

4.2.7 Onset of R8 Mistargeting Phenotype

Removing the function of *Alk* from target cells has no effect on the formation of the initial R-cell projection pattern formation during 3rd instar larval stage. However, *Alk* is required for the establishment of the adult R8 projection pattern. To demonstrate that *Alk* is required for the correct target layer selection of R8 axons during development and not some later process, I set specific time points during the development of Alk^1 target mosaic animals and assessed the R-cell projection pattern using mAb24B10. The timepoints were chosen to divide pupal development (~100 hours) into three parts, the time by which all R-cell axons have entered the optic lobe (24 hours), the stage during which R8 terminals are still observed at the distal border of the medulla neuropil (40 hours) and the stage at which R8 terminals have entered the medulla neuropil (60 hours).

Until 40 hours of pupal development, R7 and R8 growth cones are located normally in their expected positions, with R8 at the distal border and R7 within the medulla neuropil (n=18). Topographic map formation is also preserved, as each of the R7 or R8 terminals remain in their appropriate columns (Figures 24A, B). Defects in the R8 projection pattern can be detected at 60 hours of pupal development (n=20). R8 terminals in Alk^1 mosaic animals at this stage have started to develop abnormal morphology with clumped ends and appear to terminate in the wrong layer or fasciculate with R8 terminals in adjacent columns (Figure 24C). This suggests that *Alk* is required at some point during this 20-hour period for R8 target layer selection, possibly by regulating the entry of R8 axons in the medulla neuropil. *Alk* could also regulate the stabilization of connections between R8 terminals and processes of neurons

projecting in their recipient layer. Failing to stabilize these connections could subsequently cause extension or even retraction of the R8 growth cones away from the target layer or shift to an adjacent column.

The onset of the R8-specific marker Rh6-lacZ expression is around 75 hours of pupal development (Cook et al., 2003). To pinpoint the critical step during which Alk is required for R8 target selection more precisely, I used an R8-specific marker, which is expressed during larval and pupal stages. Atonal is a transcription factor expressed exclusively in R8 during late 3rd instar larval stage (Baker et al., 1996). To follow atonal expression in R8 axons during early stages of pupal development I made use of an *atonal-τ-myc* transgene, in which the atonal enhancer drives *τ-myc* expression during 3rd instar larval stage (Senti et al., 2003).

Strong *ato-τ-myc* expression is also detected during early pupal development at 40 hours (Figures 24D, D'). During this stage, R8 terminals are located correctly at the distal end of the medulla neuropil in *Alk^{1}* mosaic animals, when compared to wild type (n=17) (Figures 24D-E'). At 55 hours of pupal development, expression of the transgene is gradually down-regulated in R8 terminals. Wild type animals carrying two copies of the *atonal-τ-myc* transgene were used as control for better resolution. In these animals, R8 terminals extend fine processes towards their target layer (Figures 24F, F'). In the *Alk^{1}* mosaic animals, some R8 axons have clumped terminals, do not form the fine extensions observed in controls and are arrested at the distal border of the medulla neuropil (22/121, n=7) (Figures 24G, G').

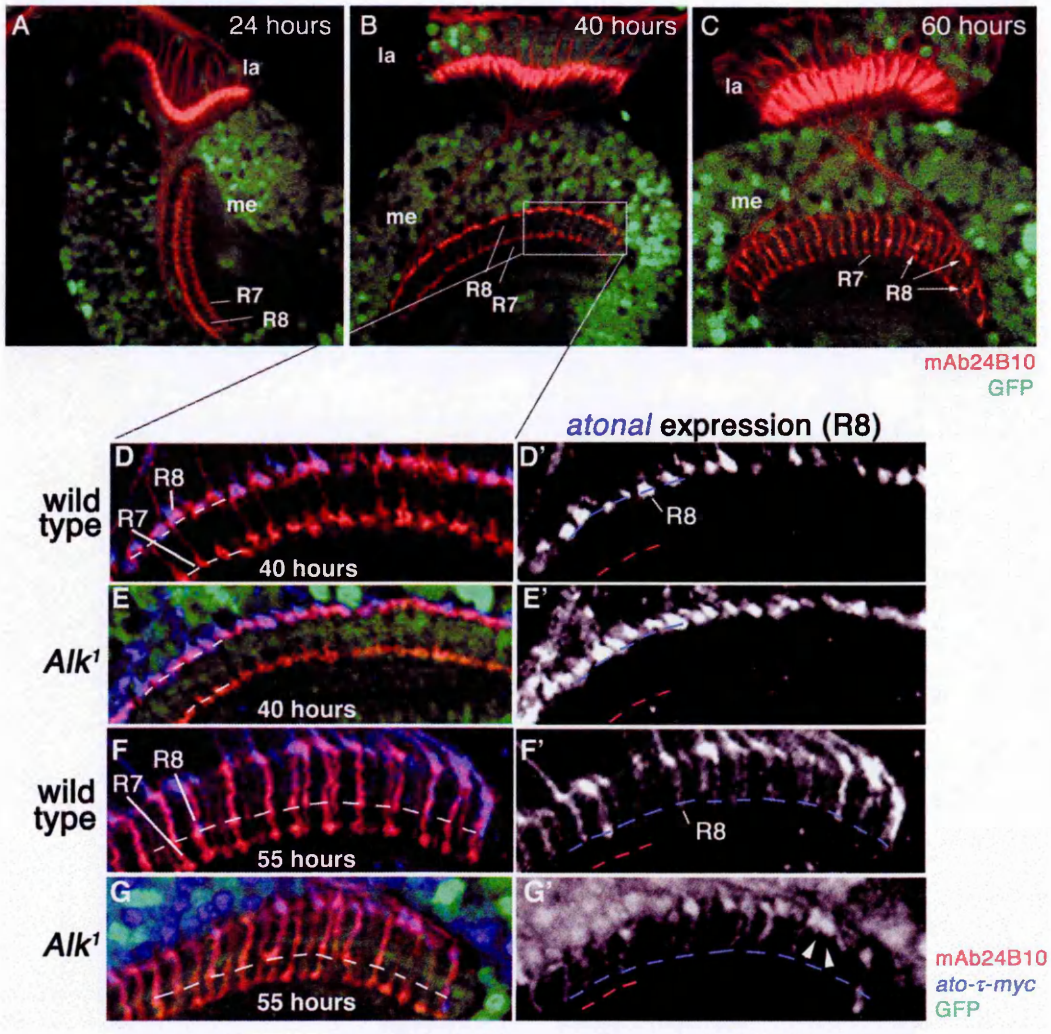

Figure 24. *Alk* is Required in Target Neurons for R8 Targeting during Mid-Pupal Development. (A-C) *Alk*^{1} *ELF* mosaic: *yw ey-Gal80; Ub-GFP PCNA FRT42D/ FRT42D Alk*^{1}*; lama-Gal4 UAS-FLP/ +*. (D-D') Heterozygous control: *yw ey-Gal80; FRT42D Alk*^{1} */ CyO Kr-GFP; lama-Gal4 UAS-FLP/ ato-τ-myc*. (F-F') *ato-τ-myc/ ato-τ-myc*. (E-E', G-G') *Alk*^{1} *ELF* mosaic: *yw ey-Gal80; Ub-GFP PCNA FRT42D/ FRT42D Alk*^{1}*; lama-Gal4 UAS-FLP/ ato-τ-myc*.

Mosaic animals do not exhibit any projection defects at 24 and 40 hours of pupal development. Defects are detected at 60 hours, including thickened R8 terminals, or R8 axons failing to terminate in their target layer (arrows in C). Somatic clones are visualized using a *Ubiquitin-GFP* transgene (green) and R-cell axons are labeled by mAb24B10 (red). R8 axons are labeled using an *atonal-τ-myc* transgene (blue in D-G). Initially, R8 terminals are found at the distal border of the neuropil in target mosaic animals, as in controls. At 55 hours, fine processes of R8 terminals enter the neuropil and extend towards their target layer (white line in F'). In *Alk*^{1} target mosaic animals, some R8 terminals can fail to form these processes and remain in the distal border of the neuropil (arrowheads in G').

These results demonstrate that the *ato-τ-myc* transgene can be used to follow R8 axons during the first half of pupal development. It is strongly expressed until 40 hours but is downregulated after 50 hours. Using two copies of the *ato-τ-myc* transgene can improve resolution of R8 axons during later stages, however, this was not possible in our case as the transgene is on the third chromosome and our mosaic animals already carry the *lama Gal4* driver there. Despite these limitations, *Alk* was shown to be non-autonomously required for the guidance of R8 axons towards their target layer around 55 hours of pupal development. Down-regulation of *Alk* in the target results in mistargeting of R8 axons in an inappropriate layer or in an adjacent column via an instructive or a permissive signal.

4.2.8 *Alk* is Not Required for R1-R6 Target Layer Specificity

To determine whether *Alk* functions in regulating targeting of R1-R6 axons in the lamina, similarly to the R8 approach, we used an *Rh1-lacZ* transgene to specifically label R1-R6 in controls and Alk^{1} *ELF* mosaic animals (Figures 25A-B'). In the adult Alk^{1} target mosaic animals, R1-R6 axons terminate correctly in the lamina and do not misproject into the medulla, as in control heterozygous animals. This demonstrates that *Alk* is not required for target layer specificity of R1-R6 axons in the lamina.

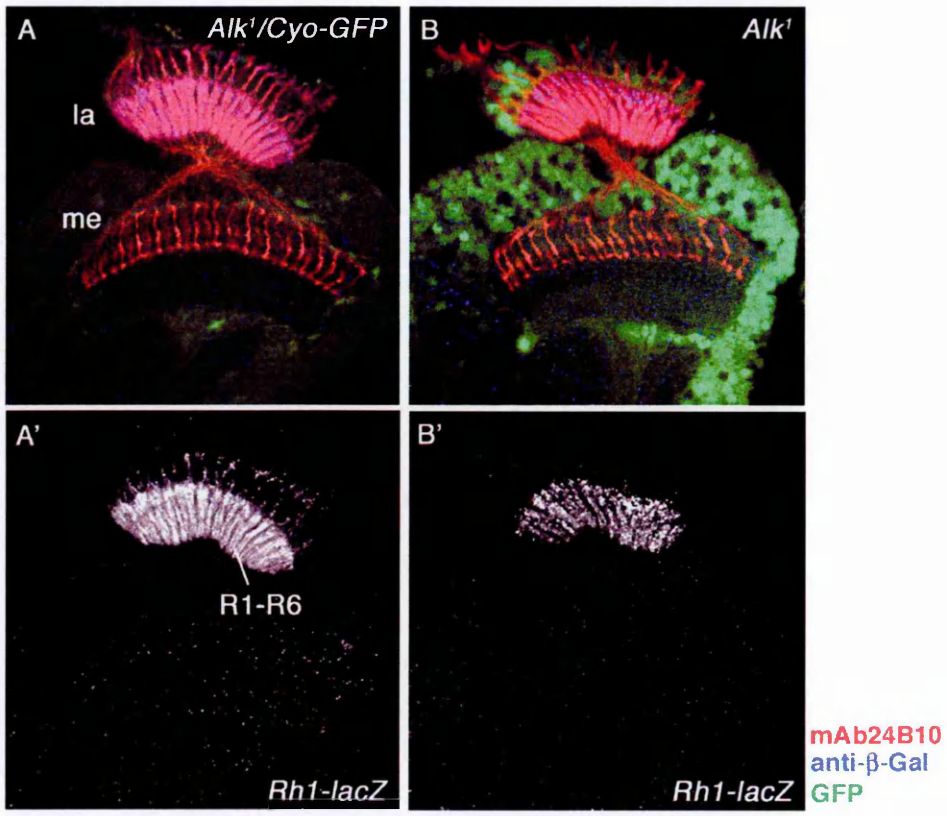

Figure 25. *Alk* is Not Required for R1-R6 Target Layer Specificity.

(A, A') Control heterozygous adult animals: *yw ey-Gal80; FRT42D Alk¹/ CyO Kr-GFP; lama-Gal4 UAS-FLP/ Rh1-lacZ.*

(B, B') Adult *Alk¹ ELF* animals: *yw ey-Gal80; Ub-GFP PCNA FRT42D/ FRT42D Alk¹; lama-Gal4 UAS-FLP/ Rh1-lacZ.* Somatic clones are visualized by the absence of GFP (green), whereas mAb24B10 (red) labels all R cells and their axons. Anti-β-Gal antibody labels R1-R6 axons (blue) terminating normally in the lamina in both controls and *Alk¹* mosaic animals.

4.2.9 *Alk* Plays a Role in the Selection of Postsynaptic Partners in the Lamina

Next, to assess whether Alk is required for the selection of appropriate postsynaptic partners by R1-R6 axons, transverse sections across the lamina were examined under the confocal microscope to visualize lamina cartridges. In the adult, these synaptic units consist of six photoreceptor axon terminals and dendrites of five lamina neurons (L1-L5). R1-R6 axons in each cartridge unit originate from a defined set of adjacent ommatidia and surround the processes of two lamina neurons, L1 and L2 (Meinertzhagen, 2000; Clandinin and Zipursky, 2002). The remaining lamina neurons,

L3, L4 and L5 are in the periphery. L3 and L4 axons are located adjacent to R5 and R6 axonal profiles, whereas L5 axon is found between R4 and R5. At the ultrastructural level, all processes can be identified within cartridges by their position relative to anterior or equatorial directions (Meinertzhagen, 2000). A simplified scheme depicting the complement of axons from lamina neurons and R-cells within the lamina cartridge unit is shown in Figure 26B.

To assess the assembly of lamina cartridges, pre-synaptic axons were labeled with anti-Highwire (Hw) antibody (Wan et al., 2000). In wild type animals, cartridge units are circular and are arranged in a regular array (n=18, Figures 26C, C'). Interestingly, in Alk^1 *ELF* mosaics, the array of these units appears disrupted. Furthermore, cartridges vary in size and morphology (n=43, Figures 26D, D'). Taken together, these data suggest that *Alk* is required for R1-R6 target selection of postsynaptic partners in the lamina.

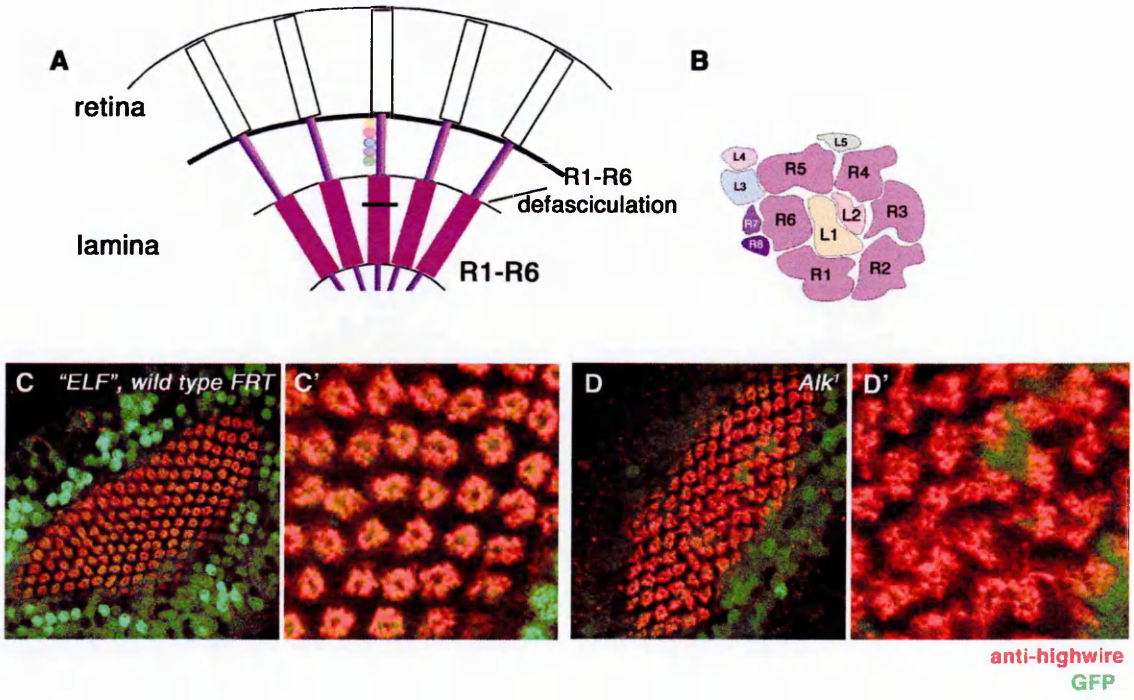

Figure 26. *Alk* is Required for Selection of Postsynaptic Partners in the Lamina.

(A) Scheme representing R1-R6 target layer specificity in the lamina in the adult.

(B) Scheme showing the main constituents of a cartridge unit, as observed in an ultrastructural transverse section of the lamina. R-cell axons surround the profiles of L1 and L2 axons. L3 and L4 axons are found adjacent to R5 and R6, and L5 axons are found between R4 and R5. B adapted from Meinertzhagen, 2000.

(C, C') Adult wild type *ELF* mosaic animals: *yw ey-Gal80; Ub-GFP PCNA FRT42D/ FRT42D; lama-Gal4 UAS-FLP mδ/ +.*

(D, D') Adult Alk^1 *ELF* animals: *yw ey-Gal80; Ub-GFP PCNA FRT42D/ FRT42D* Alk^1*; lama-Gal4 UAS-FLP mδ/ +.* Presynaptic units are visualized using Highwire antibody (red) and somatic clones are visualized by the absence of GFP. In Alk^1 mosaic animals the morphology and arrangement of lamina cartridges is irregular and their size is variable, compared to wild type. Processes of glial cells cover the space in between lamina cartridges. In both wild type and mosaic animals the majority of glial cells appear to have undergone mitotic recombination and are homozygous mutant for *Alk* (GFP-negative).

Due to the limited resolution of laser-scanning microscopic images, we were unable to determine how many lamina neurons in the disrupted cartridges are homozygous mutant or to fully demonstrate the extent of disruption in lamina cartridge assembly. To address this in greater detail, wild type and Alk^1 *ELF* mosaic animals were analyzed at the ultrastructural level (I. Salecker, unpublished observations). Consistent

with previous descriptions (Meinertzhagen, 2000), in electron microscopic sections of cartridges, pre- and postsynaptic components within each unit are clearly identified (Figure 27A-C). Glial processes surround each cartridge and send capitate projections into the photoreceptor axons (Fabian-Fine et al., 2003). These glial projections help to distinguish the profiles of R-cells from those of lamina neurons.

The presence of glial capitate projections and of darker T-bar areas, indicating formation of synaptic contacts, within R-cell axon profiles in Alk^1 mosaic animals, suggests that *Alk* does not affect lamina glia and that output synapses form normally. However, in contrast to wild type animals (Figure 27A), cartridge units in Alk^1 mosaic animals exhibited irregular shapes (Figures 27B and C). In particular, the variability in size observed under the laser-scanning microscope reflected an abnormal distribution of pre- and post-synaptic components in cartridge units at the ultrastructural level. Whereas in wild type (n=8, 54 cartridges) the majority of cartridges (80%) contained 6 R-cell profiles, in Alk^1 mosaic animals around 50% of cartridges (n=13, 69 cartridges) contained more than 8 ($\geq$7, up to 15) and less than 4 R-cell axons ($\leq$3) (Figure 27F). Interestingly, some large cartridge units were located in close proximity to smaller units, suggesting that there may be some exchange or intermixing of pre-synaptic terminals between neighbouring cartridges (Figures 27B and C). Taken together, these findings indicate that *Alk* is required for the correct assembly of the lamina cartridges and/or for the maintenance of the components within each unit.

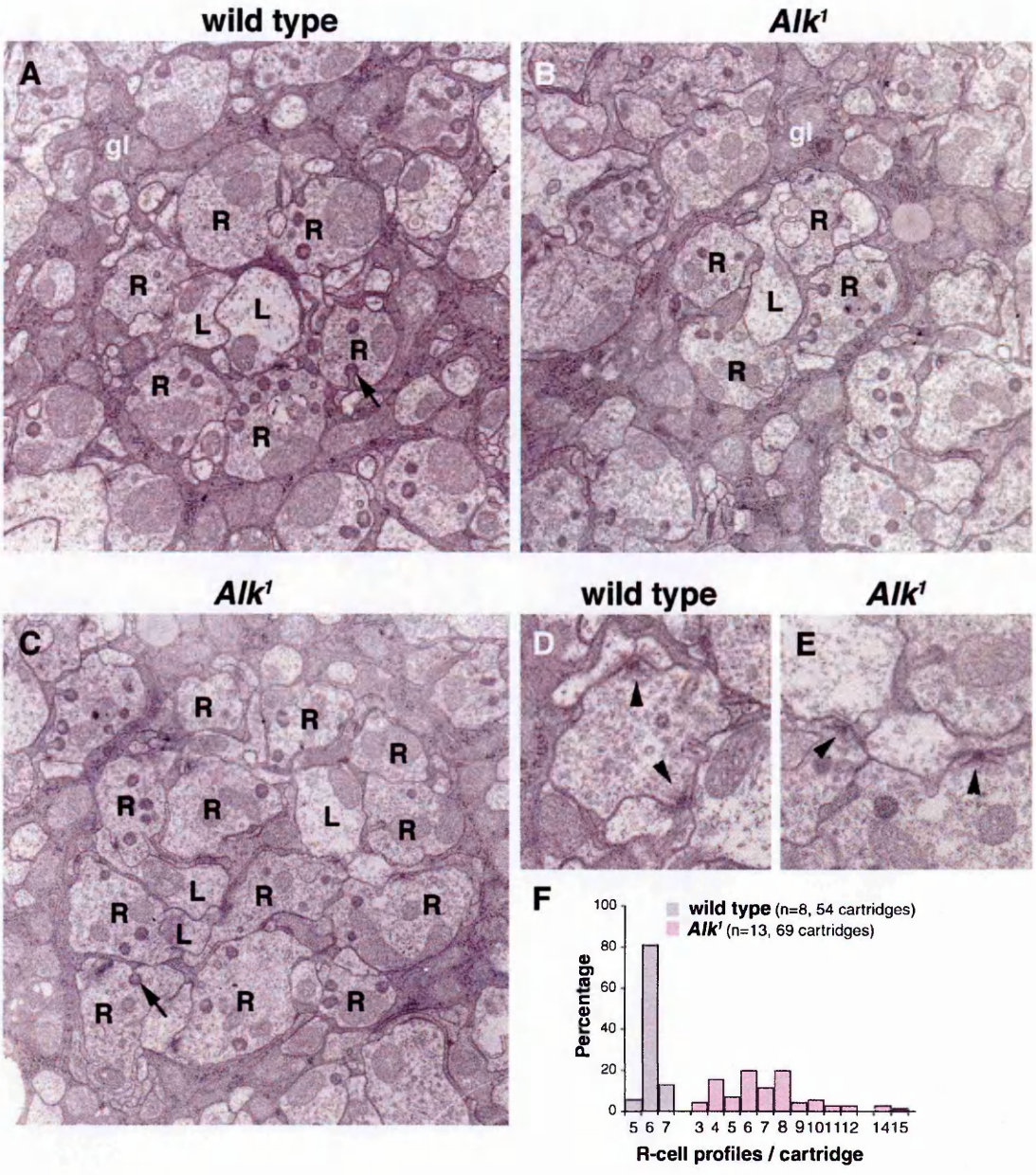

Figure 27. EM Sections Reveal an Irregular Distribution of Pre- and Post-Synaptic Units in the Lamina Cartridges of *Alk*^{1} *ELF* Animals.

(A, D) Wild type: *yw ey-Gal80; Ub-GFP PCNA FRT42D/ FRT42D +; lama-Gal4 UAS-FLP mδ/ +.* Projections of glial processes are characteristic of R-cell axon profiles (arrow in A and C).

(B, C, E) *Alk*^{1} *ELF* mosaic: *yw ey-Gal80; Ub-GFP PCNA FRT42D/ FRT42D Alk*^{1}*; lama-Gal4 UAS-FLP mδ/ +.* Output synapses are normal in *Alk*^{1} target mosaic animals (arrowheads).

(F) Distribution of R-cell terminals and lamina neuron profiles per cartridge in wild type and *Alk*^{1} mosaic animals. Figure kindly provided by I. Salecker.

4.2.10 Differentiation of R-cells is not Affected in *Alk ELF* Animals

Our loss of function analysis for *Alk* has revealed that it is required during pupal development for the R8 target layer specificity in the medulla and for connectivity between R1-R6 axons and their postsynaptic partners in the lamina. *Alk* is, therefore, non-cell-autonomously required in R-cells for target specificity. However, the guidance errors observed in Alk^1 target mosaic animals could be a consequence of defects in the formation of the eye.

To test this possibility, we used the R-cell-specific marker mAb24B10 to examine the formation of ommatidial clusters during 3rd instar larval stage (Figures 28A, B) and prepared plastic sections stained with toluidine blue to examine the position and morphology of individual R-cells in the adult (Figures 28C and D, I. Salecker, unpublished observations). Immunolabeling with mAb24B10 revealed regular rows of ommatidial clusters in Alk^1 target mosaics during late larval development (Figure 28B). Plastic sections of adult eyes stained with toluidine blue allowed the identification of individual R-cells by their position and morphology, and reveal normal arrangement of R-cells within the ommatidia of these animals. These findings suggest that the defects in pathfinding and targeting observed in Alk^1 target mosaic animals are not due to alterations in earlier steps of R-cell development.

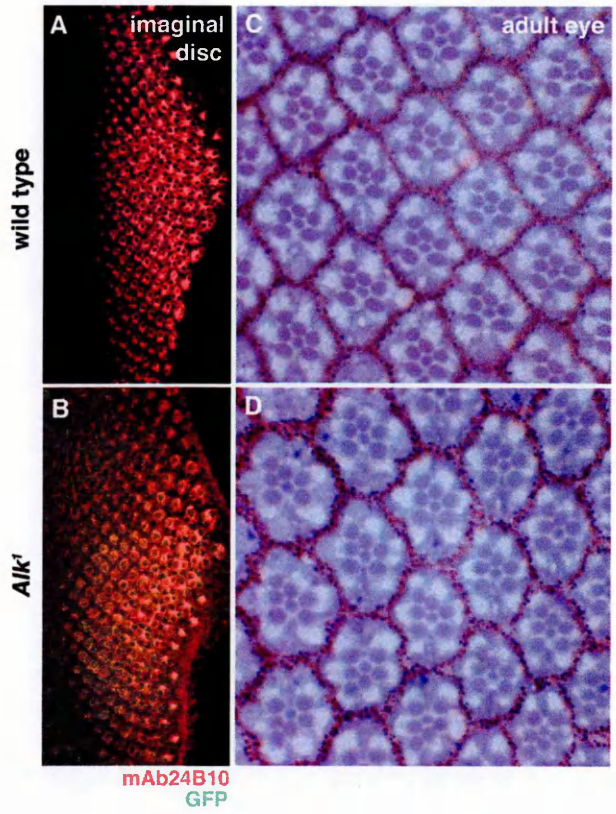

Figure 28. R cells Develop Normally in *Alk ELF* Animals.

(A, C) 3rd instar and adult wild type, respectively: *yw ey-Gal80; FRT42D Alk¹/ CyO Kr-GFP +; lama-Gal4 UAS-FLP mδ/ +.*

(B, D) 3rd instar and adult *Alk ELF* animals, respectively: *yw ey-Gal80; Ub-GFP PCNA FRT42D/ FRT42D Alk¹; lama-Gal4 UAS-FLP mδ/ +.* In A and B, R-cells in the eye imaginal disc are labeled using mAb24B10 (red). During 3rd instar larval stage R-cell clusters form regular rows. In the adult, plastic sections stained with toluidine blue reveal that in *Alk* target mosaics, ommatidia have a normal complement and arrangement of R-cells and normal polarity (D) when compared to wild type (C). C, D kindly provided by I. Salecker.

4.2.11 Cell-Autonomous Requirement of *Alk* in the Target

The observation that clone formation in the optic lobes of *Alk¹ ELF* mosaic animals appeared normal when compared to wild type indicated that proliferation of target cells is not affected. For this reason we focused on assessing the differentiation of target neurons and glia in the lamina and medulla. The development of lamina neurons was examined using Dachshund (Mardon et al., 1994) as an early differentiation marker of LPCs and lamina neurons (Figures 29A, B), Elav (Robinow and White, 1991) labeling

postmitotic differentiated neurons, and the L4- and L5-specific Brain-specific-homeobox (bsh) protein (Jones and McGinnis, 1993; Figures 29C, D). Analysis of Alk^1 mosaic and control animals with these markers demonstrated that target neurons differentiate normally in both optic ganglia. The development of glial cells was assessed using the glial-specific marker Repo (Campbell et al., 1994; Figures 29A, B). As in wild type, in Alk^1 *ELF* animals lamina glia form regular rows above and below the lamina plexus.

Our findings suggest that the projection defects observed in Alk^1 mosaic animals are not a consequence of errors in the differentiation or migration of neurons or glial cells. Our analysis revealed that *Alk* does not regulate basic aspects of neuronal fate per se. However, differentiation into different types of neurons was only assessed in L4 and L5 lamina neurons. To address whether lamina neurons L1, L2 and L3, as well as different subtypes of medulla neurons differentiate normally would require the use of additional markers for these subtypes.

Interestingly, *Alk* has been shown to promote cell survival and inhibit apoptosis when fused to nucleophosmin and in *in vitro* studies (Stoica et al., 2001; Bowden et al., 2002; Motegi et al., 2004). In the fly optic lobe, cell death has been described to occur during the proliferation and early differentiation of ganglion cells (Meinertzhagen and Hanson, 1993). Within the proliferation zones, degenerating cells are visible towards the end of the proliferative period, i.e., about 20 hours of pupal development in the proliferation zone of the medulla and about 5-10 hours later in the proliferation zones of the lamina neuropil (Meinertzhagen and Hanson, 1993).

To assess cell survival in Alk^1 mosaic animals, we used an antibody raised against activated Caspase-3, a protease that is involved in cleavage of proteins essential for cell stability and activation of DNases that lead to DNA fragmentation (reviewed in Nagata, 2000). At 24 hours of pupal development, similar sets of neurons in the lamina

and medulla are undergoing programmed cell death in both heterozygous and Alk^1 mosaic animals (Figures 29E, F). Interestingly, in addition to some neurons in the lamina and medulla, this antibody also labels processes of neurons extending in the medulla and lobula complex neuropils. Levels of activated Caspase-3 expression are not different between wild type and mosaic animals. Taken together, these results suggest that *Alk* is not required for the regulation of differentiation or survival of target neurons in the optic lobe.

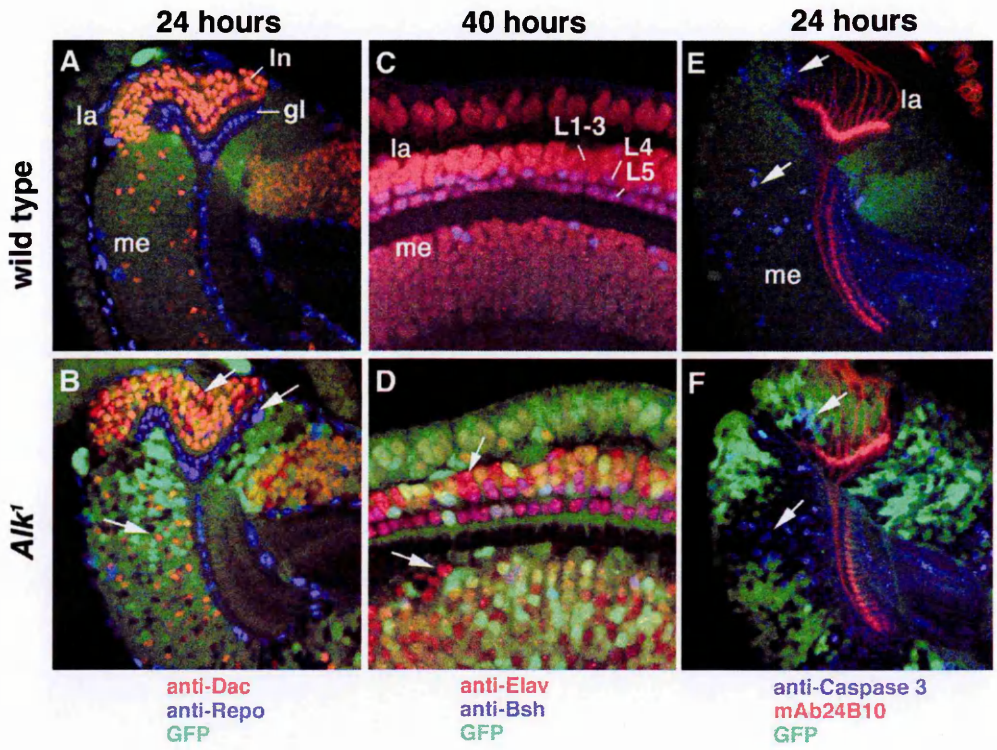

Figure 29. Target neurons and Glia Develop Normally in *Alk ELF* Animals.

(A, C, E) Wild type: *yw ey-Gal80; FRT42D Alk^1/ CyO Kr-GFP +; lama-Gal4 UAS-FLP mδ/ +.* (B, D, F) *Alk^1 ELF* animals: *yw ey-Gal80; Ub-GFP PCNA FRT42D/ FRT42D Alk^1; lama-Gal4 UAS-FLP mδ/ +.*

(B, D) *Alk* homozygous mutant neurons express the early differentiation marker Dachshund (red, arrows in A, B), as well as the late differentiation markers Elav and Bsh (red and blue in C, D, respectively). Mutant Glial cells for *Alk* also develop normally as visualized with anti-Repo labeling (blue, arrows in A, B).

During early pupal development some neurons undergo apoptosis in wild type (E). Similar levels of cell death, as visualized with activated anti-Caspase-3 (blue in E, F), are observed in *Alk^1 ELF* animals (arrows in F).

Due to a lack of specific markers for the different neuronal subtypes in lamina and medulla, I used the MARCM technique (Mosaic Analysis with a Repressible Cell Marker, Lee and Luo, 1999) to positively label target neurons in the adult and to assess whether or not *Alk* is required in these cells for extending dendrites or for choosing the correct target layer. Lamina neuron processes have been characterized in both lamina and medulla neuropils (Figure 30), whereas the medulla contains more than 50 different subtypes of neurons (Fischbach and Dittrich, 1989; Meinertzhagen and Hanson, 1993).

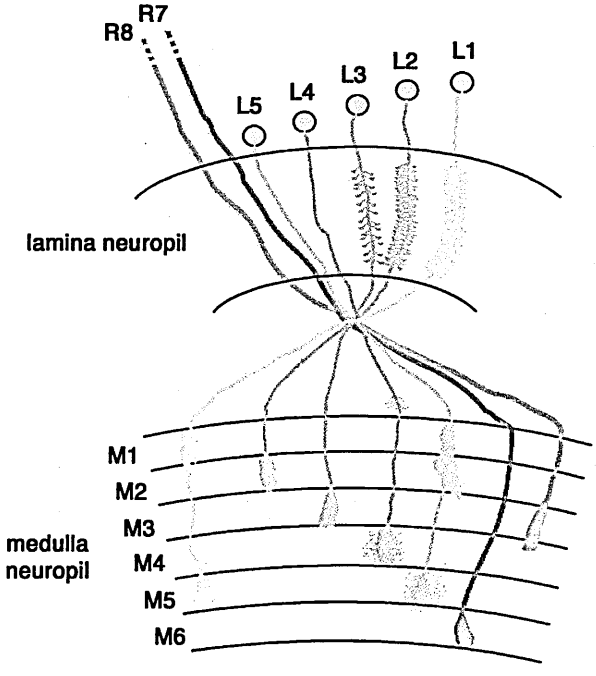

Figure 30. Lamina Neurons Innervating the Medulla Neuropil.
R7 and R8 axons extend from the eye and terminate in the M6 and M3 layer of the medulla neuropil, respectively. Lamina neurons have distinct patterns of arborizations and projections in lamina and medulla. L1 and L2 have elaborate dendrites in the lamina neuropil, whereas L3 have more scarce dendrites. L1 innervates layers M1 and M5, and L2 and L3 innervate single layers, M2 and M3, respectively. L4 and L5 axons do not possess dendrites. L4 innervates the M4 layer, whereas L5 innervates M1, M2 and M5 layers. Adapted from Fischbach and Dittrich, 1989.

To further assess the cell-autonomous effect of *Alk* on target neuron development, we focused on the morphology of dendrite arborizations and axonal projections of lamina neurons using the MARCM system. Using *elav-Gal4* as a driver, lamina neurons

were made homozygous mutant for Alk^1 and were labeled by GFP. R-cells and their axons were labeled using mAb24B10 in horizontal sections and anti-Highwire in transverse sections of the lamina. In Alk^1 MARCM mosaic animals (n=92) mutant lamina neurons extend elaborate dendritic spines as in wild type (n=48) (Figures 31A-A', D-D'). Furthermore, mutant lamina neurons extend axons, which appear to terminate in the appropriate layers of the medulla (Figures 31B-B'). Although the projection pattern of individual mutant medulla neurons could not be compared to wild type due to absence of specific medulla neuron markers, our findings reveal that these cells form processes in the medulla neuropil. Together, these data suggest that *Alk* is not required for the basic aspects of dendritogenesis and axonal outgrowth in target neurons.

In Alk^1 MARCM mosaic animals (n=15), transverse sections of lamina revealed that smaller or larger cartridges contained mutant *Alk* lamina neurons, when compared to wild type animals (n=15) (Figures 31C-C', D-D'). As in wild type animals, mutant lamina neurons form dendritic spines between the profiles of retinal axons of their respective cartridge, however, they occasionally appear larger and less regular in some large and irregular-shaped cartridges (Figures 31D-D"). These findings suggest that basic aspects of formation of branches is normal, however, the resolution is not high enough to evaluate whether all aspects of branch formation are normal. Furthermore, a more systematic analysis of target columns and columns of origin could help us distinguish between *Alk* requirement in cartridges of the original column or of the target column, as it has been demonstrated for Cad-N (Prakash et al., 2005).

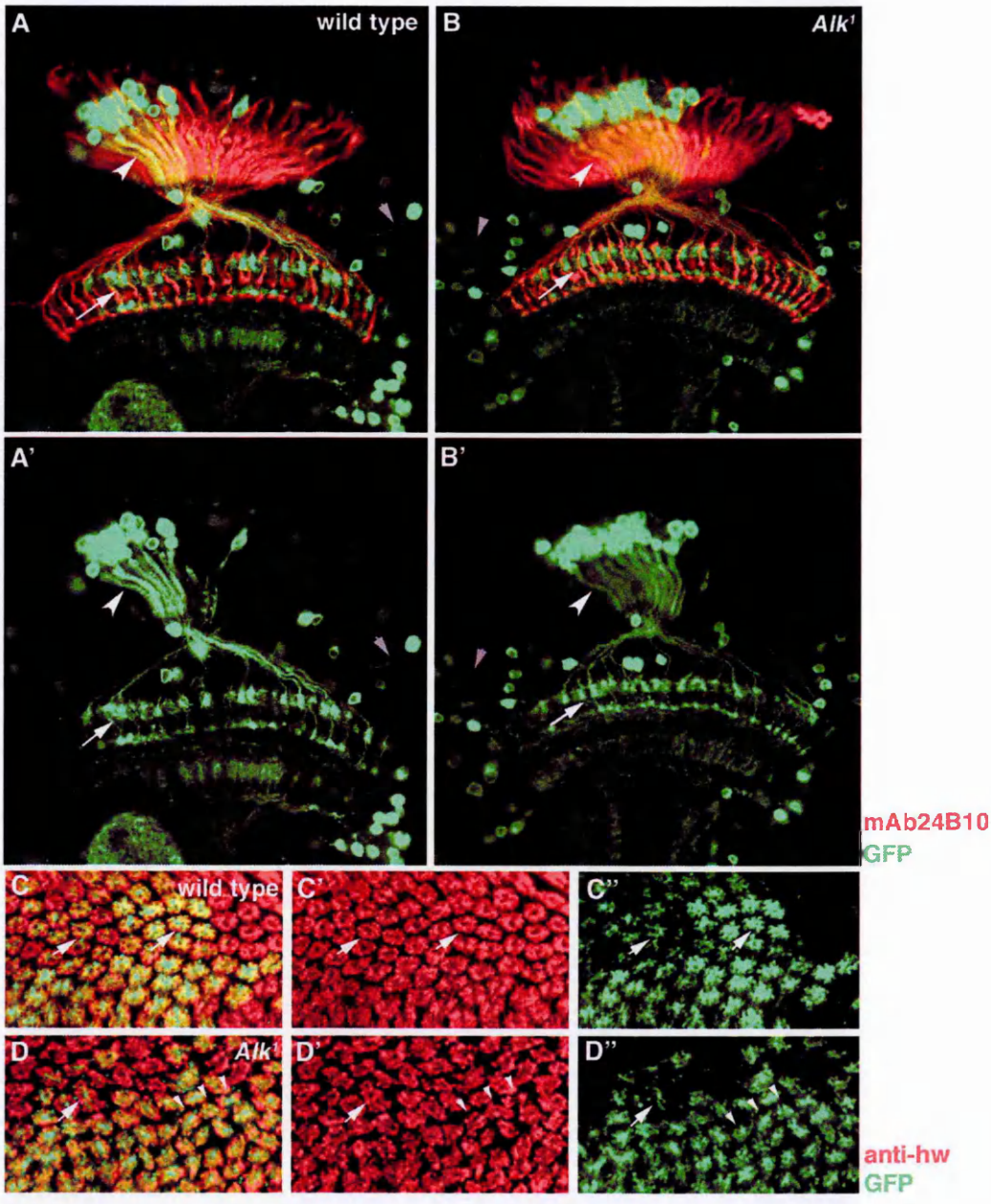

Figure 31. *Alk* does Not Appear to be Required in Lamina Neurons for Dendritogenesis and Axon Arbor Formation.

(A-A', C-C") Adult wild type MARCM animals: elav$_{C155}$-*Gal4, UAS-cd8GFP hs-FLP*^{122} *FRT42D tubP-Gal80/ FRT42D +*. (B-B', D-D") Adult *Alk*^{1} MARCM animals: elav$_{C155}$-*Gal4; UAS-cd8GFP hsFLP*^{122} *FRT42D tubP-Gal80/ FRT42D Alk*^{1}. Lamina neurons and their axons are labeled by GFP (green). R-cell axons are labeled by mAb24B10 (red in A, B) and anti-Highwire (red in C-C' and D-D').

As in wild type, lamina neurons form elaborate dendrites in the lamina in *Alk*^{1} target mosaic animals (arrowheads in A', B'). Moreover, they appear to project axons that terminate in the appropriate layers of the medulla (arrows in A', B'). In sections across the lamina, dendritic spines are present in each cartridge (arrows in C-D"), even when cartridge units appear irregular (arrowheads in C-D").

4.3 Loss-of-Function Analysis of *jelly belly*

4.3.1 The *jeb*$^{l(2)SH0422}$ Allele

Jeb has been shown to act as the activating ligand for Alk in the developing visceral mesoderm of *Drosophila* (Englund et al., 2003). To test whether the same applies in the visual system, we undertook a loss-of-function approach for *jeb*. The first published allele, *jeb*^{KG05644} exhibiting differentiation defects in the visceral mesoderm (Weiss et al., 2001; Englund et al., 2003), produced a "rough" eye phenotype when removed from R-cells using the *ey-FLP* system. Subsequent genetic tests revealed that the stock carried other P-element insertions and at least one additional lethal mutation, which may have been responsible for the eye phenotype (I. Salecker, unpublished observations). We therefore tested another lethal allele, *jeb*$^{l(2)SH0422}$, identified in a screen for mutations caused by single P-element insertions on the second chromosome (Oh et al., 2003). We showed that this allele failed to complement with *jeb*^{KG05644} and *Df(2L)BSC40*, which disrupts *jeb* transcription. To confirm the P-element insertion and determine its site, I used inverse PCR. Sequence analysis of the cDNA fragment produced showed that the insertion lies within the intron between the two exons of the *jeb* locus (position 7627278) (Figure 32C).

4.3.2 *jeb* is not Required during the 3rd Instar Larval Stage

To test whether *jeb* is required for the formation of the R-cell projection pattern, we generated *jeb*$^{l(2)SH0422}$ mosaic animals using the *ey-FLP* system (Newsome et al., 2000a), inducing mitotic recombination in the majority of R-cells but also in some cells in the target. To increase the size of somatic clones, a cell lethal mutation in *PCNA* was used. Removing *jeb* function using this tool did not cause any defects in the R-cell projection pattern during 3rd instar larval stage (Figure 32B). When compared to wild type (Figure 32A), *jeb*$^{l(2)SH0422}$ mosaic animals exhibit reduced expression of Jeb in R-cell axons and

their growth cones (Figure 32B'). The residual Jeb staining could be originating from heterozygous R-cells in the eye. Similar results are obtained when *jeb* was removed specifically from the eye, using the $ey^{3.5kb}$-*FLP* system (I. Salecker, unpublished observations). These findings show that *jeb* is not required for the initial target selection of R-cells during 3rd instar larval stage.

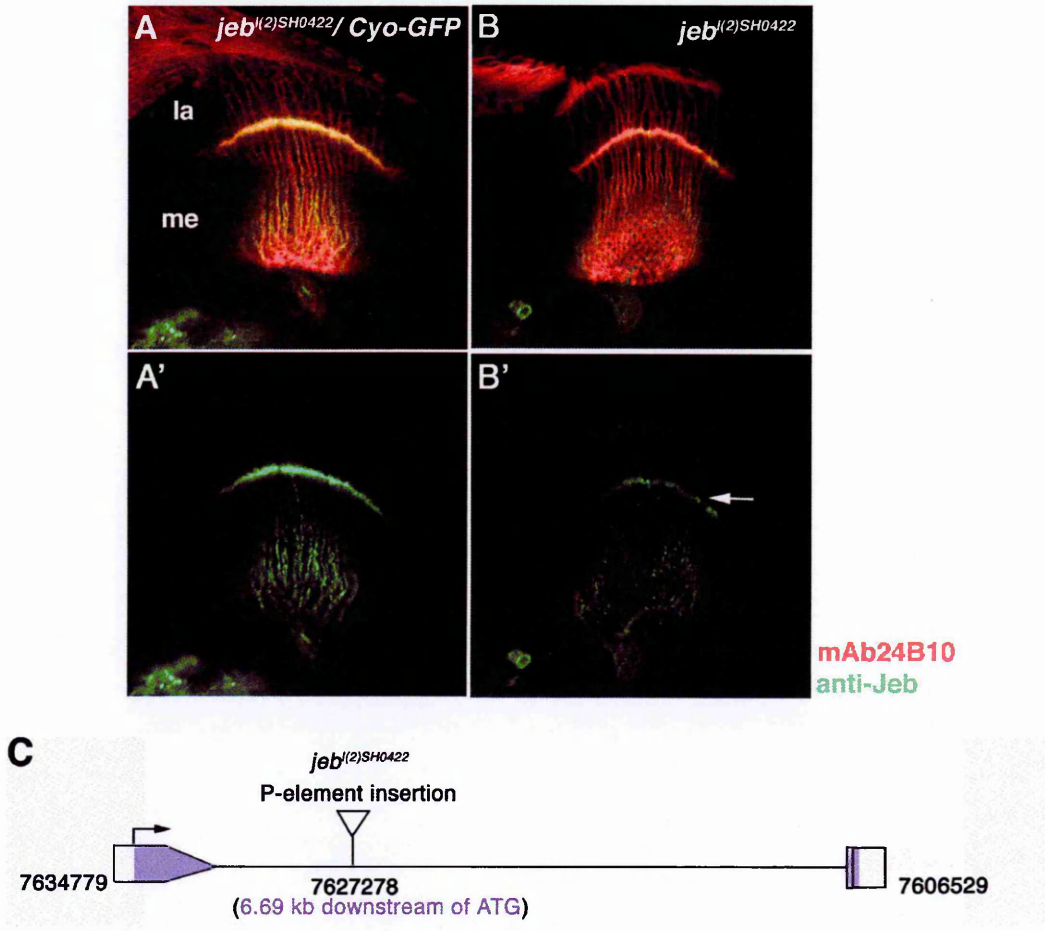

Figure 32. *jeb* is not Required in R-cells during Larval Development.

(A, A') Wild Type

(B, B') 3rd instar $jeb^{l(2)SH0422}$ mosaic: *ey-FLP; FRT42D PCNA/ FRT42D* $jeb^{l(2)SH0422}$. This system allows mitotic recombination and generation of somatic clones in the eye and also in the optic lobe. The R-cell projection pattern during 3rd instar larval stage visualized by antibody staining (mAb24B10, red) is normal in $jeb^{l(2)SH0422}$ eye mosaic animals. Jeb expression (detected by an anti-Jeb antibody, green) decreases in R-cell axons.

(C) Scheme illustrating the P-element insertion in the $jeb^{l(2)SH0422}$ allele.

4.3.3 Differentiation in both the Eye and the Target is Normal in *jeb*$^{l(2)SH0422}$ Mosaic Animals

Since Jeb is expressed in R-cells, removing its function from the eye could result in irregular assembly of ommatidial clusters and defects in the differentiation of R-cells. Therefore, the development of R8 in the ommatidial clusters in the developing eye was assessed using an antibody against Senseless (Sens) (Nolo et al., 2000). R8 cells in *jeb*$^{l(2)SH0422}$ eye mosaic animals express Sens (Figure 33C), suggesting that *jeb* is not required for R8 differentiation during larval development. To assess whether *jeb* is required in any of the late steps in the differentiation process of R-cells or their polarity, plastic sections of adult *jeb*$^{l(2)SH0422}$ mosaic eyes were stained with toluidine blue and analyzed. Sections that reveal both levels of R7 and R8 cells demonstrated that each ommatidium contains a full complement of R-cells that have normal morphology and spatial arrangement (I. Salecker, unpublished observations, Figures 33A, A').

As retinal innervation is very important for the differentiation of neurons and glia in the optic lobe, lack of *jeb* in R-cell afferents could elicit differentiation defects in the target. We therefore tested the expression of several differentiation markers in *jeb*$^{l(2)SH0422}$ mosaic animals during pupal development. Dachshund and Repo show a normal pattern of expression in the *jeb*$^{l(2)SH0422}$ mosaic animals at 24 hours of pupal development (Figures 33D, E). At 40 hours of pupal development, Elav and Bsh are also expressed normally in target neurons (Figures 33F, G). These results show that consistent with our findings in *Alk ELF* mosaics, *jeb* is not required for the differentiation of R-cells or target cells.

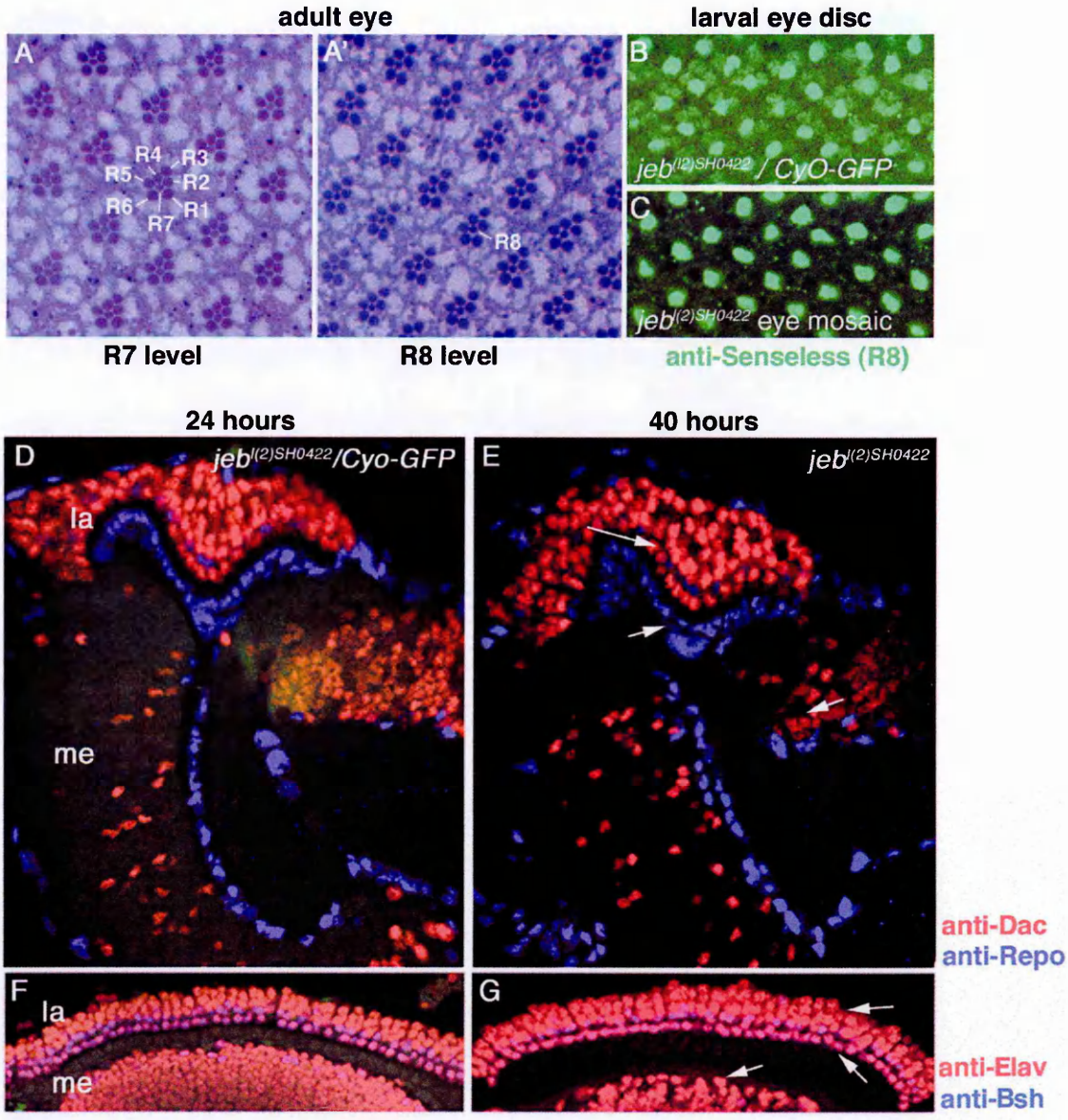

Figure 33. Differentiation of R-cells and Target Cells is Normal in *jeb*$^{l(2)SH0422}$ Eye Mosaic Animals.

(A, A', C, E, G) *jeb*$^{l(2)SH0422}$ eye mosaic: *ey-FLP; FRT42D PCNA/ FRT42D jeb*$^{l(2)SH0422}$.

(B, D, F) Wild type: *ey-FLP; FRT42D jeb*$^{l(2)SH0422}$ */ CyO Kr-GFP.*

Ommatidia in *jeb*$^{l(2)SH0422}$ eye mosaic animals show a normal complement and arrangement of R-cells, as visualized by toluidine blue (A, A'). R8 cells express anti-Senseless (green) in both wild type and *jeb*$^{l(2)SH0422}$ mosaic animals (B, C). Early neuronal and glial differentiation markers (anti-Dachshund, red and anti-Repo, blue in D and E) as well as late neuronal differentiation markers (Elav, red and Bsh, blue in F and G) are expressed normally in *jeb*$^{l(2)SH0422}$ eye mosaic animals.

4.3.4 *jeb* is Required for R8 Targeting in the Medulla

Similarly to *Alk* target mosaic animals, $jeb^{l(2)SH0422}$ eye mosaic animals do not exhibit any R-cell projection defects during 3rd instar larval stage. Intriguingly, removing *jeb* function from R-cells reproduces the same R8 phenotype observed in *Alk* target mosaic animals during late pupal development. To distinguish between a strict requirement of *jeb* in the eye and a partial requirement in the target, where it is found after midpupal development, two different genetic tools were used for this study (Figure 34B, C). The *ey-FLP* system induces mitotic recombination in both the eye and some target neurons, and the $ey^{3.5kb}$*-FLP* system restricts the recombination events to the eye. In the latter, we used a *clR-11* lethal mutation to increase the size of the somatic clones. The R8 projection pattern was assessed by labeling subpopulations of R8 cells and their axons using an *Rh6 lacZ* marker in adult $jeb^{l(2)SH0422}$ mosaics (n=6 for each *ey-FLP* approach, Figures 34B-C'). Whereas in control animals R8 terminals were found in the correct layer (Figure 34A, A'), in $jeb^{l(2)SH0422}$ mosaic animals using both *ey-FLP* approaches, R8 misprojected to the R7 recipient layer (3/75, n=3), yet more frequently were found to prematurely stop at the distal border of the medulla neuropil (23/75, n=3) (Figures 34B-C'). R7 terminals appeared to terminate properly in their recipient layer in all the samples examined.

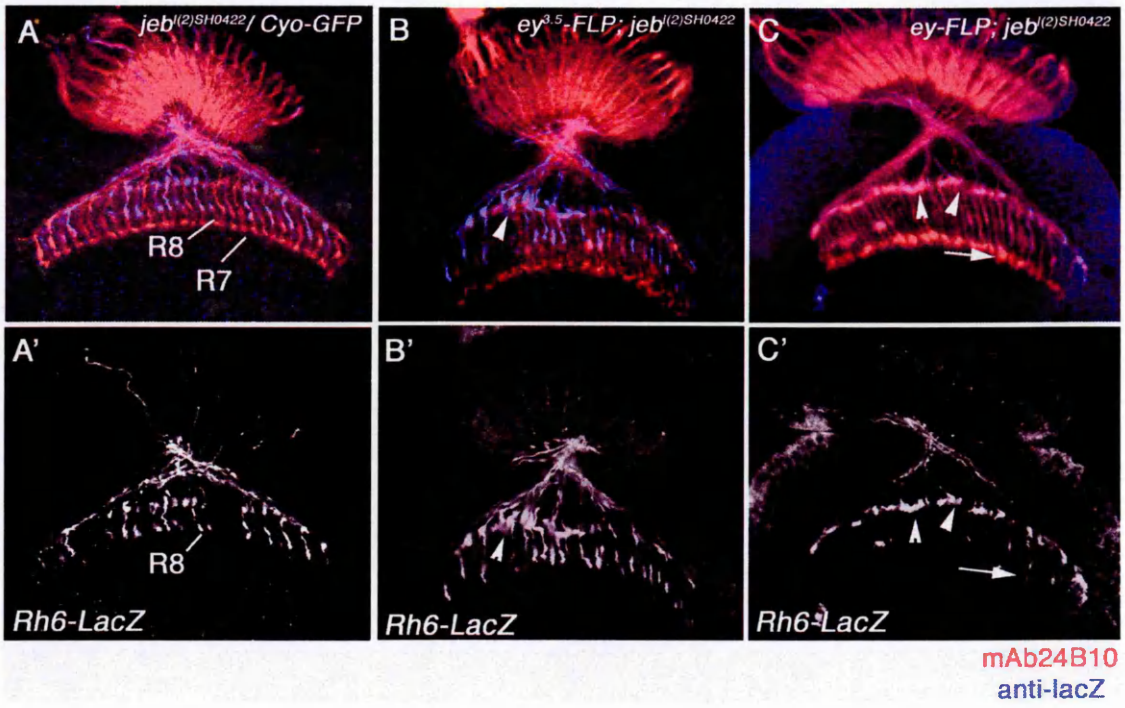

Figure 34. *jeb* is Required in the Eye for R8 Target Layer Specificity.
(A, A') Adult wild type: *ey-FLP; FRT42D jeb*$^{l(2)SH0422}$ */ Cyo Kr-GFP; Rh6-lacZ/+.*
(B, B') Adult *jeb*$^{l(2)SH0422}$ eye mosaic: *ey-FLP; FRT42D PCNA/ FRT42D jeb*$^{l(2)SH0422}$*; Rh6-lacZ/+.*
(C, C') Adult *jeb*$^{l(2)SH0422}$ eye mosaic: *ey*$^{3.5}$*-FLP; FRT42D PCNA/ FRT42D jeb*$^{l(2)SH0422}$*; Rh6-lacZ/+.*
A subgroup of R8 axons is labeled with an *Rh6-lacZ* transgene (blue) whereas mAb24B10 (red) labels all R cell axons. In both *jeb*$^{l(2)SH0422}$ eye mosaic animals, R8 terminals are thickened and axons often are found in the distal border of the medulla neuropil (arrowheads in B-C') or misproject to the R7 recipient layer (arrow in C-C').

Comparing the two *ey-FLP* approaches, the R8 phenotype appeared less severe in *jeb*$^{l(2)SH0422}$ mosaic animals in which the target cells are wild type (i.e., the ones generated with the *ey*$^{3.5kb}$*-FLP* driver). This could indicate that either recombinase activity is stronger in the *ey-FLP* system or that there is a weak requirement of *jeb* in target cells. Using the ELF system to generate homozygous mutant *jeb* clones specifically in the target showed no phenotype in the R-cell projection pattern (Figure 35B), suggesting that the differences in the strength of the phenotype using either *ey-FLP* approach to remove *jeb* from the eye may reside in differences in the strength of their recombinase activity in the eye.

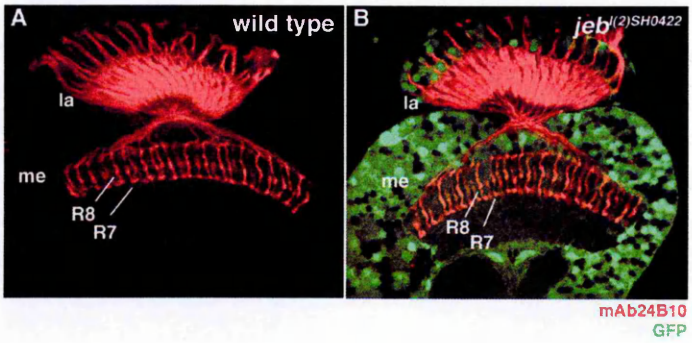

Figure 35. *jeb* is Not Required in the Target.

(A) Adult wild type.

(B) Adult *jeb*$^{l(2)SH0422}$ ELF mosaic: *yw ey-Gal80; Ub-GFP PCNA FRT42D/ FRT42D jeb*$^{l(2)SH0422}$; *lama-Gal4 UAS-FLP mδ/ +*. Somatic clones are visualized by the absence of GFP (green) while R-cells are visualized with mAb24B10 (red). R8 terminate correctly in their recipient layer in the medulla (me). Lamina (la).

Next, to show that *jeb* function is required during development, the R-cell projection pattern was assessed in *jeb*$^{l(2)SH0422}$ eye mosaics during different pupal stages using mAb24B10. Similarly to the onset of the *Alk*-induced phenotype in the medulla, R8 mistargeting was also observed around 55-60 hours of pupal development in *jeb*$^{l(2)SH0422}$ eye mosaic animals (n=7 for ~55 hours, Figure 36C).

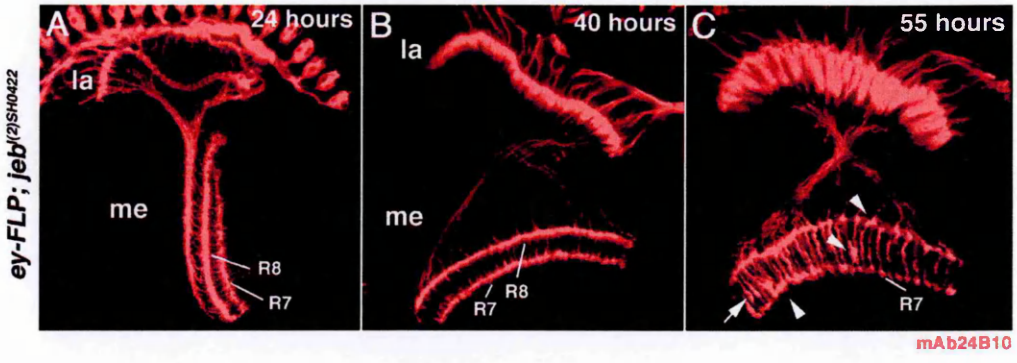

Figure 36. R8 Targeting Phenotypes Arise around 55 hours in *jeb*$^{l(2)SH0422}$ Eye Mosaic Animals.

(A-C) *jeb*$^{l(2)SH0422}$ eye mosaics: *ey-FLP; FRT42D PCNA/ FRT42D jeb*$^{l(2)SH0422}$. R-cell axons are visualized with mAb24B10 (red).

(A, B) Up to 40 hours of pupal development R8 terminate correctly in the distal part of the medulla neuropil. (C) By 55 hours, a few R8 terminals terminate in their recipient layer (arrow), whereas others are mispositioned in adjacent columns or in inappropriate layers of the medulla (me) (arrowheads). R7 terminate correctly during all stages. (la, lamina).

In our loss-of-function analysis of *jeb*, we showed that it is cell-autonomously required in R-cells for target layer specificity of R8 in the medulla neuropil during pupal development and regulates the same R8 targeting steps as *Alk*. Taken together, these findings indicate that Jeb is involved in this process in a common pathway with Alk, by acting as its activating ligand in the medulla.

4.3.5 *jeb* is Required for the Selection of Postsynaptic Partners by R1-R6 Axons in the Lamina

To assess whether *jeb* is also required for the assembly of lamina cartridges, transverse sections across the lamina were examined in adult $jeb^{l(2)SH0422}$ eye mosaic animals using both *ey-FLP* approaches to generate mosaic eyes. R-cell axons were labeled with the pre-synaptic marker Highwire. Unlike wild type (Figure 37A), lamina cartridges in $jeb^{l(2)SH0422}$ mosaic animals using either system exhibited abnormal morphology and varied in size (n=30 and n=20, respectively, in Figures 37B, C). Some cartridges appeared very small and others very large (Figures 37B, C).

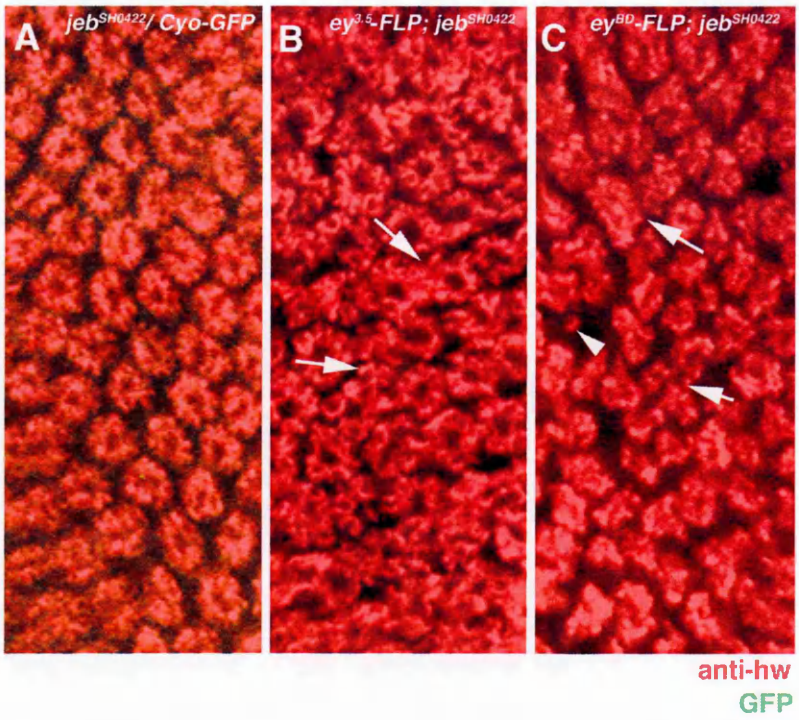

Figure 37. *jeb* is Required in R1-R6 for the Assembly of Lamina Cartridges.

(A) Adult control: *ey-FLP; FRT42D jeb$^{l(2)SH0422}$ / Cyo Kr-GFP.*

(B) Adult *ey-FLP jeb$^{l(2)SH0422}$* mosaic: *ey-FLP; FRT42D PCNA/ FRT42D jeb$^{l(2)SH0422}$.*

(C) Adult *ey$^{3.5}$-FLP jeb$^{l(2)SH0422}$* mosaic: *ey$^{3.5}$-FLP; FRT42D PCNA/ FRT42D jeb$^{l(2)SH0422}$*. R-cell axons are labeled with anti-Highwire (red). In *jeb$^{l(2)SH0422}$* mosaic animals, lamina cartridges are not orderly arranged and have variable morphology and size. Some cartridges are very small (arrowhead) and others very large (arrows).

To confirm the observations from the confocal microscope, the distribution of pre-synaptic units of *ey-FLP; jeb$^{l(2)SH042}$* and *ey$^{3.5}$-FLP; jeb$^{l(2)SH0422}$* mosaic animals was further assessed at the ultrastructural level (I. Salecker, unpublished observations). Abnormal distribution of presynaptic units per cartridge was evident in *jeb$^{l(2)SH0422}$* mosaic animals using both approaches. Using the *ey-FLP* approach, 31.6% of cartridges assessed contained either less than 5 (≤4) or more than 8 R-cell axons (≥7) (n=3, 322 cartridges), whereas with the *ey$^{3.5kb}$-FLP* approach this percentage was slightly smaller, 20.5% (n=4, 401 cartridges).

Together, these findings show that *jeb* is required for the assembly of lamina cartridges. Furthermore, the observation that removal of *jeb* from R-cells causes the

same phenotype as the one observed in *Alk* target mosaic animals, indicates that Jeb acts together with Alk for the formation of the R-cell projection pattern in both the lamina and medulla.

4.3.6 R1-R6 Projection Pattern During Pupal Development by Anterograde Labeling

The assembly of lamina cartridges in both *Alk* and *jeb* mosaic animals was assessed in adults. To show that, similarly to R8, the phenotype in the lamina arises as a consequence of targeting defect during development, we needed to pinpoint the stage during which this occurs. In wild type animals, each R1-R6 cell from a single ommatidium makes a projection of characteristic length and polarity and connects with post-synaptic lamina neurons from a different column (Clandinin and Zipursky, 2002). As R-cells in each ommatidium are not clonally related, a genetic approach for assessing defasciculation in individual retinal axon bundles has not been developed. R1-R6 axons from single ommatidia can instead be visualized by DiI anterograde labeling (Clandinin and Zipursky, 2000).

Using the ELF system to remove *Alk* from lamina neurons would not provide a good target background to assess R1-R6 projection pattern, as lamina neurons in each column are not clonally related and recombination events in target neurons occur in variable frequencies. Due to these technical limitations, the study was performed in $jeb^{l(2)SH0422}$ mosaic animals using the *ey-FLP* approach, with which the majority of R-cells can be made homozygous mutant (Newsome et al., 2000a). DiI crystals were placed on single ommatidia at 43 hours of pupal development, when defasciculation is complete and R-cell axons have not yet started to extend along the distal-proximal axis within the lamina.

Since Jeb is expressed in all R-cells, it is possible that it mediates interactions between R-cell axons in each ommatidial fascicle determining the trajectories of individual R1-R6 growth cones during or soon after defasciculation is initiated. 65 samples of $jeb^{l(2)SH0422}$ mosaic animals that took up the DiI in single ommatidia, produced 5 countable examples, which could be assessed for defective defasciculation. In these samples, most R1-6 growth cones appeared to defasciculate from the ommatidial bundle, however, they often chose an invariant pattern of projections and extended more filopodia, giving terminals an irregular morphology and length (Figure 38D) when compared with wild type terminals (Figure 38B, n=3). Taken together, these preliminary findings suggest that *jeb* is required during development for the selection of synaptic partners by R1-R6 axons. The phenotype caused by removing *jeb* from R-cells suggests that it does not prevent defasciculation, but appears to regulate the choice R-cell axons make after leaving their bundle.

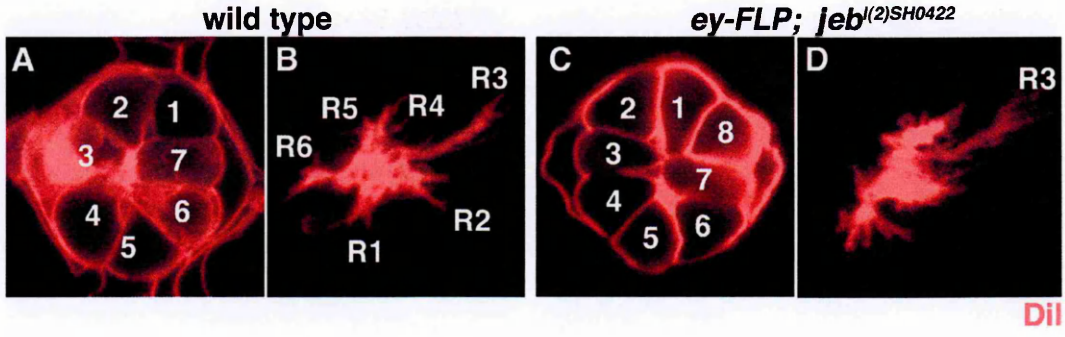

Figure 38. Defasciculation of R1-R6 Axons from the Original Bundle is Defective in $jeb^{l(2)SH0422}$ Mosaic Animals.

(A, B) Wild type. (C, D) $jeb^{l(2)SH0422}$ eye mosaic at 43 hours of pupal development: *ey-FLP; FRT42D PCNA/ FRT42D* $jeb^{l(2)SH0422}$.

(A, B) DiI-injected ommatidia (red) label all R cells (R8 is found below R7 in A).

(B) Stereotyped pattern of R-cell axons defasciculating from their original bundle at 43 hours of pupal development. (D) In $jeb^{l(2)SH0422}$ mosaic animals, some R-cell axon extensions appear irregular and more diffuse.

4.4 Cell Adhesion Molecules as Possible Downstream Targets of *Alk*

Removal of *Alk* from target cells and *jeb* from the eye results in inappropriate selection of postsynaptic partners by R1-R6 and R8 axons during pupal development. One possibility for the underlying mechanisms through which *Alk* and *jeb* regulate these processes may involve a later step in the differentiation of target cells. This would require the use of markers for specific subtypes of neurons, which are currently unavailable. In our working model, we tested the alternative possibility, that *Alk* and *jeb* modulate an axon guidance molecule. To identify candidate factors that could be modulated downstream of Alk signaling, I tested the expression of two cell adhesion molecules in Alk^1 target mosaic animals, Cad-N and Fmi.

N-Cadherin (Cad-N) is very strongly expressed in R-cell growth cones and ubiquitously in the lamina and medulla neuropils during pupal development. It is cell-autonomously required in R7 for target layer specificity and in R1-R6 for selecting their postsynaptic partners (Lee et al., 2001; Ting et al., 2005; Nern et al., 2005). There is, however, evidence that it is also required in lamina target neurons (Prakash et al., 2005).

To address whether Cad-N is modulated downstream of Alk signaling, its expression levels were tested in *Alk* mutant background. Since with the ELF system a large portion of target cells can consistently be made homozygous mutant, we used Alk^1 *ELF* target mosaic animals to test Cad-N expression levels in the medulla. During mid-pupal development, Cad-N is very strongly expressed in the lamina and medulla of Alk^1 target mosaic animals, when compared with wild type heterozygous animals (n=4, Figures 39A, B). In fact, Cad-N expression levels in Alk^1 *ELF* mosaic animals remain comparable with wild type until adulthood (n=6, Figures 39C, D). These preliminary findings suggest that Alk does not modulate the activity of Cad-N. This is consistent with previous findings that Cad-N is required in R7 for target layer selection, and not for R8 target specificity.

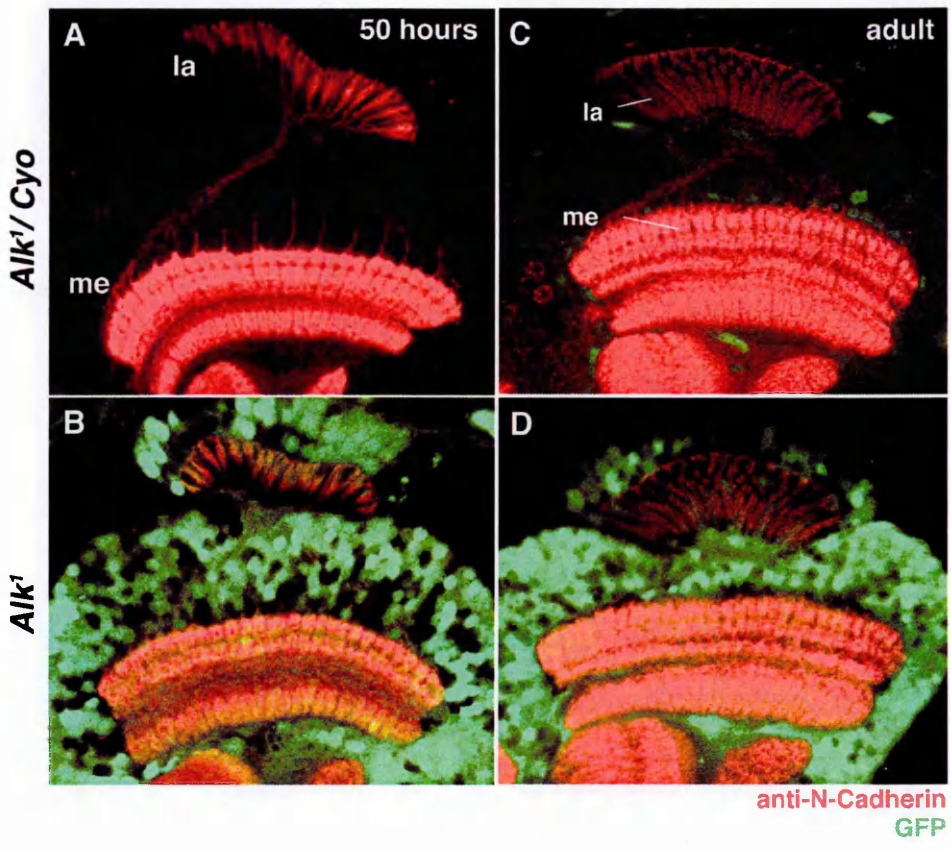

Figure 39. N-Cadherin Expression is Maintained in *Alk*^{1} *ELF* Animals.

(A, C) Wild type heterozygous animals: *yw ey-Gal80; FRT42D Alk*^{1}*/ CyO Kr-GFP; lama-Gal4 UAS-FLP/ +.*

(B, D) *Alk*^{1} *ELF* animals: *yw ey-Gal80; Ub-GFP PCNA FRT42D/ FRT42D Alk*^{1}*; lama-Gal4 UAS-FLP/ +.* Cad-N (red) is strongly expressed in all the medulla layers and at lower levels in the lamina neuropil at 50 hours of pupal development (B) and in the adult (D). Mosaic animals do not show any decreased levels of N-Cadherin expression at either stage when compared to wild type. Somatic clones are visualized by the absence of GFP (green). (la, lamina and me, medulla).

Flamingo (Fmi) has been described to be required in R-cells for the regulation of R8 target layer specificity and postsynaptic partner selection of R1-R6 axons in the lamina (Senti et al., 2003; Lee et al., 2003b).

A close examination of Fmi expression in the medulla revealed that, consistent with previous studies, at 17 hours of pupal development it is expressed in a broad band within the medulla neuropil (Figure 40A) (Senti et al., 2003). However, at 50 hours of pupal development Fmi is detected in two bands, separated by a layer that does not

express it (Figure 40C). During this stage of development, R8 axons remain at the distal border of the medulla neuropil. By 60 hours of pupal development, there is an additional layer expressing Fmi, also separated from the other two by a layer that does not express it. At this stage, R8 axons project into the second layer of the medulla neuropil expressing Fmi, which is the developing M3 layer (Figure 40E). In Alk^1 target mosaic animals, Fmi expression is maintained until 50 hours (n=10) (Figures 40B, D). However, at 60 hours of pupal development, the second layer shows reduced expression of Fmi in some columns in Alk^1 target mosaic animals (n=4) (Figure 40F). Loss of Fmi staining is variable in columns within this layer, probably due to the size and nature of the mutant medulla neurons in these animals. Taken together, these data suggest that the cell adhesion molecule Fmi is downregulated in a layer-specific manner in the Alk^1 target mosaic animals during a stage at which the R8 mistargeting phenotype arises. This raises the possibility that Flamingo is a downstream target of activated Alk in the medulla, required for the regulation of R8 target layer specificity.

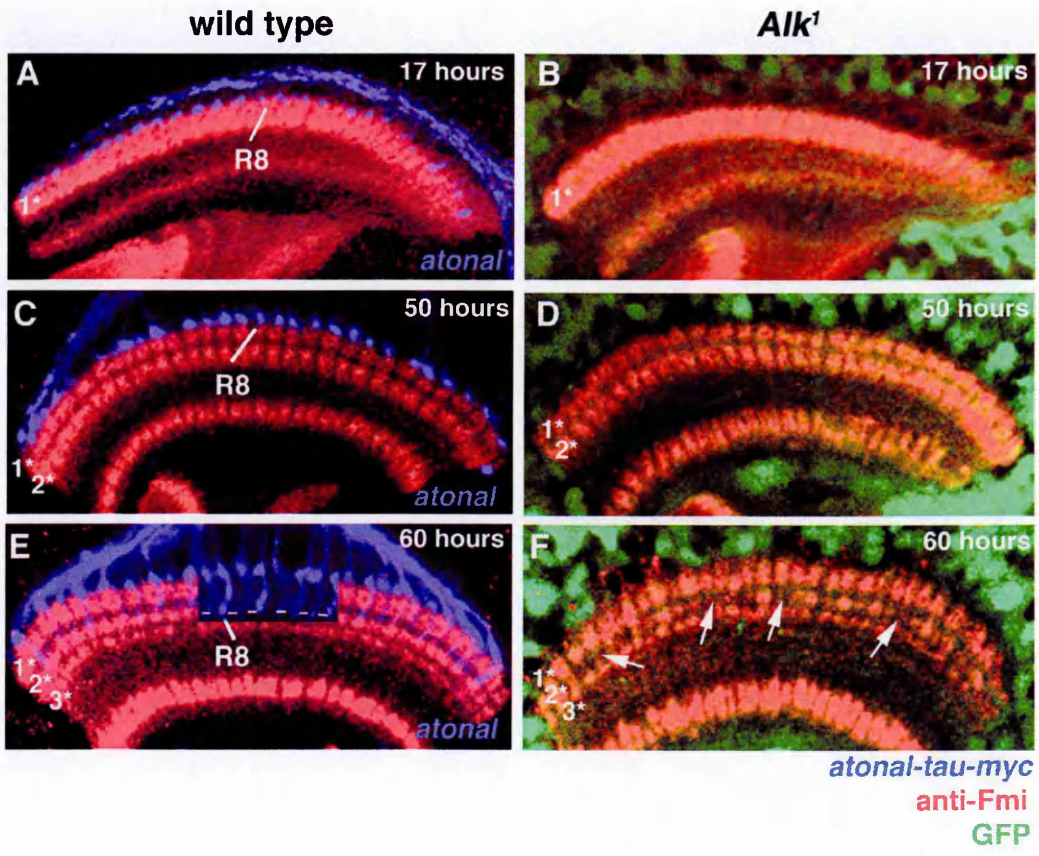

Figure 40. Flamingo Expression Levels Seem to Decrease in Some Columns of Specific Medulla Sublayers in *Alk*^{1} *ELF* Animals.

(A, C, E) Controls: *ato-τ-myc/ ato-τ-myc.*

(B, D, F) *Alk*^{1} *ELF* animals: *yw ey-Gal80; Ub-GFP PCNA FRT42D/ FRT42D Alk*^{1}*; lama-Gal4 UAS-FLP/ ato-τ-myc.* Mosaic animals do not show any decreased levels of Fmi (red) expression at 17 hours of pupal development. Flamingo is expressed in a single thick sub-layer in the proximal medulla (asterisk in A and B). At 50 hours of pupal development, there are two layers expressing Fmi (asterisks in C and D). At 60 hrs of pupal development, three sub-layers of flamingo expression are generated in the medulla neuropil (asterisks in E and F). In *Alk*^{1} mosaic animals, Flamingo expression is decreased in some columns in the second sub-layer (arrows), which is innervated by R8 terminals. Somatic clones are visualized by the absence of GFP (green) and R8 axons are visualized using the *ato-τ-myc* transgene (blue).

4.5 Discussion

Following the identification of the receptor Alk and its activating ligand Jeb in the visceral mesoderm of *Drosophila* (Weiss et al., 2001; Englund et al., 2003; Loren et al., 2003), we showed that Alk and Jeb exhibit a highly dynamic and initially complementary expression pattern in the visual system during late larval and pupal development, when major reorganization events in axonal projections take place in the target. The receptor Alk is ubiquitously expressed in the medulla neuropil throughout pupal development, whereas in lamina neuron processes its expression increases during mid-pupal stages. Although the expression pattern of Alk in the target is reminiscent of other known phosphoproteins, such as PTP69D and Lar (Clandinin et al., 2001; Garrity et al., 1999; Newsome et al., 2000a), unlike them, it is not found in R-cells. Jeb is initially expressed in R-cells and their axons, however during mid-pupal development it is down-regulated in R-cell growth cones and is slightly up-regulated in processes of target neurons adjacent to R7 and R8 terminals. Since Jeb carries a secretory signal peptide and has indeed been shown to be secreted in vitro (Weiss et al., 2001), it is likely that Jeb is released from R-cell axon terminals and the staining in developing medulla layers reflects its uptake by target neurons expressing Alk. Although the range of Jeb diffusion in the lamina or its uptake by postsynaptic neurons are not yet known, it appears that at least initially, Jeb is released in a column-specific fashion in the medulla, closely adjacent to R8 axon terminals.

4.5.1 Alk Signaling Regulates Axon Guidance in the Fly Visual System

Removal of *Alk* function from the target and of *jeb* from R-cells indicated that R1-R6 and R8 axons extend towards inappropriate postsynaptic partners in the lamina and the medulla, respectively, during reorganization events in connections between R-cell axons and target neurons. Disruption of R1-R6 target specificity results in cartridge units with

abnormal morphology and variable size, whereas R8 terminals either fail to enter the medulla neuropil or misproject to the R7 recipient layer long before synapse formation occurs. These findings suggest that the receptor Alk and the secretory molecule Jeb regulate axon guidance in the developing visual system of *Drosophila* through a common signaling pathway.

4.5.2 Mistargeting During Development

Using anterograde labeling to visualize the trajectories of R1-R6 across the lamina as they form during mid-pupal development, we demonstrated that loss of *jeb* does not prevent defasciculation, but rather regulates the choice R-cell axons make after leaving their bundle. On the contrary, when the function of two other molecules involved in the formation of lamina cartridge assembly, *Cad-N* and *Lar,* is removed from R-cells, R1-R6 growth cones fail to defasciculate from their original bundle (Lee et al., 2001; Clandinin et al., 2001). Interestingly, the phenotype observed in $jeb^{l(2)SH0422}$ eye mosaics resembles the defects observed in *Fmi* eye mosaics, where most axons extend away from the ommatidial bundle but reach inappropriate synaptic partners and form extensive filopodia (Lee et al., 2003). These preliminary findings suggest that *Fmi* and *jeb/Alk* may regulate the same steps of target selection in the lamina, which may be distinct from those regulated by *Cad-N* and *Lar.*

Using the *ato-τ-myc* transgene to label R8 axons in the medulla, we demonstrated that in Alk^{1} target mosaic animals the R8 targeting defects arise at a stage when R8 terminals actually extend processes to deeper layers of the medulla neuropil, but not before. This underpins the notion that initial steps in the transition of R8 terminals from the temporary to the recipient layer have been affected. To observe and record the movement of the R8 terminals in living animals, one could label R8 axons using a *cd8GFP* transgene driven by an R8-specific marker expressed during the crucial

period of 50 to 60 hours of pupal development. Previous reports suggest that pupae can develop normally outside the pupa case from stage 40 onwards and that eye-brain complexes can develop normally in culture (Gibbs and Truman, 1998).

As the phenotype in the adult includes R8 mistargeting to adjacent columns in either the M3 or M6 layer of the medulla neuropil, these findings also reveal a role for *Alk* and *jeb* in regulating topographic map formation in the medulla. However, defects in topographic map formation usually manifest during earlier stages of projection pattern formation and show high penetrance (Garrity et al., 1996; Lee et al., 2003; Shinza-Kameda et al., 2006). In the absence of Alk signaling such phenotype is observed during the transition of R8 axons from the temporary layer to the developing M3 recipient layer, suggesting either that distinct aspects of topographic map formation are developmentally regulated by different mechanisms or that jeb/*Alk* rather have a more local effect in the target for the formation or maintenance of the topographic map.

Interestingly, the choice of several different synaptic partners by R8 axons in *jeb* and *Alk* mosaic animals, suggests a model in which at the distal end of the medulla neuropil in each individual column, the growth cone may "decide" on whether to enter the neuropil or remain at the distal end. At this stage, *Alk* could provide R8 terminals with an initial permissive cue to enter the neuropil. Subsequently, after R8 terminals enter the neuropil, they may receive various information for connecting with processes of neurons in the appropriate layer of the medulla neuropil, through a combination of attractive and repulsive guidance cues. *Alk* could regulate one or a combination of such cues. Alternatively, *Alk* could regulate the cell fate of target cells.

4.5.3 *Alk* and *jeb* do not Affect the Differentiation or Survival of the Eye or the Target

Similarly to the approach taken for the analysis of our screen candidates, to distinguish between a requirement of *Alk* or *jeb* for the normal development of the eye or the target area and a role in axon guidance, we subjected both mosaic animals to tests with R-cell and target cell-specific markers. Neuron- and glia-specific markers in the target were expressed normally in both mosaics and the assessment of the ommatidia assembly in the adult excluded the possibility that through retrograde signaling *Alk* may regulate R-cell differentiation. Furthermore, MARCM analysis showed that *Alk* is not required in target neurons for the formation of dendrites or extension of axons. The resolution of our analysis indicated that lamina and medulla neurons differentiate normally in *Alk* and *jeb* mosaic animals. However, the cell fate identity of different subpopulations of neurons in the two optic ganglia was not tested, apart from the fate of L4 and L5 lamina neurons.

So far there has been no evidence to show that R-cell axons develop greater affinity for particular subtypes of lamina neurons when they defasciculate from their original bundle. On the contrary, it has been demonstrated that at least for N-Cadherin, the contribution of a guidance signal from each lamina neuron in the target column to individual R1-R6 axons is equal (Prakash et al., 2005). However, cell-fate transformation amongst populations of medulla neurons could result in the loss of R8-specific guidance cues from the recipient layer to another location, and thus be responsible for the mistargeting of R8 axons. To demonstrate that different populations of neurons in each optic ganglion differentiate normally in the absence of Alk signaling, one would need to identify more specific markers for lamina and medulla neurons expressed during later stages of development and test them in *Alk* and *jeb* mosaic animals.

4.5.4 Potential Downstream Effectors of Alk Signaling

An alternative explanation for the targeting defects observed in the absence of Alk signaling could be that upon Alk activation by Jeb, target cells activate or modulate one or more guidance cues. Since Alk is ubiquitously expressed in both lamina and medulla neuropils during pupal development, the regulation of R1-R6 and R8 axon final target selection may depend on either the restricted localization of its activating ligand or on the modulation of guidance molecules downstream of Alk signaling that have a more restricted expression pattern in these regions.

Whereas *Alk* is non-cell autonomously required in target neurons for the regulation of R-cell target specificity, *jeb* is cell-autonomously required in R-cells. Although removal of *jeb* specifically affects R8 axon targeting, it is expressed by both R7 and R8. To our resolution, Jeb appears to localize more strongly in the developing M3 layer of the medulla neuropil around 60 hours of pupal development, however, it is not known whether the source of Jeb in that region is R8 or R7 terminals. It would therefore be an interesting issue for further analysis to address the cell-autonomous role of *jeb* in individual R8 and R7 axons. An additional issue concerning *jeb*, is whether it is required in its original column or it can influence targeting of axons in adjacent columns. Using MARCM analysis to compare between single mutant R8 (or R7) axons and clones of adjacent mutant axons, could provide with some valuable information on these matters.

In the case where the specific function of *Alk* in R1-R6 and R8 is regulated by its downstream effectors, the activation/modulation of such factors could be achieved by their direct phosphorylation by activated Alk. Alternatively, it could be a result of the activation of the MAPK pathway regulating the transcription of downstream targets. In the visceral mesoderm of *Drosophila*, *Alk* has been shown to activate the MAPK pathway (Loren et al., 2001; Englund et al., 2003). One way to test whether the MAPK

is required in mediating axon targeting in the visual system as well, would be to test whether phenotypes observed in *Alk* target mosaic animals can be rescued by overexpressing activated Ras in the target. Such an approach, however, is likely to be inconclusive for the role of MAPK downstream of Alk signaling, as Ras overexpression in the optic lobe would cause upregulation of EGFR signaling, which uses the Ras/Raf/MAPK effector pathway (reviewed in Kurada and White, 1999). This could subsequently cause disruption of lamina neuron differentiation, which depends on EGFR signaling (Huang et al., 1998). Due to these technical limitations, the subsequent separation between Alk and EGFR signaling would not be possible in our working system and thus the hypothesis that *Alk* signals through the MAPK pathway in the visual system of *Drosophila* cannot be tested at this stage.

In a first attempt to identify potential downstream targets of *Alk*, the expression levels of two cell adhesion molecules regulating axon guidance in the visual system of *Drosophila* were tested, N-Cadherin (Cad-N) and Flamingo (Fmi). Cad-N is required cell-autonomously in R-cells (Lee et al., 2001; Ting et al., 2005; Nern et al., 2005) but has also been shown to have a non-cell autonomous requirement in target lamina neurons for the establishment of the R1-R6 projection pattern (Prakash et al., 2005). Phosphorylation of the β-catenin-Cad-N complex has been shown to disrupt Cad-N-mediated adhesion (reviewed in Lilien and Balsamo, 2005). In addition, Alk and Cad-N have similar ubiquitous expression patterns in the target (Lee et al., 2001). These findings led us to test whether Cad-N could be a potential downstream target of Alk signaling. However, in *Alk* target mosaic animals the levels of Cad-N remain normal in comparison with the wild type.

Fmi is expressed, similarly to Cad-N, along R-afferents as well as in target cells (Lee et al., 2003b). When removed from the eye, it causes projection defects in R1-R6 axons across the lamina and R8 mistargeting in inappropriate layers of the medulla (Lee

et al., 2003b; Senti et al., 2003). Our analysis illustrated that Fmi is expressed in a more restrictive pattern than Cad-N or Alk in the target. During mid-pupal development, Fmi is no longer found in the lamina but is specifically expressed in the R8 recipient layer (M3) and not in the developing M6 layer where R7 terminate (my observations and unpublished observations of H. Apitz). My results show that in the absence of *Alk* from target neurons, Fmi is down-regulated in some columns of the developing M3 layer. These findings suggest that, in addition to a cell-autonomous requirement in the eye (Senti et al., 2003; Lee et al., 2003b), *Fmi* may also have a previously unknown requirement in the target. Its M3 layer-specific downregulation in *Alk ELF* animals suggests that it may be one of the cell adhesion molecules activated/modulated by Alk signaling that could regulate R8 target layer specificity. To confirm these observations, analysis of *Fmi ELF* mosaic animals during pupal development will need to be performed. In addition, overexpression of Alk could demonstrate whether there is ectopic activation or extended expression of Fmi, which could further support the notion that it is a downstream target of Alk signaling.

The balance between attractive and repulsive guidance cues present in the environment of the R8 terminals are responsible for defining the trajectory of the axons towards their synaptic partners. *Alk* could be required for the activation or modulation of both cues in different layers of the medulla neuropil. In fact, recently, the chemorepellent Semaphorin was found to be strongly expressed in all other layers of the medulla neuropil apart from M3 (I.Salecker, unpublished observations). Subsequent characterization of its expression levels in *Alk* target mosaic animals and loss-of-function analysis for *Semaphorin* in the visual system will resolve whether it is found downstream of Alk signaling.

4.5.4.1 Adhesion Molecules from the Visceral Mesoderm

Other candidates for downstream targets of Alk signaling could also include the cell adhesion molecules activated by Alk in the visceral mesoderm, provided that they are expressed in the visual system during the crucial time at which the phenotypes in the R-cell projection pattern arise. In the visceral mesoderm, Alk activates the cell adhesion molecule Dumbfounded (Duf) (Englund et al., 2003), required for the muscle fusion process. Duf expressed on the surface of muscle founder cells (Ruiz-Gomez et al., 2000), recognizes an Ig-containing cell adhesion molecule, Sticks and Stones (Sns), present on the surface of migrating FCMs (Bour et al., 2000). Muscle fusion occurs with additional support by the paralog of Duf, Irregular chiasmC- roughest (IrreC-rst), which is also present in muscle founder cells (Galletta et al., 2004).

Although the role of Duf in the visual system is not known, recent data in the lab demonstrate that it is expressed in lamina neurons during pupal development (I. Salecker, unpublished observations). Its paralog, IrreC-rst, is also strongly expressed in the visual system of *Drosophila*, along photoreceptor axons as well as in lamina and medulla neuropils (Schneider et al., 1995). Protein levels in the lamina cannot be detected past mid-pupal development whereas in the medulla, down-regulation begins a few hours later and expression ceases by 74 hours of pupal development (Schneider et al., 1995). In the lamina, only L3 and L4 express IrreC-rst, whereas in the medulla the immunoreactivity of distal layers becomes organized in a columnar manner during pupal development (Schneider et al., 1995). If gene hierarchies are conserved between the visceral mesoderm and the visual system, then maybe Sns expressed along R-cell afferents (Dworak et al., 2001) could recognize the extracellular domains of Duf or IrreC-rst in processes of target neurons to establish connections between the two. An alternative hypothesis for this connectivity could involve cleavage and release of the extracellular domain of Duf (Menon et al., 2005), in which case R-cell growth cones

would move towards their postsynaptic partners by responding to gradients of the secreted Duf domain. Future analysis will show whether any of these factors are part of the Alk signaling pathway.

Finally, as Alk shows prolonged expression in the target until adult stages, it may also be required for the formation or stabilization of specific synapses between R-cell axons and processes of target neurons at later stages of development. A possible candidate to be regulated by *Alk* in such a process could be the member of the "leucine rich repeat" family of cell adhesion molecules, Capricious (Caps) or the member of the exocyst component, Sec15. Caps is required for synapse formation between motor neurons and muscles and was recently shown to be cell-autonomously required for R8 target specificity (Shishido et al., 1998; Taniguchi et al., 2000; Shinza-Kameda et al., 2006). Its expression pattern in the medulla neuropil and the phenotype *caps* mosaic animals exhibit (Shinza-Kameda et al., 2006) suggest that it may be a downstream target of Alk signaling regulating R8 targeting. Exocyst components are known for their role in docking and fusion of secretory vesicles (reviewed in Novick and Guo, 2002). Sec15 is expressed in both R-cell axons and in the target, and *sec15* eye mosaic animals exhibit defects in synaptic specificity of R-cell axons in the lamina and medulla (Mehta et al., 2005). The expression pattern of Caps and Sec15, as well as the phenotype they cause in their absence suggest that they could be downstream effectors of Alk signaling.

Our preliminary observations suggest that the timing of axonal growth must be tightly coordinated with the temporal expression of axon guidance cues in the medulla, and therefore, *Alk* could be regulating the timing of expression of such relevant guidance cues. Alternatively, *Alk* could regulate the activity of downstream signals by controling their localization or trafficking within the cell or even to the extracellular space.

4.5.5 Novel Anterograde Signaling in the Developing Visual System

Demonstrating that Jeb could be the activating ligand for the receptor Alk in the visual system of *Drosophila* not only highlighted the importance of interactions between R-cells and the target, but also revealed a novel anterograde signaling pathway.

The communication between the target and the growth cone is very often achieved via retrograde signaling. An example of this is set in the distribution of ephrin ligands in the target optic tectum and the presence of the Eph receptors along retinal ganglion cell (RGC) afferents (Hindges et al., 2002). Interestingly, anterograde signaling pathways regulating the formation of neuronal connections with target cells are not well understood. In the *Drosophila* neuromuscular junction, Wingless has been shown to act as an anterograde signal from motoneurons to muscle fibers mediating synapse maturation (Packard et al., 2002). In vertebrates, RGC axons have been described to transport neurotrophins by anterograde axonal transport to their targets in the brain, where they promote survival and mediate synapse plasticity and remodeling (Spalding et al., 2002; Menna et al., 2003; Wang et al., 2003).

To date, two well-characterized anterograde signals exist in the *Drosophila* visual system, Hh and Spitz. Although both regulate patterning of the eye (Dominguez and Hafen, 1997; Tio and Moses, 1997), in the target, R-cell axon-derived Hh also induces proliferation of LPCs, differentiation of lamina neurons and their assembly into columns in the target, whereas Spitz is responsible for their further maturation (Huang and Kunes, 1996; Huang et al., 1998). Our data suggest that Alk and Jeb form a third anterograde signaling pathway in the fly visual system: Jeb released from R-cell terminals activates the receptor Alk in the target, which then regulates the guidance of R1-R6 and R8 axons towards their postsynaptic partners during mid-pupal development (Figure 41).

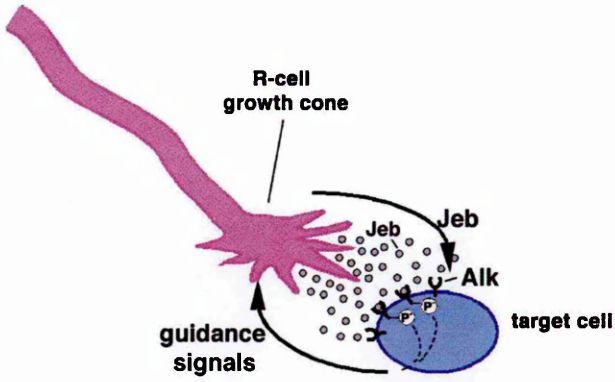

Figure 41. Proposed Model

Jeb released from R-cell growth cones activates the receptor Alk in target cells. Subsequently, downstream effectors of *Alk* signal back to R-cell growth cones to provide them with guidance signals.

5. Concluding Remarks

The goal of my thesis was to identify target-area required factors regulating the guidance of R-cell axons in the visual system of *Drosophila*, and also to try and understand the mechanisms through which they accomplish this.

Two approaches were used to address these fundamental questions: a forward mutagenesis screen and a candidate approach. The first approach began to illustrate the efficiency of the novel ELF system in studying the function of genes required in target neurons and glia.

The candidate approach revealed a novel function for the receptor tyrosine kinase Alk and its activating ligand Jeb in the developing nervous system, and in particular the visual system of *Drosophila.* My results suggest that, through a novel anterograde signaling pathway, Jeb transmitted along R-cell afferents activates the receptor Alk in target neurons and together they regulate R1-R6 targeting in the lamina and R8 target layer specificity in the medulla. We propose that these processes may be regulated by the modulation of one or more guidance factors by the receptor Alk. My studies indicate that Fmi may be such a candidate.

Future issues for resolving the exact role of Alk in the visual system involve epistasis analysis, through which downstream targets and interacting factors of *Alk* can be identified. Finally, it remains to elucidate the role of the two family members discovered as the *Drosophila* homologues for PTN and MK, miple 1 and miple 2 (Englund et al., 2005). Mutant flies for either *miple 1* or *miple 2* have not been generated yet, but since the expression of miple 1 in particular complements the expression of Alk in the central nervous system, it may act as another activating ligand for Alk there. As mentioned in the introduction, the mammalian and *Drosophila* Alk proteins show a high degree of similarity, including domains in their extracellular region (Loren et al., 2001). One would expect their respective ligands to share structural

features. However, miple1 and miple2 are structurally unrelated to Jeb. It could, therefore, be possible, that activation of Alk by these proteins could initiate a signaling cascade distinct from the one induced by Jeb, either in the visual system or in another part of the *Drosophila* nervous system.

REFERENCES

Amet, L. E., Lauri, S. E., Hienola, A., Croll, S. D., Lu, Y., Levorse, J. M., Prabhakaran, B., Taira, T., Rauvala, H., and Vogt, T. F. (2001). Enhanced hippocampal long-term potentiation in mice lacking heparin-binding growth-associated molecule. Mol Cell Neurosci 17, 1014-1024.

Ashe, H. L. and J. Briscoe (2006). The interpretation of morphogen gradients. Development 133(3): 385-94.

Augsburger, A., Schuchardt, A., Hoskins, S., Dodd, J., and Butler, S. (1999). BMPs as mediators of roof plate repulsion of commissural neurons. Neuron 24, 127-141.

Awasaki, T., Saito, M., Sone, M., Suzuki, E., Sakai, R., Ito, K., and Hama, C. (2000). The Drosophila trio plays an essential role in patterning of axons by regulating their directional extension. Neuron 26, 119-131.

Azpiazu, N., and Frasch, M. (1993). tinman and bagpipe: two homeo box genes that determine cell fates in the dorsal mesoderm of Drosophila. Genes Dev 7, 1325-1340.

Azpiazu, N., Lawrence, P. A., Vincent, J. P., and Frasch, M. (1996). Segmentation and specification of the Drosophila mesoderm. Genes Dev 10, 3183-3194.

Bai, R. Y., Dieter, P., Peschel, C., Morris, S. W., and Duyster, J. (1998). Nucleophosmin-anaplastic lymphoma kinase of large-cell anaplastic lymphoma is a constitutively active tyrosine kinase that utilizes phospholipase C-gamma to mediate its mitogenicity. Mol Cell Biol 18, 6951-6961.

Bai, R. Y., Ouyang, T., Miething, C., Morris, S. W., Peschel, C., and Duyster, J. (2000). Nucleophosmin-anaplastic lymphoma kinase associated with anaplastic large-cell lymphoma activates the phosphatidylinositol 3-kinase/Akt antiapoptotic signaling pathway. Blood 96, 4319-4327.

Babu, K., S. Bahri, et al. (2005). "Bifocal and PP1 interaction regulates targeting of the R-cell growth cone in Drosophila." Dev Biol 288(2): 372-86.

Baker, N.E., Yu, S. and Han, D (1996). "Evolution of proneural atonal expression during distinct regulatory phases in the developing Drosophila." Current Biology 6(10): 1290-301.

Barlow, A., E. de Graaff, et al. (2003). "Enteric nervous system progenitors are coordinately controlled by the G protein-coupled receptor EDNRB and the receptor tyrosine kinase RET." Neuron 40(5): 905-16.

Bashaw, G. J., and Goodman, C. S. (1999). Chimeric axon guidance receptors: the cytoplasmic domains of slit and netrin receptors specify attraction versus repulsion. Cell 97, 917-926.

Bashaw, G. J., Hu, H., Nobes, C. D., and Goodman, C. S. (2001). A novel Dbl family RhoGEF promotes Rho-dependent axon attraction to the central nervous system midline in Drosophila and overcomes Robo repulsion. J Cell Biol 155, 1117-1122.

Bashaw, G. J., Kidd, T., Murray, D., Pawson, T., and Goodman, C. S. (2000). Repulsive axon guidance: Abelson and Enabled play opposing roles downstream of the roundabout receptor. Cell 101, 703-715.

Bateman, J., Shu, H., and Van Vactor, D. (2000). The guanine nucleotide exchange factor trio mediates axonal development in the Drosophila embryo. Neuron 26, 93-106.

Beckmann, G. and P. Bork (1993). "An adhesive domain detected in functionally diverse receptors." Trends Biochem Sci 18(2): 40-1.

Beggs, H. E., Soriano, P., and Maness, P. F. (1994). NCAM-dependent neurite outgrowth is inhibited in neurons from Fyn-minus mice. J Cell Biol 127, 825-833.

Bello, B., Resendez-Perez, D., and Gehring, W. J. (1998). Spatial and temporal targeting of gene expression in Drosophila by means of a tetracycline-dependent transactivator system. Development 125, 2193-2202.

Ben-Neriah, Y., and Bauskin, A. R. (1988). Leukocytes express a novel gene encoding a putative transmembrane protein-kinase devoid of an extracellular domain. Nature 333, 672-676.

Berger, J., Suzuki, T., Senti, K. A., Stubbs, J., Schaffner, G., and Dickson, B. J. (2001). Genetic mapping with SNP markers in Drosophila. Nat Genet 29, 475-481.

Bischof, D., Pulford, K., Mason, D. Y., and Morris, S. W. (1997). Role of the nucleophosmin (NPM) portion of the non-Hodgkin's lymphoma-associated NPM-anaplastic lymphoma kinase fusion protein in oncogenesis. Mol Cell Biol 17, 2312-2325.

Blume-Jensen, P., and Hunter, T. (2001). Oncogenic kinase signalling. Nature 411, 355-365.

Borer, R. A., Lehner, C. F., Eppenberger, H. M., and Nigg, E. A. (1989). Major nucleolar proteins shuttle between nucleus and cytoplasm. Cell 56, 379-390.

Bour, B. A., Chakravarti, M., West, J. M., and Abmayr, S. M. (2000). Drosophila SNS, a member of the immunoglobulin superfamily that is essential for myoblast fusion. Genes Dev 14, 1498-1511.

Bourikas, D., Pekarik, V., Baeriswyl, T., Grunditz, A., Sadhu, R., Nardo, M., and Stoeckli, E. T. (2005). Sonic hedgehog guides commissural axons along the longitudinal axis of the spinal cord. Nat Neurosci 8, 297-304.

Bornemann, D. J., J. E. Duncan, et al. (2004). "Abrogation of heparan sulfate synthesis in Drosophila disrupts the Wingless, Hedgehog and Decapentaplegic signaling pathways." Development 131(9): 1927-38.

Bovolenta, P., and Fernaud-Espinosa, I. (2000). Nervous system proteoglycans as modulators of neurite outgrowth. Prog Neurobiol 61, 113-132.

Bowden, E. T., Stoica, G. E., and Wellstein, A. (2002). Anti-apoptotic signaling of pleiotrophin through its receptor, anaplastic lymphoma kinase. J Biol Chem 277, 35862-35868.

Braisted, J. E., T. McLaughlin, et al. (1997). "Graded and lamina-specific distributions of ligands of EphB receptor tyrosine kinases in the developing retinotectal system." Dev Biol 191(1): 14-28.

Braitenberg, V. (1967). Patterns of projection in the visual system of the fly. I. Retina-lamina projections. Exp Brain Res 3, 271-298.

Brankatschk, M., and Dickson, B. J. (2006). Netrins guide Drosophila commissural axons at short range. Nat Neurosci 9, 188-194.

Briscoe, J., Chen, Y., Jessell, T. M., and Struhl, G. (2001). A hedgehog-insensitive form of patched provides evidence for direct long-range morphogen activity of sonic hedgehog in the neural tube. Mol Cell 7, 1279-1291.

Brittis, P. A., Lu, Q., and Flanagan, J. G. (2002). Axonal protein synthesis provides a mechanism for localized regulation at an intermediate target. Cell 110, 223-235.

Brose, K., Bland, K. S., Wang, K. H., Arnott, D., Henzel, W., Goodman, C. S., Tessier-Lavigne, M., and Kidd, T. (1999). Slit proteins bind Robo receptors and have an evolutionarily conserved role in repulsive axon guidance. Cell 96, 795-806.

Brown, A., P. A. Yates, et al. (2000). "Topographic mapping from the retina to the midbrain is controlled by relative but not absolute levels of EphA receptor signaling." Cell 102(1): 77-88.

Bruckner, K., Pasquale, E. B., and Klein, R. (1997). Tyrosine phosphorylation of transmembrane ligands for Eph receptors. Science 275, 1640-1643.

Brunet, I., C. Weinl, et al. (2005). "The transcription factor Engrailed-2 guides retinal axons." Nature 438(7064): 94-8.

Buck, K. B., and Zheng, J. Q. (2002). Growth cone turning induced by direct local modification of microtubule dynamics. J Neurosci 22, 9358-9367.

Cafferty, P., L. Yu, et al. (2004). "The receptor tyrosine kinase Off-track is required for layer-specific neuronal connectivity in Drosophila." Development 131(21): 5287-95.

Campbell, D. S., and Holt, C. E. (2001). Chemotropic responses of retinal growth cones mediated by rapid local protein synthesis and degradation. Neuron 32, 1013-1026.

Campbell, G., Goring, H., Lin, T., Spana, E., Andersson, S., Doe, C. Q., and Tomlinson, A. (1994). RK2, a glial-specific homeodomain protein required for embryonic nerve cord condensation and viability in Drosophila. Development 120, 2957-2966.

Carnegie, G. K., and Scott, J. D. (2003). A-kinase anchoring proteins and neuronal signaling mechanisms. Genes Dev 17, 1557-1568.

Carrasco, H., G. H. Olivares, et al. (2005). "Heparan sulfate proteoglycans exert positive and negative effects in Shh activity." J Cell Biochem 96(4): 831-8.

Cayuso, J., and Marti, E. (2005). Morphogens in motion: growth control of the neural tube. J Neurobiol 64, 376-387.

Chan, P. K. and F. Y. Chan (1995). "Nucleophosmin/B23 (NPM) oligomer is a major and stable entity in HeLa cells." Biochim Biophys Acta 1262(1): 37-42.

Chan, S. S., Zheng, H., Su, M. W., Wilk, R., Killeen, M. T., Hedgecock, E. M., and Culotti, J. G. (1996). UNC-40, a C. elegans homolog of DCC (Deleted in Colorectal Cancer), is required in motile cells responding to UNC-6 netrin cues. Cell 87, 187-195.

Charron, F., Stein, E., Jeong, J., McMahon, A. P., and Tessier-Lavigne, M. (2003). The morphogen sonic hedgehog is an axonal chemoattractant that collaborates with netrin-1 in midline axon guidance. Cell 113, 11-23.

Cheng, H. J., A. Bagri, et al. (2001). "Plexin-A3 mediates semaphorin signaling and regulates the development of hippocampal axonal projections." Neuron 32(2): 249-63.

Cheng, H. J., Nakamoto, M., Bergemann, A. D., and Flanagan, J. G. (1995). Complementary gradients in expression and binding of ELF-1 and Mek4 in

development of the topographic retinotectal projection map. Cell 82, 371-381.

Chiarle, R., Gong, J. Z., Guasparri, I., Pesci, A., Cai, J., Liu, J., Simmons, W. J., Dhall, G., Howes, J., Piva, R., and Inghirami, G. (2003). NPM-ALK transgenic mice spontaneously develop T-cell lymphomas and plasma cell tumors. Blood 101, 1919-1927.

Chiarle, R., W. J. Simmons, et al. (2005). "Stat3 is required for ALK-mediated lymphomagenesis and provides a possible therapeutic target." Nat Med 11(6): 623-9.

Chin-Sang, I. D., George, S. E., Ding, M., Moseley, S. L., Lynch, A. S., and Chisholm, A. D. (1999). The ephrin VAB-2/EFN-1 functions in neuronal signaling to regulate epidermal morphogenesis in C. elegans. Cell 99, 781-790.

Chotard, C., Leung, W., and Salecker, I. (2005). glial cells missing and gcm2 cell autonomously regulate both glial and neuronal development in the visual system of Drosophila. Neuron 48, 237-251.

Chotard, C., and Salecker, I. (2004). Neurons and glia: team players in axon guidance. Trends Neurosci 27, 655-661.

Chou, W. H., K. J. Hall, et al. (1996). "Identification of a novel Drosophila opsin reveals specific patterning of the R7 and R8 photoreceptor cells." Neuron 17(6): 1101-15.

Chung, K. Y., Taylor, J. S., Shum, D. K., and Chan, S. O. (2000). Axon routing at the optic chiasm after enzymatic removal of chondroitin sulfate in mouse embryos. Development 127, 2673-2683.

Clandinin, T. R., Lee, C. H., Herman, T., Lee, R. C., Yang, A. Y., Ovasapyan, S., and Zipursky, S. L. (2001). Drosophila LAR regulates R1-R6 and R7 target specificity in the visual system. Neuron 32, 237-248.

Clandinin, T. R., and Zipursky, S. L. (2000). Afferent growth cone interactions control synaptic specificity in the Drosophila visual system. Neuron 28, 427-436.

Clandinin, T. R. and S. L. Zipursky (2002). "Making connections in the fly visual system." Neuron 35(5): 827-41.

Colamarino, S. A., and Tessier-Lavigne, M. (1995). The role of the floor plate in axon guidance. Annu Rev Neurosci 18, 497-529.

Colavita, A., Krishna, S., Zheng, H., Padgett, R. W., and Culotti, J. G. (1998). Pioneer axon guidance by UNC-129, a C. elegans TGF-beta. Science 281, 706-709.

T. Cook, F. Pichaud, R. Sonneville, D. Papatsenko, C. Desplan (2003). Distinction between Color Photoreceptor Cell Fates Is Controlled by Prospero in Drosophila. Developmental Cell 4 (6), Pages 853-864.

Cook, T., and Desplan, C. (2001). Photoreceptor subtype specification: from flies to humans. Semin Cell Dev Biol 12, 509-518.

Cowan, C. A. and M. Henkemeyer (2001). "The SH2/SH3 adaptor Grb4 transduces B-ephrin reverse signals." Nature 413(6852): 174-9.

Curtiss, J., and Mlodzik, M. (2000). Morphogenetic furrow initiation and progression during eye development in Drosophila: the roles of decapentaplegic, hedgehog and eyes absent. Development 127, 1325-1336.

Cussac, D., Greenland, C., Roche, S., Bai, R. Y., Duyster, J., Morris, S. W., Delsol, G., Allouche, M., and Payrastre, B. (2004). Nucleophosmin-anaplastic lymphoma kinase of anaplastic large-cell lymphoma recruits, activates, and uses pp60c-src to mediate its mitogenicity. Blood 103, 1464-1471.

Dan, C., Kelly, A., Bernard, O., and Minden, A. (2001). Cytoskeletal changes regulated by the PAK4 serine/threonine kinase are mediated by LIM kinase 1 and cofilin. J Biol Chem 276, 32115-32121.

Davis, J. Q., and Bennett, V. (1994). Ankyrin binding activity shared by the neurofascin/L1/NrCAM family of nervous system cell adhesion molecules. J Biol Chem 269, 27163-27166.

Davy, A., Aubin, J., and Soriano, P. (2004). Ephrin-B1 forward and reverse signaling are required during mouse development. Genes Dev 18, 572-583.

Dawe, H. R., Minamide, L. S., Bamburg, J. R., and Cramer, L. P. (2003). ADF/cofilin controls cell polarity during fibroblast migration. Curr Biol 13, 252-257.

Dearborn, R., Jr., and Kunes, S. (2004). An axon scaffold induced by retinal axons directs glia to destinations in the Drosophila optic lobe. Development 131, 2291-2303.

Dearborn, R., Jr., Q. He, et al. (2002). "Eph receptor tyrosine kinase-mediated formation of a topographic map in the Drosophila visual system." J Neurosci 22(4): 1338-49.

Debant, A., Serra-Pages, C., Seipel, K., O'Brien, S., Tang, M., Park, S. H., and Streuli, M. (1996). The multidomain protein Trio binds the LAR transmembrane tyrosine phosphatase, contains a protein kinase domain, and has separate rac-

specific and rho-specific guanine nucleotide exchange factor domains. Proc Natl Acad Sci U S A 93, 5466-5471.

Dent, E. W., and Gertler, F. B. (2003). Cytoskeletal dynamics and transport in growth cone motility and axon guidance. Neuron 40, 209-227.

Dent, E. W., and Kalil, K. (2001). Axon branching requires interactions between dynamic microtubules and actin filaments. J Neurosci 21, 9757-9769.

Dickson, B. J. (2001). Rho GTPases in growth cone guidance. Curr Opin Neurobiol 11, 103-110.

Dickson, B. J. (2002). Molecular mechanisms of axon guidance. Science 298, 1959-1964.

Dirks, W. G., Fahnrich, S., Lis, Y., Becker, E., MacLeod, R. A., and Drexler, H. G. (2002). Expression and functional analysis of the anaplastic lymphoma kinase (ALK) gene in tumor cell lines. Int J Cancer 100, 49-56.

Drescher, U., F. Bonhoeffer, et al. (1997). "The Eph family in retinal axon guidance." Curr Opin Neurobiol 7(1): 75-80.

Duyster, J., Bai, R. Y., and Morris, S. W. (2001). Translocations involving anaplastic lymphoma kinase (ALK). Oncogene 20, 5623-5637.

Dworak, H. A., Charles, M. A., Pellerano, L. B., and Sink, H. (2001). Characterization of Drosophila hibris, a gene related to human nephrin. Development 128, 4265-4276.

Dworak, H. A., and Sink, H. (2002). Myoblast fusion in Drosophila. Bioessays 24, 591-601.

Englund, C., Birve, A., Falileeva, L., Grabbe, C., and Palmer, R. H. (2005). Miple1 and miple2 encode a family of MK/PTN homologues in Drosophila melanogaster. Dev Genes Evol, 1-9.

Englund, C., Loren, C. E., Grabbe, C., Varshney, G. K., Deleuil, F., Hallberg, B., and Palmer, R. H. (2003). Jeb signals through the Alk receptor tyrosine kinase to drive visceral muscle fusion. Nature 425, 512-516.

Erskine, L., Williams, S. E., Brose, K., Kidd, T., Rachel, R. A., Goodman, C. S., Tessier-Lavigne, M., and Mason, C. A. (2000). Retinal ganglion cell axon guidance in the mouse optic chiasm: expression and function of robos and slits. J Neurosci 20, 4975-4982.

Fabian-Fine, R., Verstreken, P., Hiesinger, P. R., Horne, J. A., Kostyleva, R., Zhou, Y., Bellen, H. J., and Meinertzhagen, I. A. (2003). Endophilin promotes a late step

in endocytosis at glial invaginations in Drosophila photoreceptor terminals. J Neurosci 23, 10732-10744.

Falk, J., Bechara, A., Fiore, R., Nawabi, H., Zhou, H., Hoyo-Becerra, C., Bozon, M., Rougon, G., Grumet, M., Puschel, A. W., et al. (2005). Dual functional activity of semaphorin 3B is required for positioning the anterior commissure. Neuron 48, 63-75.

Fan, Q. W., Muramatsu, T., and Kadomatsu, K. (2000). Distinct expression of midkine and pleiotrophin in the spinal cord and placental tissues during early mouse development. Dev Growth Differ 42, 113-119.

Fan, X., Labrador, J. P., Hing, H., and Bashaw, G. J. (2003). Slit stimulation recruits Dock and Pak to the roundabout receptor and increases Rac activity to regulate axon repulsion at the CNS midline. Neuron 40, 113-127.

Fan, Y., Soller, M., Flister, S., Hollmann, M., Muller, M., Bello, B., Egger, B., White, K., Schafer, M. A., and Reichert, H. (2005). The egghead gene is required for compartmentalization in Drosophila optic lobe development. Dev Biol 287, 61-73.

Feiguin, F., M. Hannus, et al. (2001). "The ankyrin repeat protein Diego mediates Frizzled-dependent planar polarization." Dev Cell 1(1): 93-101.

Feldheim, D. A., Kim, Y. I., Bergemann, A. D., Frisen, J., Barbacid, M., and Flanagan, J. G. (2000). Genetic analysis of ephrin-A2 and ephrin-A5 shows their requirement in multiple aspects of retinocollicular mapping. Neuron 25, 563-574.

Fenstermaker, V., Chen, Y., Ghosh, A., and Yuste, R. (2004). Regulation of dendritic length and branching by semaphorin 3A. J Neurobiol 58, 403-412.

Forcet, C., Stein, E., Pays, L., Corset, V., Llambi, F., Tessier-Lavigne, M., and Mehlen, P. (2002). Netrin-1-mediated axon outgrowth requires deleted in colorectal cancer-dependent MAPK activation. Nature 417, 443-447.

Forsthoefel, D. J., Liebl, E. C., Kolodziej, P. A., and Seeger, M. A. (2005). The Abelson tyrosine kinase, the Trio GEF and Enabled interact with the Netrin receptor Frazzled in Drosophila. Development 132, 1983-1994.

Frankfort, B. J. and G. Mardon (2004). Senseless represses nuclear transduction of Egfr pathway activation. Development 131(3): 563-70.

Fricke, C., Lee, J.S., Geiger-Rudolph, S., Bonhoeffer, F., Chien, C.B. (2001). Astray, a zebrafish roundabout homolog required for retinal axon guidance. Science 292 (5516):507-10.

Frisen, J., P. A. Yates, et al. (1998). "Ephrin-A5 (AL-1/RAGS) is essential for proper retinal axon guidance and topographic mapping in the mammalian visual system Neuron 20(2): 235-43.

Fujimoto, J., Shiota, M., Iwahara, T., Seki, N., Satoh, H., Mori, S., and Yamamoto, T. (1996). Characterization of the transforming activity of p80, a hyperphosphorylated protein in a Ki-1 lymphoma cell line with chromosomal translocation t(2;5). Proc Natl Acad Sci U S A 93, 4181-4186.

Gabay, L., Seger, R., and Shilo, B. Z. (1997). MAP kinase in situ activation atlas during Drosophila embryogenesis. Development 124, 3535-3541.

Gale, N.W., Holland, S.J., Valenzuela, D.M., Flenniken, A., Pan, L., Ryan, T.E., Henkemeyer, M., Strebhardt, K., Hirai, H., Wilkinson, D.G. *et al.*, (1996). Eph receptors and ligands comprise two major specificity subclasses and are reciprocally compartmentalized during embryogenesis. Neuron 17, 9–19.

Galletta, B. J., Chakravarti, M., Banerjee, R., and Abmayr, S. M. (2004). SNS: Adhesive properties, localization requirements and ectodomain dependence in S2 cells and embryonic myoblasts. Mech Dev 121, 1455-1468.

Gao, F. B., Kohwi, M., Brenman, J. E., Jan, L. Y., and Jan, Y. N. (2000). Control of dendritic field formation in Drosophila: the roles of flamingo and competition between homologous neurons. Neuron 28, 91-101.

Garcia-Alonso, L., R. D. Fetter, et al. (1996). "Genetic analysis of Laminin A in Drosophila: extracellular matrix containing laminin A is required for ocellar axon pathfinding." Development 122(9): 2611-21.

Garrity, P. A., Lee, C. H., Salecker, I., Robertson, H. C., Desai, C. J., Zinn, K., and Zipursky, S. L. (1999). Retinal axon target selection in Drosophila is regulated by a receptor protein tyrosine phosphatase. Neuron 22, 707-717.

Garrity, P. A., Rao, Y., Salecker, I., McGlade, J., Pawson, T., and Zipursky, S. L. (1996). Drosophila photoreceptor axon guidance and targeting requires the dreadlocks SH2/SH3 adapter protein. Cell 85, 639-650.

Gavard, J., M. Lambert, et al. (2004). "Lamellipodium extension and cadherin adhesion: two cell responses to cadherin activation relying on distinct signalling pathways." J Cell Sci 117(Pt 2): 257-70.

Gehring, W. J. (1996). "The master control gene for morphogenesis and evolution of the eye." Genes Cells 1(1): 11-5.

George, S. E., Simokat, K., Hardin, J., and Chisholm, A. D. (1998). The VAB-1 Eph receptor tyrosine kinase functions in neural and epithelial morphogenesis in C. elegans. Cell 92, 633-643.

Georgiou, M., and Tear, G. (2002). Commissureless is required both in commissural neurones and midline cells for axon guidance across the midline. Development 129, 2947-2956.

Gibbs, S. M., and Truman, J. W. (1998). Nitric oxide and cyclic GMP regulate retinal patterning in the optic lobe of Drosophila. Neuron 20, 83-93.

Gitai, Z., Yu, T. W., Lundquist, E. A., Tessier-Lavigne, M., and Bargmann, C. I. (2003). The netrin receptor UNC-40/DCC stimulates axon attraction and outgrowth through enabled and, in parallel, Rac and UNC-115/AbLIM. Neuron 37, 53-65.

Greenwood, S., and Struhl, G. (1999). Progression of the morphogenetic furrow in the Drosophila eye: the roles of Hedgehog, Decapentaplegic and the Raf pathway. Development 126, 5795-5808.

Gumbiner, B. M. (2000). "Regulation of cadherin adhesive activity." J Cell Biol 148(3): 399-404.

Gumbiner, B. M. (2005). "Regulation of cadherin-mediated adhesion in morphogenesis." Nat Rev Mol Cell Biol 6(8): 622-34.

Hakeda-Suzuki, S., Ng, J., Tzu, J., Dietzl, G., Sun, Y., Harms, M., Nardine, T., Luo, L., and Dickson, B. J. (2002). Rac function and regulation during Drosophila development. Nature 416, 438-442.

Hantschel, O., and Superti-Furga, G. (2004). Regulation of the c-Abl and Bcr-Abl tyrosine kinases. Nat Rev Mol Cell Biol 5, 33-44.

Harbott, L. K. and C. D. Nobes (2005). "A key role for Abl family kinases in EphA receptor-mediated growth cone collapse." Mol Cell Neurosci 30(1): 1-11.

Harris, R., Sabatelli, L. M., and Seeger, M. A. (1996). Guidance cues at the Drosophila CNS midline: identification and characterization of two Drosophila Netrin/UNC-6 homologs. Neuron 17, 217-228.

He, Z., and Tessier-Lavigne, M. (1997). Neuropilin is a receptor for the axonal chemorepellent Semaphorin III. Cell 90, 739-751.

Heberlein, U., Wolff, T., and Rubin, G. M. (1993). The TGF beta homolog dpp and the segment polarity gene hedgehog are required for propagation of a morphogenetic wave in the Drosophila retina. Cell 75, 913-926.

Heberlein, U., and Moses, K. (1995). Mechanisms of Drosophila retinal morphogenesis: the virtues of being progressive. Cell 81, 987-990.

Heberlein, U., Wolff, T., and Rubin, G. M. (1993). The TGF beta homolog dpp and the segment polarity gene hedgehog are required for propagation of a morphogenetic wave in the Drosophila retina. Cell 75, 913-926.

Hedgecock, E. M., Culotti, J. G., and Hall, D. H. (1990). The unc-5, unc-6, and unc-40 genes guide circumferential migrations of pioneer axons and mesodermal cells on the epidermis in C. elegans. Neuron 4, 61-85.

Himanen, J. P., Chumley, M. J., Lackmann, M., Li, C., Barton, W. A., Jeffrey, P. D., Vearing, C., Geleick, D., Feldheim, D. A., Boyd, A. W., et al. (2004). Repelling class discrimination: ephrin-A5 binds to and activates EphB2 receptor signaling. Nat Neurosci 7, 501-509.

Hindges, R., McLaughlin, T., Genoud, N., Henkemeyer, M., and O'Leary, D. D. (2002). EphB forward signaling controls directional branch extension and arborization required for dorsal-ventral retinotopic mapping. Neuron 35, 475-487.

Hing, H., Xiao, J., Harden, N., Lim, L., and Zipursky, S. L. (1999). Pak functions downstream of Dock to regulate photoreceptor axon guidance in Drosophila. Cell 97, 853-863.

Hiramoto, M., Hiromi, Y., Giniger, E., and Hotta, Y. (2000). The Drosophila Netrin receptor Frazzled guides axons by controlling Netrin distribution. Nature 406, 886-889.

Holt, C. E. and B. J. Dickson (2005). "Sugar codes for axons?" Neuron 46(2): 169-72.

Hong, K., Hinck, L., Nishiyama, M., Poo, M. M., Tessier-Lavigne, M., and Stein, E. (1999). A ligand-gated association between cytoplasmic domains of UNC5 and DCC family receptors converts netrin-induced growth cone attraction to repulsion. Cell 97, 927-941.

Hopker, V. H., D. Shewan, et al. (1999). "Growth-cone attraction to netrin-1 is converted to repulsion by laminin-1." Nature 401(6748): 69-73.

Hu, H., Marton, T. F., and Goodman, C. S. (2001). Plexin B mediates axon guidance in Drosophila by simultaneously inhibiting active Rac and enhancing RhoA signaling. Neuron 32, 39-51.

Huai, J. and U. Drescher (2001). "An ephrin-A-dependent signaling pathway controls integrin function and is linked to the tyrosine phosphorylation of a 120-kDa protein." J Biol Chem 276(9): 6689-94.

Huang, C. C., D. H. Hall, et al. (2003). "Laminin alpha subunits and their role in C. elegans development." Development 130(14): 3343-58.

Huang, Z., and Kunes, S. (1996). Hedgehog, transmitted along retinal axons, triggers neurogenesis in the developing visual centers of the Drosophila brain. Cell 86, 411-422.

Huang, Z., Shilo, B. Z., and Kunes, S. (1998). A retinal axon fascicle uses spitz, an EGF receptor ligand, to construct a synaptic cartridge in the brain of Drosophila. Cell 95, 693-703.

Huber, A. B., Kania, A., Tran, T. S., Gu, C., De Marco Garcia, N., Lieberam, I., Johnson, D., Jessell, T. M., Ginty, D. D., and Kolodkin, A. L. (2005). Distinct roles for secreted semaphorin signaling in spinal motor axon guidance. Neuron 48, 949-964.

Hummel, T., S. Attix, et al. (2002). "Temporal control of glial cell migration in the Drosophila eye requires gilgamesh, hedgehog, and eye specification genes." Neuron 33(2): 193-203.

Hummel, T., M. L. Vasconcelos, et al. (2003). "Axonal targeting of olfactory receptor neurons in Drosophila is controlled by Dscam." Neuron 37(2): 221-31.

Hummel, T. and S. L. Zipursky (2004). "Afferent induction of olfactory glomeruli requires N-cadherin." Neuron 42(1): 77-88.

Huot, J. (2004). Ephrin signaling in axon guidance. Prog Neuropsychopharmacol Biol Psychiatry 28, 813-818.

Hutter, H. (2003). Extracellular cues and pioneers act together to guide axons in the ventral cord of C. elegans. Development 130, 5307-5318.

Hynes, R. O. (2002). "Integrins: bidirectional, allosteric signaling machines." Cell 110(6): 673-87.

Ignelzi, M. A., Jr., D. R. Miller, et al. (1994). "Impaired neurite outgrowth of src-minus cerebellar neurons on the cell adhesion molecule L1." Neuron 12(4): 873-84.

Irie, A., E. A. Yates, et al. (2002). "Specific heparan sulfate structures involved in retinal axon targeting." Development 129(1): 61-70.

Iwahara, T., Fujimoto, J., Wen, D., Cupples, R., Bucay, N., Arakawa, T., Mori, S., Ratzkin, B., and Yamamoto, T. (1997). Molecular characterization of ALK, a

receptor tyrosine kinase expressed specifically in the nervous system. Oncogene 14, 439-449.

Iwai, Y., Usui, T., Hirano, S., Steward, R., Takeichi, M., and Uemura, T. (1997). Axon patterning requires DN-cadherin, a novel neuronal adhesion receptor, in the Drosophila embryonic CNS. Neuron 19, 77-89.

Iwasaki, W., Nagata, K., Hatanaka, H., Inui, T., Kimura, T., Muramatsu, T., Yoshida, K., Tasumi, M., and Inagaki, F. (1997). Solution structure of midkine, a new heparin-binding growth factor. Embo J 16, 6936-6946.

Jarman, A. P., E. H. Grell, et al. (1994). "Atonal is the proneural gene for Drosophila photoreceptors." Nature 369(6479): 398-400.

Jarman, A. P., Y. Sun, et al. (1995). "Role of the proneural gene, atonal, in formation of Drosophila chordotonal organs and photoreceptors." Development 121(7): 2019-30.

Jessell, T. M. (2000). Neuronal specification in the spinal cord: inductive signals and transcriptional codes. Nat Rev Genet 1, 20-29.

Jin, Z., and Strittmatter, S. M. (1997). Rac1 mediates collapsin-1-induced growth cone collapse. J Neurosci 17, 6256-6263.

Johnson, K. G., A. Ghose, et al. (2004). "Axonal heparan sulfate proteoglycans regulate the distribution and efficiency of the repellent slit during midline axon guidance." Curr Biol 14(6): 499-504.

Jones, B., and McGinnis, W. (1993). A new Drosophila homeobox gene, bsh, is expressed in a subset of brain cells during embryogenesis. Development 117, 793-806.

Jones, B. W., Fetter, R. D., Tear, G., and Goodman, C. S. (1995). glial cells missing: a genetic switch that controls glial versus neuronal fate. Cell 82, 1013-1023.

Kadomatsu, K. and T. Muramatsu (2004). "Midkine and pleiotrophin in neural development and cancer." Cancer Lett 204(2): 127-43.

Kaminker, J. S., Canon, J., Salecker, I., and Banerjee, U. (2002). Control of photoreceptor axon target choice by transcriptional repression of Runt. Nat Neurosci 5, 746-750.

Kantor, D. B., Chivatakarn, O., Peer, K. L., Oster, S. F., Inatani, M., Hansen, M. J., Flanagan, J. G., Yamaguchi, Y., Sretavan, D. W., Giger, R. J., and Kolodkin, A. L. (2004). Semaphorin 5A is a bifunctional axon guidance cue regulated by heparan and chondroitin sulfate proteoglycans. Neuron 44, 961-975.

Keino-Masu, K., Masu, M., Hinck, L., Leonardo, E. D., Chan, S. S., Culotti, J. G., and Tessier-Lavigne, M. (1996). Deleted in Colorectal Cancer (DCC) encodes a netrin receptor. Cell 87, 175-185.

Keleman, K., and Dickson, B. J. (2001). Short- and long-range repulsion by the Drosophila Unc5 netrin receptor. Neuron 32, 605-617.

Keleman, K., Rajagopalan, S., Cleppien, D., Teis, D., Paiha, K., Huber, L. A., Technau, G. M., and Dickson, B. J. (2002). Comm sorts robo to control axon guidance at the Drosophila midline. Cell 110, 415-427.

Keleman, K., Ribeiro, C., and Dickson, B. J. (2005). Comm function in commissural axon guidance: cell-autonomous sorting of Robo in vivo. Nat Neurosci 8, 156-163.

Kennedy, T. E., Serafini, T., de la Torre, J. R., and Tessier-Lavigne, M. (1994). Netrins are diffusible chemotropic factors for commissural axons in the embryonic spinal cord. Cell 78, 425-435.

Kidd, T., Bland, K. S., and Goodman, C. S. (1999). Slit is the midline repellent for the robo receptor in Drosophila. Cell 96, 785-794.

Kidd, T., Brose, K., Mitchell, K. J., Fetter, R. D., Tessier-Lavigne, M., Goodman, C. S., and Tear, G. (1998). Roundabout controls axon crossing of the CNS midline and defines a novel subfamily of evolutionarily conserved guidance receptors. Cell 92, 205-215.

Kirkpatrick, C. A., B. D. Dimitroff, et al. (2004). "Spatial regulation of Wingless morphogen distribution and signaling by Dally-like protein." Dev Cell 7(4): 513-23.

Kirschfeld, K. (1967). [The projection of the optical environment on the screen of the rhabdomere in the compound eye of the Musca]. Exp Brain Res 3, 248-270.

Knoll, B. and U. Drescher (2004). "Src family kinases are involved in EphA receptor-mediated retinal axon guidance." J Neurosci 24(28): 6248-57.

Kolodkin, A. L., Matthes, D. J., and Goodman, C. S. (1993). The semaphorin genes encode a family of transmembrane and secreted growth cone guidance molecules. Cell 75, 1389-1399.

Kolodziej, P. A., Timpe, L. C., Mitchell, K. J., Fried, S. R., Goodman, C. S., Jan, L. Y., and Jan, Y. N. (1996). frazzled encodes a Drosophila member of the DCC immunoglobulin subfamily and is required for CNS and motor axon guidance. Cell 87, 197-204.

Kolpak, A., Zhang, J., and Bao, Z. Z. (2005). Sonic hedgehog has a dual effect on the growth of retinal ganglion axons depending on its concentration. J Neurosci 25, 3432-3441.

Kuefer, M. U., Look, A. T., Pulford, K., Behm, F. G., Pattengale, P. K., Mason, D. Y., and Morris, S. W. (1997). Retrovirus-mediated gene transfer of NPM-ALK causes lymphoid malignancy in mice. Blood 90, 2901-2910.

Kullander, K., and Klein, R. (2002). Mechanisms and functions of Eph and ephrin signalling. Nat Rev Mol Cell Biol 3, 475-486.

Kumar, J. P. and K. Moses (2001). "EGF receptor and Notch signaling act upstream of Eyeless/Pax6 to control eye specification." Cell 104(5): 687-97.

Kurada, P. and K. White (1999). "Epidermal growth factor receptor: its role in Drosophila eye differentiation and cell survival." Apoptosis 4(4): 239-43.

Land, M. F. (1997). "Visual acuity in insects." Annu Rev Entomol 42: 147-77.

Laplante, I., R. Beliveau, et al. (2004). "RhoA/ROCK and Cdc42 regulate cell-cell contact and N-cadherin protein level during neurodetermination of P19 embryonal stem cells." J Neurobiol 60(3): 289-307.

Lebrand, C., Dent, E. W., Strasser, G. A., Lanier, L. M., Krause, M., Svitkina, T. M., Borisy, G. G., and Gertler, F. B. (2004). Critical role of Ena/VASP proteins for filopodia formation in neurons and in function downstream of netrin-1. Neuron 42, 37-49.

Lee, C. H., Herman, T., Clandinin, T. R., Lee, R., and Zipursky, S. L. (2001). N-cadherin regulates target specificity in the Drosophila visual system. Neuron 30, 437-450.

Lee, H., Engel, U., Rusch, J., Scherrer, S., Sheard, K., and Van Vactor, D. (2004). The microtubule plus end tracking protein Orbit/MAST/CLASP acts downstream of the tyrosine kinase Abl in mediating axon guidance. Neuron 42, 913-926.

Lee, H. H., Norris, A., Weiss, J. B., and Frasch, M. (2003b). Jelly belly protein activates the receptor tyrosine kinase Alk to specify visceral muscle pioneers. Nature 425, 507-512.

Lee, R. C., Clandinin, T. R., Lee, C. H., Chen, P. L., Meinertzhagen, I. A., and Zipursky, S. L. (2003b). The protocadherin Flamingo is required for axon target selection in the Drosophila visual system. Nat Neurosci 6, 557-563.

Lee, T., and Luo, L. (1999). Mosaic analysis with a repressible cell marker for studies of gene function in neuronal morphogenesis. Neuron 22, 451-461.

Li, W., Lee, J., Vikis, H. G., Lee, S. H., Liu, G., Aurandt, J., Shen, T. L., Fearon, E. R., Guan, J. L., Han, M., et al. (2004). Activation of FAK and Src are receptor-proximal events required for netrin signaling. Nat Neurosci 7, 1213-1221.

Liebl, E. C., Forsthoefel, D. J., Franco, L. S., Sample, S. H., Hess, J. E., Cowger, J. A., Chandler, M. P., Shupert, A. M., and Seeger, M. A. (2000). Dosage-sensitive, reciprocal genetic interactions between the Abl tyrosine kinase and the putative GEF trio reveal trio's role in axon pathfinding. Neuron 26, 107-118.

Liem, K. F., Jr., T. M. Jessell, et al. (2000). "Regulation of the neural patterning activity of sonic hedgehog by secreted BMP inhibitors expressed by notochord and somites." Development 127(22): 4855-66.

Lilien, J. and J. Balsamo (2005). "The regulation of cadherin-mediated adhesion by tyrosine phosphorylation/dephosphorylation of beta-catenin." Curr Opin Cell Biol 17(5): 459-65.

Liu, G., Beggs, H., Jurgensen, C., Park, H. T., Tang, H., Gorski, J., Jones, K. R., Reichardt, L. F., Wu, J., and Rao, Y. (2004). Netrin requires focal adhesion kinase and Src family kinases for axon outgrowth and attraction. Nat Neurosci 7, 1222-1232.

Long, H., Sabatier, C., Ma, L., Plump, A., Yuan, W., Ornitz, D. M., Tamada, A., Murakami, F., Goodman, C. S., and Tessier-Lavigne, M. (2004). Conserved roles for Slit and Robo proteins in midline commissural axon guidance. Neuron 42, 213-223.

Loren, C. E., Englund, C., Grabbe, C., Hallberg, B., Hunter, T., and Palmer, R. H. (2003). A crucial role for the Anaplastic lymphoma kinase receptor tyrosine kinase in gut development in Drosophila melanogaster. EMBO Rep 4, 781-786.

Loren, C. E., Scully, A., Grabbe, C., Edeen, P. T., Thomas, J., McKeown, M., Hunter, T., and Palmer, R. H. (2001). Identification and characterization of DAlk: a novel Drosophila melanogaster RTK which drives ERK activation in vivo. Genes Cells 6, 531-544.

Lum, L. and P. A. Beachy (2004). "The Hedgehog response network: sensors, switches, and routers." Science 304(5678): 1755-9.

Luo, L. (2000). Rho GTPases in neuronal morphogenesis. Nat Rev Neurosci 1, 173-180.

Luo, Y., Raible, D., and Raper, J. A. (1993). Collapsin: a protein in brain that induces the collapse and paralysis of neuronal growth cones. Cell 75, 217-227.

Lyuksyutova, A. I., Lu, C. C., Milanesio, N., King, L. A., Guo, N., Wang, Y., Nathans, J., Tessier-Lavigne, M., and Zou, Y. (2003). Anterior-posterior guidance of commissural axons by Wnt-frizzled signaling. Science 302, 1984-1988.

Maeda, N., and Noda, M. (1998). Involvement of receptor-like protein tyrosine phosphatase zeta/RPTPbeta and its ligand pleiotrophin/heparin-binding growth-associated molecule (HB-GAM) in neuronal migration. J Cell Biol 142, 203-216.

Mann, F., Ray, S., Harris, W., and Holt, C. (2002). Topographic mapping in dorsoventral axis of the Xenopus retinotectal system depends on signaling through ephrin-B ligands. Neuron 35, 461-473.

Mardon, G., Solomon, N. M., and Rubin, G. M. (1994). dachshund encodes a nuclear protein required for normal eye and leg development in Drosophila. Development 120, 3473-3486.

Marillat, V., Cases, O., Nguyen-Ba-Charvet, K. T., Tessier-Lavigne, M., Sotelo, C., and Chedotal, A. (2002). Spatiotemporal expression patterns of slit and robo genes in the rat brain. J Comp Neurol 442, 130-155.

Mason, D. Y., Pulford, K. A., Bischof, D., Kuefer, M. U., Butler, L. H., Lamant, L., Delsol, G., and Morris, S. W. (1998). Nucleolar localization of the nucleophosmin-anaplastic lymphoma kinase is not required for malignant transformation. Cancer Res 58, 1057-1062.

Mast, J. D., S. Prakash, et al. (2005). "The mechanisms and molecules that connect photoreceptor axons to their targets in Drosophila." Semin Cell Dev Biol.

Maurel-Zaffran, C., Suzuki, T., Gahmon, G., Treisman, J. E., and Dickson, B. J. (2001). Cell-autonomous and -nonautonomous functions of LAR in R7 photoreceptor axon targeting. Neuron 32, 225-235.

Mehta, S. Q., P. R. Hiesinger, et al. (2005). "Mutations in Drosophila sec15 reveal a function in neuronal targeting for a subset of exocyst components." Neuron 46(2): 219-32.

Meinertzhagen, I. A. and Hanson, T.E. (1993). The development of the optic lobe. In the Development of Drosophila Melanogaster. Cold Spring Harbor, New York: Cold Spring Harbor Laboratory Press, 1363-1491.

Meinertzhagen, I. A. (2000). Wiring the fly's eye. Neuron 28, 310-313.

Menna, E., M. C. Cenni, et al. (2003). "The anterogradely transported BDNF promotes retinal axon remodeling during eye specific segregation within the LGN." Mol Cell Neurosci 24(4): 972-83.

Menon, S. D., Osman, Z., Chenchill, K., and Chia, W. (2005). A positive feedback loop between Dumbfounded and Rolling pebbles leads to myotube enlargement in Drosophila. J Cell Biol 169, 909-920.

Meriane, M., Tcherkezian, J., Webber, C. A., Danek, E. I., Triki, I., McFarlane, S., Bloch-Gallego, E., and Lamarche-Vane, N. (2004). Phosphorylation of DCC by Fyn mediates Netrin-1 signaling in growth cone guidance. J Cell Biol 167, 687-698.

Michaud, N. and D. S. Goldfarb (1991). "Multiple pathways in nuclear transport: the import of U2 snRNP occurs by a novel kinetic pathway." J Cell Biol 112(2): 215-23.

Ming, G., Henley, J., Tessier-Lavigne, M., Song, H., and Poo, M. (2001). Electrical activity modulates growth cone guidance by diffusible factors. Neuron 29, 441-452.

Mitchell, K. J., Doyle, J. L., Serafini, T., Kennedy, T. E., Tessier-Lavigne, M., Goodman, C. S., and Dickson, B. J. (1996). Genetic analysis of Netrin genes in Drosophila: Netrins guide CNS commissural axons and peripheral motor axons. Neuron 17, 203-215.

Mlodzik, M., Y. Hiromi, et al. (1990). "The Drosophila seven-up gene, a member of the steroid receptor gene superfamily, controls photoreceptor cell fates." Cell 60(2): 211-24.

Montell, C., K. Jones, et al. (1987). "A second opsin gene expressed in the ultraviolet-sensitive R7 photoreceptor cells of Drosophila melanogaster." J Neurosci 7(5): 1558-66.

Morris, S. W., Kirstein, M. N., Valentine, M. B., Dittmer, K. G., Shapiro, D. N., Saltman, D. L., and Look, A. T. (1994). Fusion of a kinase gene, ALK, to a nucleolar protein gene, NPM, in non-Hodgkin's lymphoma. Science 263, 1281-1284.

Morris, S. W., Naeve, C., Mathew, P., James, P. L., Kirstein, M. N., Cui, X., and Witte, D. P. (1997). ALK, the chromosome 2 gene locus altered by the t(2;5) in non-Hodgkin's lymphoma, encodes a novel neural receptor tyrosine kinase that is highly related to leukocyte tyrosine kinase (LTK). Oncogene 14, 2175-2188.

Motegi, A., Fujimoto, J., Kotani, M., Sakuraba, H., and Yamamoto, T. (2004). ALK receptor tyrosine kinase promotes cell growth and neurite outgrowth. J Cell Sci 117, 3319-3329.

Muramatsu, T. (2002). Midkine and pleiotrophin: two related proteins involved in development, survival, inflammation and tumorigenesis. J Biochem (Tokyo) 132, 359-371.

Nagata, S. (2000). "Apoptotic DNA fragmentation." Exp Cell Res 256(1): 12-8.

Nakagawa, H., Miki, H., Ito, M., Ohashi, K., Takenawa, T., and Miyamoto, S. (2001). N-WASP, WAVE and Mena play different roles in the organization of actin cytoskeleton in lamellipodia. J Cell Sci 114, 1555-1565.

Nakagawa, S., C. Brennan, et al. (2000). "Ephrin-B regulates the Ipsilateral routing of retinal axons at the optic chiasm." Neuron 25(3): 599-610.

Nakamura, F., Tanaka, M., Takahashi, T., Kalb, R. G., and Strittmatter, S. M. (1998). Neuropilin-1 extracellular domains mediate semaphorin D/III-induced growth cone collapse. Neuron 21, 1093-1100.

Nakashiba, T., Nishimura, S., Ikeda, T., and Itohara, S. (2002). Complementary expression and neurite outgrowth activity of netrin-G subfamily members. Mech Dev 111, 47-60.

Nern, A., Nguyen, L. V., Herman, T., Prakash, S., Clandinin, T. R., and Zipursky, S. L. (2005). An isoform-specific allele of Drosophila N-cadherin disrupts a late step of R7 targeting. Proc Natl Acad Sci U S A 102, 12944-12949.

Newsome, T. P., Asling, B., and Dickson, B. J. (2000a). Analysis of Drosophila photoreceptor axon guidance in eye-specific mosaics. Development 127, 851-860.

Newsome, T. P., Schmidt, S., Dietzl, G., Keleman, K., Asling, B., Debant, A., and Dickson, B. J. (2000b). Trio combines with dock to regulate Pak activity during photoreceptor axon pathfinding in Drosophila. Cell 101, 283-294.

Ng, J., and Luo, L. (2004). Rho GTPases regulate axon growth through convergent and divergent signaling pathways. Neuron 44, 779-793.

Ng, J., Nardine, T., Harms, M., Tzu, J., Goldstein, A., Sun, Y., Dietzl, G., Dickson, B. J., and Luo, L. (2002). Rac GTPases control axon growth, guidance and branching. Nature 416, 442-447.

Nieborowska-Skorska, M., Slupianek, A., Xue, L., Zhang, Q., Raghunath, P. N., Hoser, G., Wasik, M. A., Morris, S. W., and Skorski, T. (2001). Role of signal

transducer and activator of transcription 5 in nucleophosmin/ anaplastic lymphoma kinase-mediated malignant transformation of lymphoid cells. Cancer Res 61, 6517-6523.

Niwa, R., Nagata-Ohashi, K., Takeichi, M., Mizuno, K., and Uemura, T. (2002). Control of actin reorganization by Slingshot, a family of phosphatases that dephosphorylate ADF/cofilin. Cell 108, 233-246.

Nolo, R., Abbott, L. A., and Bellen, H. J. (2000). Senseless, a Zn finger transcription factor, is necessary and sufficient for sensory organ development in Drosophila. Cell 102, 349-362.

Norton, W. H., J. Ledin, et al. (2005). "HSPG synthesis by zebrafish Ext2 and Extl3 is required for Fgf10 signalling during limb development." Development 132(22): 4963-73.

O'Brien, T., Cranston, D., Fuggle, S., Bicknell, R., and Harris, A. L. (1996). The angiogenic factor midkine is expressed in bladder cancer, and overexpression correlates with a poor outcome in patients with invasive cancers. Cancer Res 56, 2515-2518.

O'Tousa, J. E., W. Baehr, et al. (1985). "The Drosophila ninaE gene encodes an opsin." Cell 40(4): 839-50.

Oh, S. W., Kingsley, T., Shin, H. H., Zheng, Z., Chen, H. W., Chen, X., Wang, H., Ruan, P., Moody, M., and Hou, S. X. (2003). A P-element insertion screen identified mutations in 455 novel essential genes in Drosophila. Genetics 163, 195-201.

Ohashi, K., Nagata, K., Maekawa, M., Ishizaki, T., Narumiya, S., and Mizuno, K. (2000). Rho-associated kinase ROCK activates LIM-kinase 1 by phosphorylation at threonine 508 within the activation loop. J Biol Chem 275, 3577-3582.

Ogiso, H., R. Ishitani, et al. (2002). "Crystal structure of the complex of human epidermal growth factor and receptor extracellular domains." Cell 110(6): 775-87.

Okuda, M., Horn, H. F., Tarapore, P., Tokuyama, Y., Smulian, A. G., Chan, P. K., Knudsen, E. S., Hofmann, I. A., Snyder, J. D., Bove, K. E., and Fukasawa, K. (2000). Nucleophosmin/B23 is a target of CDK2/cyclin E in centrosome duplication. Cell 103, 127-140.

Packard, M., E. S. Koo, et al. (2002). "The Drosophila Wnt, wingless, provides an essential signal for pre- and postsynaptic differentiation." Cell 111(3): 319-30.

Pantaloni, D., Le Clainche, C., and Carlier, M. F. (2001). Mechanism of actin-based motility. Science 292, 1502-1506.

Papatsenko, D., G. Sheng, et al. (1997). "A new rhodopsin in R8 photoreceptors of Drosophila: evidence for coordinate expression with Rh3 in R7 cells." Development 124(9): 1665-73.

Paratcha, G., Ledda, F., and Ibanez, C. F. (2003). The neural cell adhesion molecule NCAM is an alternative signaling receptor for GDNF family ligands. Cell 113, 867-879.

Pasquale, E. B. (2005). Eph receptor signalling casts a wide net on cell behaviour. Nat Rev Mol Cell Biol 6, 462-475.

Paulus, J. D. and M. C. Halloran (2006). "Zebrafish bashful/laminin-alpha 1 mutants exhibit multiple axon guidance defects." Dev Dyn 235(1): 213-24.

Perez, S. E., and Steller, H. (1996a). Migration of glial cells into retinal axon target field in Drosophila melanogaster. J Neurobiol 30, 359-373.

Perez, S. E., and Steller, H. (1996b). Molecular and genetic analyses of lama, an evolutionarily conserved gene expressed in the precursors of the Drosophila first optic ganglion. Mech Dev 59, 11-27.

Plump, A. S., Erskine, L., Sabatier, C., Brose, K., Epstein, C. J., Goodman, C. S., Mason, C. A., and Tessier-Lavigne, M. (2002). Slit1 and Slit2 cooperate to prevent premature midline crossing of retinal axons in the mouse visual system. Neuron 33, 219-232.

Poeck, B., Fischer, S., Gunning, D., Zipursky, S. L., and Salecker, I. (2001). Glial cells mediate target layer selection of retinal axons in the developing visual system of Drosophila. Neuron 29, 99-113.

Polleux, F., Morrow, T., and Ghosh, A. (2000). Semaphorin 3A is a chemoattractant for cortical apical dendrites. Nature 404, 567-573.

Prakash, S., Caldwell, J. C., Eberl, D. F., and Clandinin, T. R. (2005). Drosophila N-cadherin mediates an attractive interaction between photoreceptor axons and their targets. Nat Neurosci 8, 443-450.

Prehoda, K. E., and Lim, W. A. (2002). How signaling proteins integrate multiple inputs: a comparison of N-WASP and Cdk2. Curr Opin Cell Biol 14, 149-154.

Pulford, K., Lamant, L., Espinos, E., Jiang, Q., Xue, L., Turturro, F., Delsol, G., and Morris, S. W. (2004). The emerging normal and disease-related roles of anaplastic lymphoma kinase. Cell Mol Life Sci 61, 2939-2953.

Rajagopalan, S., Nicolas, E., Vivancos, V., Berger, J., and Dickson, B. J. (2000). Crossing the midline: roles and regulation of Robo receptors. Neuron 28, 767-777.

Ranscht, B. (2000). "Cadherins: molecular codes for axon guidance and synapse formation." Int J Dev Neurosci 18(7): 643-51.

Ranscht, B. and M. T. Dours-Zimmermann (1991). "T-cadherin, a novel cadherin cell adhesion molecule in the nervous system lacks the conserved cytoplasmic region." Neuron 7(3): 391-402.

Rao, Y., Pang, P., Ruan, W., Gunning, D., and Zipursky, S. L. (2000). brakeless is required for photoreceptor growth-cone targeting in Drosophila. Proc Natl Acad Sci U S A 97, 5966-5971.

Raper, J. A. (2000). Semaphorins and their receptors in vertebrates and invertebrates. Curr Opin Neurobiol 10, 88-94.

Rawson, J. M., B. Dimitroff, et al. (2005). "The heparan sulfate proteoglycans Dally-like and Syndecan have distinct functions in axon guidance and visual-system assembly in Drosophila." Curr Biol 15(9): 833-8.

Redner, R. L., E. A. Rush, et al. (1996). "The t(5;17) variant of acute promyelocytic leukemia expresses a nucleophosmin-retinoic acid receptor fusion." Blood 87(3): 882-6.

Reinke, R. and S. L. Zipursky (1988). "Cell-cell interaction in the Drosophila retina: the bride of sevenless gene is required in photoreceptor cell R8 for R7 cell development." Cell 55(2): 321-30.

Rhiner, C., S. Gysi, et al. (2005). "Syndecan regulates cell migration and axon guidance in C. elegans." Development 132(20): 4621-33.

Riehl, R., K. Johnson, et al. (1996). "Cadherin function is required for axon outgrowth in retinal ganglion cells in vivo." Neuron 17(5): 837-48.

Ren, X. R., Ming, G. L., Xie, Y., Hong, Y., Sun, D. M., Zhao, Z. Q., Feng, Z., Wang, Q., Shim, S., Chen, Z. F., et al. (2004). Focal adhesion kinase in netrin-1 signaling. Nat Neurosci 7, 1204-1212.

Roberts, D. B (1998) Drosophila: A Practical Approach. Oxford, Oxford University Press.

Robinow, S., and White, K. (1991). Characterization and spatial distribution of the ELAV protein during Drosophila melanogaster development. J Neurobiol 22, 443-461.

Ruan, W., H. Long, et al. (2002). "Bifocal is a downstream target of the Ste20-like serine/threonine kinase misshapen in regulating photoreceptor growth cone targeting in Drosophila." Neuron 36(5): 831-42.

Ruiz-Gomez, M., Coutts, N., Price, A., Taylor, M. V., and Bate, M. (2000). Drosophila dumbfounded: a myoblast attractant essential for fusion. Cell 102, 189-198.

Sabatier, C., Plump, A. S., Le, M., Brose, K., Tamada, A., Murakami, F., Lee, E. Y., and Tessier-Lavigne, M. (2004). The divergent Robo family protein rig-1/Robo3 is a negative regulator of slit responsiveness required for midline crossing by commissural axons. Cell 117, 157-169.

Salecker, I., Clandinin, T. R., and Zipursky, S. L. (1998). Hedgehog and Spitz: making a match between photoreceptor axons and their targets. Cell 95, 587-590.

Salecker, I. and J. Boeckh (1995). "Embryonic development of the antennal lobes of a hemimetabolous insect, the cockroach Periplaneta americana: light and electron microscopic observations." J Comp Neurol 352(1): 33-54.

Sano, K., H. Tanihara, et al. (1993). "Protocadherins: a large family of cadherin-related molecules in central nervous system." Embo J 12(6): 2249-56.

Santoro, M., F. Carlomagno, et al. (2004). "Dysfunction of the RET receptor in human cancer." Cell Mol Life Sci 61(23): 2954-64.

Sato, M., D. Umetsu, et al. (2006). "DWnt4 regulates the dorsoventral specificity of retinal projections in the Drosophila melanogaster visual system." Nat Neurosci 9(1): 67-75.

Schaefer, A. W., Kabir, N., and Forscher, P. (2002). Filopodia and actin arcs guide the assembly and transport of two populations of microtubules with unique dynamic parameters in neuronal growth cones. J Cell Biol 158, 139-152.

Schlessinger, J. (2000). Cell signaling by receptor tyrosine kinases. Cell 103, 211-225.

Schmitt, A. M., Shi, J., Wolf, A. M., Lu, C. C., King, L. A., and Zou, Y. (2006). Wnt-Ryk signalling mediates medial-lateral retinotectal topographic mapping. Nature 439, 31-37.

Schneider, T., Reiter, C., Eule, E., Bader, B., Lichte, B., Nie, Z., Schimansky, T., Ramos, R. G., and Fischbach, K. F. (1995). Restricted expression of the irreC-rst

protein is required for normal axonal projections of columnar visual neurons. Neuron 15, 259-271.

Scott, E. K., and Luo, L. (2001). How do dendrites take their shape? Nat Neurosci 4, 359-365.

Scully, A. L., McKeown, M., and Thomas, J. B. (1999). Isolation and characterization of Dek, a Drosophila eph receptor protein tyrosine kinase. Mol Cell Neurosci 13, 337-347.

Semaphorin Nomenclature Committee (1999). Cell 97(5):551-2.

Senti, K., Keleman, K., Eisenhaber, F., and Dickson, B. J. (2000). brakeless is required for lamina targeting of R1-R6 axons in the Drosophila visual system. Development 127, 2291-2301.

Senti, K. A., Usui, T., Boucke, K., Greber, U., Uemura, T., and Dickson, B. J. (2003). Flamingo regulates R8 axon-axon and axon-target interactions in the Drosophila visual system. Curr Biol 13, 828-832.

Serafini, T., Colamarino, S. A., Leonardo, E. D., Wang, H., Beddington, R., Skarnes, W. C., and Tessier-Lavigne, M. (1996). Netrin-1 is required for commissural axon guidance in the developing vertebrate nervous system. Cell 87, 1001-1014.

Serafini, T., Kennedy, T. E., Galko, M. J., Mirzayan, C., Jessell, T. M., and Tessier-Lavigne, M. (1994). The netrins define a family of axon outgrowth-promoting proteins homologous to C. elegans UNC-6. Cell 78, 409-424.

Shamah, S. M., M. Z. Lin, et al. (2001). "EphA receptors regulate growth cone dynamics through the novel guanine nucleotide exchange factor ephexin." Cell 105(2): 233-44.

Shekarabi, M., and Kennedy, T. E. (2002). The netrin-1 receptor DCC promotes filopodia formation and cell spreading by activating Cdc42 and Rac1. Mol Cell Neurosci 19, 1-17.

Shewan, D., Dwivedy, A., Anderson, R., and Holt, C. E. (2002). Age-related changes underlie switch in netrin-1 responsiveness as growth cones advance along visual pathway. Nat Neurosci 5, 955-962.

Shimoyama, Y., G. Tsujimoto, et al. (2000). "Identification of three human type-II classic cadherins and frequent heterophilic interactions between different subclasses of type-II classic cadherins." Biochem J 349(Pt 1): 159-67.

Shinza-Kameda, M., E. Takasu, et al. (2006). "Regulation of layer-specific targeting by reciprocal expression of a cell adhesion molecule, capricious." Neuron 49(2): 205-13.

Shiota, M., Nakamura, S., Ichinohasama, R., Abe, M., Akagi, T., Takeshita, M., Mori, N., Fujimoto, J., Miyauchi, J., Mikata, A., et al. (1995). Anaplastic large cell lymphomas expressing the novel chimeric protein p80NPM/ALK: a distinct clinicopathologic entity. Blood 86, 1954-1960.

Shishido, E., Takeichi, M., and Nose, A. (1998). Drosophila synapse formation: regulation by transmembrane protein with Leu-rich repeats, CAPRICIOUS. Science 280, 2118-2121.

Silos-Santiago, I., Yeh, H. J., Gurrieri, M. A., Guillerman, R. P., Li, Y. S., Wolf, J., Snider, W., and Deuel, T. F. (1996). Localization of pleiotrophin and its mRNA in subpopulations of neurons and their corresponding axonal tracts suggests important roles in neural-glial interactions during development and in maturity. J Neurobiol 31, 283-296.

Simpson, J. H., Kidd, T., Bland, K. S., and Goodman, C. S. (2000). Short-range and long-range guidance by slit and its Robo receptors. Robo and Robo2 play distinct roles in midline guidance. Neuron 28, 753-766.

Slupianek, A., Nieborowska-Skorska, M., Hoser, G., Morrione, A., Majewski, M., Xue, L., Morris, S. W., Wasik, M. A., and Skorski, T. (2001). Role of phosphatidylinositol 3-kinase-Akt pathway in nucleophosmin/anaplastic lymphoma kinase-mediated lymphomagenesis. Cancer Res 61, 2194-2199.

Song, H., Ming, G., He, Z., Lehmann, M., McKerracher, L., Tessier-Lavigne, M., and Poo, M. (1998). Conversion of neuronal growth cone responses from repulsion to attraction by cyclic nucleotides. Science 281, 1515-1518.

Song, H. J., G. L. Ming, et al. (1997). "cAMP-induced switching in turning direction of nerve growth cones." Nature 388(6639): 275-9.

Souttou, B., Carvalho, N. B., Raulais, D., and Vigny, M. (2001). Activation of anaplastic lymphoma kinase receptor tyrosine kinase induces neuronal differentiation through the mitogen-activated protein kinase pathway. J Biol Chem 276, 9526-9531.

Spalding, K. L., M. M. Tan, et al. (2002). "Anterograde transport and trophic actions of BDNF and NT-4/5 in the developing rat visual system." Mol Cell Neurosci 19(4): 485-500.

Sperry, R. W. (1963). Chemoaffinity In The Orderly Growth Of Nerve Fiber Patterns And Connections. Proc Natl Acad Sci U S A 50, 703-710.

Steigemann, P., A. Molitor, et al. (2004). "Heparan sulfate proteoglycan syndecan promotes axonal and myotube guidance by slit/robo signaling." Curr Biol 14(3): 225-30.

Stein, E., and Tessier-Lavigne, M. (2001). Hierarchical organization of guidance receptors: silencing of netrin attraction by slit through a Robo/DCC receptor complex. Science 291, 1928-1938.

Stein, H., Foss, H. D., Durkop, H., Marafioti, T., Delsol, G., Pulford, K., Pileri, S., and Falini, B. (2000). CD30(+) anaplastic large cell lymphoma: a review of its histopathologic, genetic, and clinical features. Blood 96, 3681-3695.

Stoeckli, E. T., and Landmesser, L. T. (1995). Axonin-1, Nr-CAM, and Ng-CAM play different roles in the in vivo guidance of chick commissural neurons. Neuron 14, 1165-1179.

Stoica, G. E., Kuo, A., Aigner, A., Sunitha, I., Souttou, B., Malerczyk, C., Caughey, D. J., Wen, D., Karavanov, A., Riegel, A. T., and Wellstein, A. (2001). Identification of anaplastic lymphoma kinase as a receptor for the growth factor pleiotrophin. J Biol Chem 276, 16772-16779.

Stoica, G. E., Kuo, A., Powers, C., Bowden, E. T., Sale, E. B., Riegel, A. T., and Wellstein, A. (2002). Midkine binds to anaplastic lymphoma kinase (ALK) and acts as a growth factor for different cell types. J Biol Chem 277, 35990-35998.

Strasser, G. A., Rahim, N. A., VanderWaal, K. E., Gertler, F. B., and Lanier, L. M. (2004). Arp2/3 is a negative regulator of growth cone translocation. Neuron 43, 81-94.

Strunkelnberg, M., Bonengel, B., Moda, L. M., Hertenstein, A., de Couet, H. G., Ramos, R. G., and Fischbach, K. F. (2001). rst and its paralogue kirre act redundantly during embryonic muscle development in Drosophila. Development 128, 4229-4239.

Stute, C., Schimmelpfeng, K., Renkawitz-Pohl, R., Palmer, R. H., and Holz, A. (2004). Myoblast determination in the somatic and visceral mesoderm depends on Notch signalling as well as on milliways(mili(Alk)) as receptor for Jeb signalling. Development 131, 743-754.

Suh, G. S., Poeck, B., Chouard, T., Oron, E., Segal, D., Chamovitz, D. A., and Zipursky, S. L. (2002). Drosophila JAB1/CSN5 acts in photoreceptor cells to induce glial cells. Neuron 33, 35-46.

Sur, M., and Rubenstein, J. L. (2005). Patterning and plasticity of the cerebral cortex. Science 310, 805-810.

Suter, D. M., and Forscher, P. (2000). Substrate-cytoskeletal coupling as a mechanism for the regulation of growth cone motility and guidance. J Neurobiol 44, 97-113.

Suter, D. M., Schaefer, A. W., and Forscher, P. (2004). Microtubule dynamics are necessary for SRC family kinase-dependent growth cone steering. Curr Biol 14, 1194-1199.

Sutherland, J. D., and Way, M. (2002). Looking over the edge: a new role for Ena/VASP proteins in lamellipodial dynamics. Dev Cell 2, 692-694.

Tabata, T. and T. B. Kornberg (1994). "Hedgehog is a signaling protein with a key role in patterning Drosophila imaginal discs." Cell 76(1): 89-102.

Tamagnone, L., Artigiani, S., Chen, H., He, Z., Ming, G. I., Song, H., Chedotal, A., Winberg, M. L., Goodman, C. S., Poo, M., et al. (1999). Plexins are a large family of receptors for transmembrane, secreted, and GPI-anchored semaphorins in vertebrates. Cell 99, 71-80.

Tamagnone, L., and Comoglio, P. M. (2000). Signalling by semaphorin receptors: cell guidance and beyond. Trends Cell Biol 10, 377-383.

Taniguchi, H., Shishido, E., Takeichi, M., and Nose, A. (2000). Functional dissection of Drosophila capricious: its novel roles in neuronal pathfinding and selective synapse formation. J Neurobiol 42, 104-116.

Tayler, T. D., Robichaux, M. B., and Garrity, P. A. (2004). Compartmentalization of visual centers in the Drosophila brain requires Slit and Robo proteins. Development 131, 5935-5945.

Tessier-Lavigne, M., and Goodman, C. S. (1996). The molecular biology of axon guidance. Science 274, 1123-1133.

Ting, C. Y., Yonekura, S., Chung, P., Hsu, S. N., Robertson, H. M., Chiba, A., and Lee, C. H. (2005). Drosophila N-cadherin functions in the first stage of the two-stage layer-selection process of R7 photoreceptor afferents. Development 132, 953-963.

Tio, M., and Moses, K. (1997). The Drosophila TGF alpha homolog Spitz acts in photoreceptor recruitment in the developing retina. Development 124, 343-351.

Tomlinson, A., D. D. Bowtell, et al. (1987). "Localization of the sevenless protein, a putative receptor for positional information, in the eye imaginal disc of Drosophila." Cell 51(1): 143-50.

Trousse, F., Marti, E., Gruss, P., Torres, M., and Bovolenta, P. (2001). Control of retinal ganglion cell axon growth: a new role for Sonic hedgehog. Development 128, 3927-3936.

Turturro, F., Arnold, M. D., Frist, A. Y., and Pulford, K. (2002). Model of inhibition of the NPM-ALK kinase activity by herbimycin A. Clin Cancer Res 8, 240-245.

Ueno, H., Hirano, N., Kozutsumi, H., Sasaki, K., Tanaka, T., Yazaki, Y., and Hirai, H. (1995). An epidermal growth factor receptor-leukocyte tyrosine kinase chimeric receptor generates ligand-dependent growth signals through the Ras signaling pathway. J Biol Chem 270, 20135-20142.

Ueno, H., Sasaki, K., Kozutsumi, H., Miyagawa, K., Mitani, K., Yazaki, Y., and Hirai, H. (1996). Growth and survival signals transmitted via two distinct NPXY motifs within leukocyte tyrosine kinase, an insulin receptor-related tyrosine kinase. J Biol Chem 271, 27707-27714.

Umetsu, D., S. Murakami, et al. (2006). "The highly ordered assembly of retinal axons and their synaptic partners is regulated by Hedgehog/Single-minded in the Drosophila visual system." Development 133(5): 791-800.

Usui, T., Y. Shima, et al. (1999). "Flamingo, a seven-pass transmembrane cadherin, regulates planar cell polarity under the control of Frizzled." Cell 98(5): 585-95.

Van der Geer, P., Wiley, S., Lai, V. K., Olivier, J. P., Gish, G. D., Stephens, R., Kaplan, D., Shoelson, S., and Pawson, T. (1995). A conserved amino-terminal Shc domain binds to phosphotyrosine motifs in activated receptors and phosphopeptides. Curr Biol 5, 404-412.

Van Raay, T. J., S. M. Foskett, et al. (1997). "The NTN2L gene encoding a novel human netrin maps to the autosomal dominant polycystic kidney disease region on chromosome 16p13.3." Genomics 41(2): 279-82.

Vasiliauskas, D., and Stern, C. D. (2001). Patterning the embryonic axis: FGF signaling and how vertebrate embryos measure time. Cell 106, 133-136.

Vikis, H. G., Li, W., and Guan, K. L. (2002). The plexin-B1/Rac interaction inhibits PAK activation and enhances Sema4D ligand binding. Genes Dev 16, 836-845.

Wahl, S., Barth, H., Ciossek, T., Aktories, K., and Mueller, B. K. (2000). Ephrin-A5 induces collapse of growth cones by activating Rho and Rho kinase. J Cell Biol 149, 263-270.

Walsh, F. S., and Doherty, P. (1997). Neural cell adhesion molecules of the immunoglobulin superfamily: role in axon growth and guidance. Annu Rev Cell Dev Biol 13, 425-456.

Wan, H. I., DiAntonio, A., Fetter, R. D., Bergstrom, K., Strauss, R., and Goodman, C. S. (2000). Highwire regulates synaptic growth in Drosophila. Neuron 26, 313-329.

Wang, G., Wang, B., and Jiang, J. (1999a). Protein kinase A antagonizes Hedgehog signaling by regulating both the activator and repressor forms of Cubitus interruptus. Genes Dev 13, 2828-2837.

Wang, H., Copeland, N. G., Gilbert, D. J., Jenkins, N. A., and Tessier-Lavigne, M. (1999b). Netrin-3, a mouse homolog of human NTN2L, is highly expressed in sensory ganglia and shows differential binding to netrin receptors. J Neurosci 19, 4938-4947.

Wang, K. H., Brose, K., Arnott, D., Kidd, T., Goodman, C. S., Henzel, W., and Tessier-Lavigne, M. (1999c). Biochemical purification of a mammalian slit protein as a positive regulator of sensory axon elongation and branching. Cell 96, 771-784.

Wang, X., R. Butowt, et al. (2003). "Presynaptic neurotrophin-3 increases the number of tectal synapses, vesicle density, and number of docked vesicles in chick embryos." J Comp Neurol 458(1): 62-77.

Weiss, J. B., Suyama, K. L., Lee, H. H., and Scott, M. P. (2001). Jelly belly: a Drosophila LDL receptor repeat-containing signal required for mesoderm migration and differentiation. Cell 107, 387-398.

Wilkinson, D. G. (2001). Multiple roles of EPH receptors and ephrins in neural development. Nat Rev Neurosci 2, 155-164.

Williams, E. J., Furness, J., Walsh, F. S., and Doherty, P. (1994). Activation of the FGF receptor underlies neurite outgrowth stimulated by L1, N-CAM, and N-cadherin. Neuron 13, 583-594.

Wilson, S. W. and C. Houart (2004). "Early steps in the development of the forebrain." Dev Cell 6(2): 167-81.

Winberg, M. L., Noordermeer, J. N., Tamagnone, L., Comoglio, P. M., Spriggs, M. K., Tessier-Lavigne, M., and Goodman, C. S. (1998). Plexin A is a neuronal semaphorin receptor that controls axon guidance. Cell 95, 903-916.

Winberg, M. L., Perez, S. E., and Steller, H. (1992). Generation and early differentiation of glial cells in the first optic ganglion of Drosophila melanogaster. Development 115, 903-911.

Wojtowicz, W. M., J. J. Flanagan, et al. (2004). "Alternative splicing of Drosophila Dscam generates axon guidance receptors that exhibit isoform-specific homophilic binding." Cell 118(5): 619-33.

Wolff T. and Ready, D. F. (1993). Pattern formation in the Drosophila retina. In the Development of Drosophila Melanogaster. Cold Spring Harbor, New York: Cold Spring Harbor Laboratory Press, 1277-1325.

Wong, K., Ren, X. R., Huang, Y. Z., Xie, Y., Liu, G., Saito, H., Tang, H., Wen, L., Brady-Kalnay, S. M., Mei, L., et al. (2001). Signal transduction in neuronal migration: roles of GTPase activating proteins and the small GTPase Cdc42 in the Slit-Robo pathway. Cell 107, 209-221.

Wu, Q., T. Zhang, et al. (2001). "Comparative DNA sequence analysis of mouse and human protocadherin gene clusters." Genome Res 11(3): 389-404.

Yang, L. and N. E. Baker (2001). "Role of the EGFR/Ras/Raf pathway in specification of photoreceptor cells in the Drosophila retina." Development 128(7): 1183-91.

Yang, N., Higuchi, O., Ohashi, K., Nagata, K., Wada, A., Kangawa, K., Nishida, E., and Mizuno, K. (1998). Cofilin phosphorylation by LIM-kinase 1 and its role in Rac-mediated actin reorganization. Nature 393, 809-812.

Yaron, A., P. H. Huang, et al. (2005). "Differential requirement for Plexin-A3 and -A4 in mediating responses of sensory and sympathetic neurons to distinct class 3 Semaphorins." Neuron 45(4): 513-23.

Yin, Y., J. R. Sanes, et al. (2000). "Identification and expression of mouse netrin-4." Mech Dev 96(1): 115-9.

Yoneda-Kato, N., Look, A. T., Kirstein, M. N., Valentine, M. B., Raimondi, S. C., Cohen, K. J., Carroll, A. J., and Morris, S. W. (1996). The t(3;5)(q25.1;q34) of myelodysplastic syndrome and acute myeloid leukemia produces a novel fusion gene, NPM-MLF1. Oncogene 12, 265-275.

Yu, T. W., Hao, J. C., Lim, W., Tessier-Lavigne, M., and Bargmann, C. I. (2002). Shared receptors in axon guidance: SAX-3/Robo signals via UNC-34/Enabled and a Netrin-independent UNC-40/DCC function. Nat Neurosci 5, 1147-1154.

Zallen, J. A., Yi, B. A., and Bargmann, C. I. (1998). The conserved immunoglobulin superfamily member SAX-3/Robo directs multiple aspects of axon guidance in C. elegans. Cell 92, 217-227.

Zamo, A., Chiarle, R., Piva, R., Howes, J., Fan, Y., Chilosi, M., Levy, D. E., and Inghirami, G. (2002). Anaplastic lymphoma kinase (ALK) activates Stat3 and protects hematopoietic cells from cell death. Oncogene 21, 1038-1047.

Zhai, R. G., Hiesinger, P. R., Koh, T. W., Verstreken, P., Schulze, K. L., Cao, Y., Jafar-Nejad, H., Norga, K. K., Pan, H., Bayat, V., et al. (2003). Mapping Drosophila mutations with molecularly defined P element insertions. Proc Natl Acad Sci U S A 100, 10860-10865.

Zhang, H. Y., and Hoffmann, K. P. (1993). Retinal projections to the pretectum, accessory optic system and superior colliculus in pigmented and albino ferrets. Eur J Neurosci 5, 486-500.

Zhou, F. Q., Waterman-Storer, C. M., and Cohan, C. S. (2002). Focal loss of actin bundles causes microtubule redistribution and growth cone turning. J Cell Biol 157, 839-849.

Zhu, H. and L. Luo (2004). "Diverse functions of N-cadherin in dendritic and axonal terminal arborization of olfactory projection neurons." Neuron 42(1): 63-75.

Zou, Y., Stoeckli, E., Chen, H., and Tessier-Lavigne, M. (2000). Squeezing axons out of the gray matter: a role for slit and semaphorin proteins from midline and ventral spinal cord. Cell 102, 363-375.